



UNIVERSIDAD NACIONAL DE COLOMBIA

REACTION PATHWAYS FOR IN SITU COMBUSTION

Luisa Fernanda Carvajal Díaz

Universidad Nacional de Colombia, Sede Medellín

Facultad de Minas

Medellín, Colombia

2015

REACTION PATHWAYS FOR IN SITU COMBUSTION

Luisa Fernanda Carvajal Díaz

Thesis presented as a partial requirement to obtain the degree of:
M.Sc. in Chemical Engineering

Advisor:

Alejandro Molina

Co-advisor:

Astrid Elena Sanchez Pino

Research group:

Bioprocesos y Flujos Reactivos

Universidad Nacional de Colombia, Sede Medellín

Facultad de Minas

Medelln, Colombia

2015

ABSTRACT

This study proposes reaction pathways to explain chemical routes that the fractions of a heavy crude oil follow during the thermal cracking and low temperature oxidation stages of in situ combustion (ISC). ISC is an enhanced oil recovery method that has as operating principle a combustion process inside a reservoir. Coke is produced during this process by thermal cracking and oxidation at low temperature and reacts to release energy in the form of heat that reduces the viscosity of the crude oil and facilitates its extraction. Current reaction schemes for ISC do not give details about the chemistry involved in this process. Based on that, this research studied the process from a chemical point of view in order to get a better understanding on the products formation and reactions.

Surrogate compounds with physical and chemical properties representative of the different fractions of a crude oil were carefully selected. Given the complexity of the surrogate molecular structures, the reactive sites in the molecules were determined from the analysis of bond orders and reactivity indexes provided by electronic structure calculations. Quantum chemistry simulations of the possible reaction pathways of these surrogates indicated the most probable reactions that take place during ISC. Validation of the proposed reaction pathways was undertaken by assessing the agreement of intermediate species, products and reaction energies with experimental data available in the literature. The agreement was good and gave confidence that proposed pathways can improve the understanding of the chemistry associated with the ISC process and, therefore, enhance the probability of success of new ISC projects.

Keywords: In situ combustion, reaction pathway, thermal cracking, low temperature oxidation, electronic structure calculations

RESUMEN

El presente estudio propone reaction pathways para explicar las rutas químicas que las fracciones de un crudo pesado siguen durante las etapas de craqueo térmico y oxidación a baja temperatura de la combustión in situ (CIS). CIS es un método de recobro mejorado de crudo que tiene como principio operativo un proceso de combustión al interior del yacimiento. El coque es producido durante este proceso debido al craqueo térmico y la oxidación a baja temperatura y reacciona para liberar energía en forma de calor, la cual reduce la viscosidad del crudo y facilita su extracción. Los esquemas de reacción actuales para CIS no proveen detalles sobre la química implicada en este proceso. Con base en esto, esta investigación estudió la CIS desde un punto de vista químico con el fin de obtener un mejor entendimiento en la formación de productos y las reacciones.

Sucedáneos con propiedades físicas y químicas representativas de las diferentes fracciones de un crudo fueron cuidadosamente seleccionadas. Dada la complejidad de las estructuras moleculares de los sucedáneos, los sitios de mayor reactividad en dichas moléculas fueron determinados mediante el análisis de ordenes de enlace e índices de reactividad provistos por cálculos de estructura electrónica. Simulaciones en química cuántica de los posibles reaction pathways de estos sucedáneos indicaron las reacciones que más posiblemente tienen lugar durante la CIS. La validación de los reaction pathways propuestos fue realizada mediante la evaluación de la concordancia entre especies intermedias, productos y reacciones con datos experimentales disponibles en la literatura. Se obtuvo un buen acuerdo entre los resultados y lo reportado, lo que sugiere que los reaction pathways propuestos pueden mejorar el entendimiento de la química asociada con el proceso CIS y por lo tanto, aumentar la probabilidad de éxito de nuevos proyectos en este campo.

Palabras claves: Combustión in situ, reaction pathway, craqueo térmico, oxidación a baja temperatura, cálculos de estructura electrónica

Agradecimientos

Al programa de investigación: «Herramientas tecnológicas para incrementar el factor de recobro de crudos pesados», por la financiación parcial de esta maestría y de la pasantía de investigación realizada en la Universidad de Cambridge.

A la Facultad de Minas de la Universidad Nacional de Colombia Sede Medellín por otorgarme la Beca de Exención de derechos académicos durante tres periodos.

Al programa de la Facultad de Minas: «Internacionalización del conocimiento 2013-2015», por el apoyo económico para la realización de la pasantía de investigación.

Al profesor Alejandro Molina, por ser un gran maestro y ser humano. De nada vale ser bueno si alguien no te da la oportunidad de demostrarlo y eso es lo que usted hizo por mí. Gracias por estar presente y brindarme todo el apoyo durante la realización de esta investigación. Su disciplina es un ejemplo a seguir para mí.

A la profesora Astrid Sánchez, quien más que una profesora ha sido una amiga. Conocer personas como tú que iluminan vidas con su gran corazón y filosofía de servicio, es una suerte. Gracias por haber llegado en uno de los puntos más críticos de este trabajo para aportar una nueva visión que fue más que fundamental en su realización.

To Professor Markus Kraft, for gave me the opportunity to assist and work in one of the best universities in the world, University of Cambridge. Thanks for your advices and recommendations.

A mi familia, porque gracias a ellos soy persona y profesional. Ustedes son el regalo más hermoso que Dios me dio. En especial agradezco a mi madre por ser la más hermosa de las mujeres, esa que nunca me ha abandonado, la que sufrió todos mis trasnochos y angustias.

A Héctor, por ser el hermoso sol que ilumina mi vida. Gracias por ser el tibio abrazo y la palabra de aliento que siempre me reconfortan. Lo logramos! Superamos las tres reglas. Te amo!

A todos mis compañeros de FRUN, por escuchar cada una de mis presentaciones, por todos los valiosos aportes que me han hecho y por los buenos momentos que pasamos juntos. En especial a Juan David y Laura, excelentes seres humanos que fueron más que una compañía en este proceso.

A María Luisa Botero, María Mercedes Bacadare y Silvia González por brindarme su amistad y ser

un gran apoyo en todos los nuevos retos y experiencias que viví en Inglaterra.

Contents

ABSTRACT	III
RESUMEN	IV
Agradecimientos	V
List of Figures	XII
List of Tables	1
1. Introduction	2
1.1. Motivation	3
1.2. Objective	3
1.3. Specific Objectives	3
1.4. Description of the Thesis	4
2. Fundamentals and Background	6
2.1. In Situ Combustion (ISC)	6
2.1.1. Thermal cracking reactions	9
2.1.2. Low temperature oxidation reactions (LTO)	13
2.1.3. High temperature oxidation reactions (HTO)	15
2.2. Reactions and reaction mechanism	17
2.2.1. Thermal-cracking reaction mechanisms for hydrocarbons	18
2.2.2. Low temperature oxidation mechanisms for hydrocarbons	22
2.3. Computational chemistry to model hydrocarbon species	26
3. Methodology	28
3.1. Surrogate selection	28
3.2. ISC chemistry study and ISC chemical division	29

3.3. Study of typical reaction mechanisms	30
3.3.1. Thermal cracking	30
3.3.2. Low temperature oxidation	30
3.4. Computational methodology	31
3.4.1. Model chemistry definition	31
3.4.2. Geometry optimizations	31
3.4.3. Natural bond orbital (NBO) calculations	32
3.4.4. Topological Fukui calculations	32
3.4.5. Condensed Fukui function calculations	33
3.4.6. Scans	34
3.5. Reaction pathways	34
3.5.1. Low temperature oxidation	35
3.5.2. Thermal cracking	37
3.5.3. Construction of reactive schemes	40
3.6. Thematic DataBase	41
3.7. Validation	41
4. Surrogate selection and stages associated to the chemical processes in ISC	42
4.1. Surrogate selection	42
4.2. Stages associated to the chemical processes in ISC	49
5. LTO reaction pathways	50
5.1. Methodology	50
5.2. Results for saturate and aromatic surrogates	51
5.2.1. Initiation	51
5.2.2. Propagation	62
5.2.3. Termination and degenerate branching steps	66
5.3. Analysis for resin and asphaltene surrogates	71
5.4. Conclusions	74
6. Thermal cracking reaction pathways	76
6.1. Methodology	76
6.2. Results	78
6.2.1. Formation of free radicals	78
6.2.2. Initiation	81

6.2.3. Propagation	91
6.2.4. Other intermediate formation and Termination	92
6.2.5. Reaction route for coke formation	94
6.2.6. Thematic DataBase results	100
6.3. Validation	101
6.4. Conclusions	102
7. Conclusions	104
7.1. Future work	105
References	115
A. Reaction schemes	116

List of Figures

2.1. a) Scheme of the main phenomena involved in ISC. b) Temperature profile of ISC zones [1,2]	8
5.1. Methodology diagram for the formulation of the LTO reaction pathways	51
5.2. Contours of electrophilic topological Fukui function for Cyclic Saturate (CS)	52
5.3. Contours of electrophilic topological Fukui function for Normal Saturate (NS)	54
5.4. Contours of electrophilic topological Fukui function for Monocyclic Aromatic (MA)	56
5.5. Contours of electrophilic topological Fukui function for Polycyclic Aromatic (PA)	57
5.6. Molecular structure of the olefin surrogate	59
5.7. LTO Initiation products. a) $\bullet R$ radical from CS. b) $\bullet R$ radical from NS. c) $\bullet R$ radical from MA. d) $ROO\bullet$ radical from PA. e) $ROO\bullet$ radical from Olefin	60
5.8. LTO propagation products from β -scission reactions. a) Radical olefin from CS. b) $\bullet R$ radical from NS. c) Ethylene from NS	63
5.9. LTO propagation products from intermolecular H-abstraction. a) External olefin from CS. b) Internal olefin (methylcyclohexene) from CS. c) Terminal olefin from NS	64
5.10. LTO propagation products from intramolecular H-abstraction. a) $\bullet QOOH$ radical from CS. b) $\bullet QOOH$ radical from NS. c) $\bullet QOOH$ radical from MA. d) $\bullet QOOH$ radical from PA.	64
5.11. LTO propagation products from intermolecular addition of O_2 . a) $ROO\bullet$ from CS. b) $ROO\bullet$ from NS. c) $ROO\bullet$ from MA.	65
5.12. Reaction scheme for the evolution of radical peroxides	67
5.13. Reaction scheme for the evolution of peroxy radicals	68
5.14. Termination event products from CS surrogate	69
5.15. Termination event products from NS surrogate	69
5.16. Termination event products from MA surrogate	70
5.17. Termination event products from PA surrogate	70

5.18. Reactive sites (circles) in the CR structure with substituent labels	72
5.19. Reactive sites (circles) in the CA structure with substituent labels	73
6.1. Methodology diagram for the formulation of the thermal cracking reaction pathways .	77
6.2. Symmetry planes of saturate structures. a) Symmetry planes for the CS surrogate. b) Symmetry planes for the NS surrogate.	79
6.3. Symmetry planes of aromatic structures	81
6.4. Saturate initiation products (SIP). a) Hydrogen radical from CS. b) Tertiary cyclic radical from CS. c) Biradical from CS. d) Secondary radical from NS. e) Hydrogen radical from NS. f and g) Primary radicals from NS	82
6.5. Aromatic unimolecular and bimolecular initiation products (AIP). Unimolecular initiation reactions: a) Stabilized by resonance radical from MA b) Secondary radical from PA c) Hydrogen radical from PA d) Secondary radical from PA e) Hydrogen radical from PA. Bimolecular initiation reactions: f) Stabilized by resonance radical from MA g) Dihexene radical from MA h) Stabilized by resonance radical from MA i) Secondary radical from PA j) Secondary radical from PA k) Secondary radical from PA.	84
6.6. Frequency plot for bond order for the bonds in the CR surrogate	86
6.7. Castilla Resin structure. The red lines indicate the places where it is more possible that the bonds break	87
6.8. Castilla resin initiation products (RIP)	88
6.9. Castilla Asphaltene structure. The red lines indicate the places where it is more possible that the bonds break	89
6.10. Castilla Asphaltene (CA) initiation products (AsIP)	91
6.11. First step in the reaction route for coke formation - Initiation reactions. Reaction energies in kcal/mol	95
6.12. Second step in the reaction route for coke formation - Propagation reactions. Reaction energies in kcal/mol	96
6.13. Third step in the reaction route for coke formation - Coke formation	98
6.14. Fourth step in the reaction route for coke formation - Maturation. Reaction energies in kcal/mol	100
A.1. Reaction scheme for the LTO of the CS surrogate	116
A.2. Reaction scheme for the LTO of the NS surrogate	117
A.3. Reaction scheme for the LTO of the MA surrogate	117
A.4. Reaction scheme for the LTO of the PA surrogate	118

A.5. Reaction scheme for the thermal cracking of the saturate surrogates	119
A.6. Reaction scheme for the thermal cracking of the resin surrogate	120
A.7. Reaction scheme for the thermal cracking of the asphaltene surrogate	121

List of Tables

2.1. LTO free radicals, production reactions and reaction routes	25
4.1. Molecular structures in 2D and 3D of saturate surrogates	45
4.2. Molecular structures in 2D and 3D of aromatic surrogates	46
4.3. Molecular structures in 2D of resins and asphaltene surrogates	48
5.1. Results of electrophilic condensed Fukui function for Cyclic Saturate (CS)	53
5.2. Results of electrophilic condensed Fukui function for Normal Saturate (NS)	54
5.3. Results of electrophilic condensed Fukui function for Monocyclic Aromatic (MA)	56
5.4. Results of electrophilic condensed Fukui function for Polycyclic Aromatic (PA)	58
5.5. Results of electrophilic condensed Fukui function for the olefin surrogate 1-heptene	59
5.6. Summary of LTO initiation event with O_2 as oxidant agent	61
5.7. Summary of LTO initiation event with $\bullet OH$ and $HO_2\bullet$ as oxidant agents by the inter-molecular H-abstraction route	62
5.8. Summary of LTO propagation event	66
5.9. Summary of LTO termination event	71
6.1. Results of free-radical formation study for Cyclic Saturate (CS)	79
6.2. Results of free-radical formation study for Normal Saturate (NS)	80
6.3. Results of free-radical formation study for Monocyclic Aromatic (MA)	81
6.4. Results of free-radical formation study for Polycyclic Aromatic (PA)	81
6.5. Summary of unimolecular initiation reactions for saturate and aromatic surrogates	83
6.6. Summary of bimolecular initiation reactions for aromatic surrogates	85
6.7. Summary of $C - C$ cleavage as initiation reactions for Castilla Resin (CR)	88
6.8. Summary of $C - C$ cleavage as initiation reactions for Castilla Asphaltene (CA)	90
6.9. Summary of Other intermediate formation	93
6.10. Summary of Termination	94

6.11. Summary of results for scan relaxed calculations applied to Saturate surrogates 101

Chapter 1

Introduction

Hydrocarbons are still the main energy source of the world. Almost every product and process require materials or fuels derived from petroleum. Typical reservoirs have been exploited with good results; however, light oil reservoirs are becoming less abundant [3], which motivates the petroleum industry to look for other sources. Unconventional reservoirs have been evaluated as one of the main options to replace the energy supply. These type of reservoirs challenge the industry, because conventional extraction techniques do not perform properly in their cases [4]. In the last decades a vast amount of heavy crude oil and bitumen reservoirs have been identified and explored. Some studies estimate reserves of these resources around 9-13 trillion barrels [3, 5].

In situ combustion (ISC) was developed for Enhanced Oil Recovery (EOR) in order to increase the recovery factor of heavy crude oil and bitumen and is useful when common or conventional methods are not enough or appropriate. ISC is a thermal oil recovery technique where a combustion front is formed and propagated along the reservoir, taking advantage of important physical-chemical phenomena.

ISC has been traditionally divided in three stages: low temperature oxidation (LTO), thermal cracking and high temperature oxidation [1, 4, 6–8]. Low temperature oxidation is the first process stage and has as main products oxygenated compounds and coke. These products undergo an oxidation process at high temperature, producing combustion gases, carbon monoxide (CO), carbon dioxide (CO_2) and water vapor. Combustion gases propagate through the reservoir and make contact with the cold crude oil bank, which undergoes an increase in its energy that causes thermal cracking, an important stage, because, in addition to coke production, upgrades the oil, increasing the fraction of lighter compounds recovered.

This research proposes reaction pathways that describe, in detail, the chemical evolution of heavy crude oil fractions during low temperature oxidation and thermal cracking stages of ISC process. The first step in developing such a mechanism involved the selection of surrogate species representative of

the most important oil fractions. In addition, the most accepted reaction mechanisms proposed for low temperature oxidation [9–20], and thermal cracking [21–37] of hydrocarbons were analyzed. Based on that, it was possible to determine the reactions that could occur under ISC conditions. Furthermore, in order to study the possible routes that the different species follow, the software Gaussian 09 [38] was used to obtain optimized structures of surrogate compounds selected, ground-state energies, bond orders (through Wiberg Index) and a characterization of possible reactive sites (through topological and electrophilic condensed Fukui Functions). All of these parameters were taken into account to formulate the reaction pathways.

1.1. Motivation

Physical phenomena associated to ISC technique are well-known by the petroleum industry, particularly those associated with the flow through porous media. The chemical approach of this process, however, has not been largely explored or described, although chemical phenomena provide key information for a better understanding of the process [4, 11]. Typical reaction schemes to explain ISC chemistry [1, 6–8, 39] have been proposed based on experimental data. The reactions that usually integrate them involve pseudocomponents such as maltenes and consider products such as gases. Current reaction schemes do not give details about most of the products that the complex processes of low temperature oxidation and thermal cracking form, whereas there is an extensive development of high temperature oxidation mechanisms for several fuels [40–43]. Taking this into account, this research attempted to obtain a deeper chemical knowledge for the low temperature oxidation and thermal cracking stages of the ISC process, which would improve the performance of simulation tools [4, 11], the understanding of possible environmental consequences of its application and enhance the probability of success of new ISC projects.

1.2. Objective

To develop a reaction pathway to explain the chemical transformations during in situ combustion

1.3. Specific Objectives

1. To divide the ISC process in stages according to the chemical reactions involved
2. To identify chemical species that, working as surrogates for the most important fractions in a crude oil, allow the study of the chemical processes in ISC

3. To propose the chemical reactions responsible for the transformations of the surrogates during ISC

1.4. Description of the Thesis

This document contains six chapters. The present chapter presents the introduction, motivation and objectives of this research. Chapter 2 introduces the fundamentals and background studied for the development of this thesis. The chapter defines in situ combustion and its stages. It presents a brief compilation of main reaction schemes that have been proposed for the three stage of the process. In addition, Chapter 2 introduces a definition of reaction mechanisms and types of reactions, and presents a summary of the most accepted reaction mechanisms formulated for low temperature oxidation and thermal cracking processes of hydrocarbon molecules. The use of computational chemistry tools was fundamental to conduct this research, and therefore to describe the current state of the use of these tools was mandatory. Because this is the first research in ISC that takes advantage of computational chemistry calculations, Chapter 2 describes briefly the present usage of this kind of tools to study other processes that involve hydrocarbons chemistry.

Chapter 3 explains the methodology developed to conduct this research. That applied mechanistic-study methodologies to ISC to develop reaction pathways to explain, in detail, the complex chemical evolution of crude oil fractions. Three main parts could be identified in the methodology. The first one that was based on a literature review, which allowed to select surrogates, products and reactions. The second part involved the computational methodology employed, calculations procedures and analysis of obtained results. The third part associated the methodology to formulate the reaction pathways.

Results are presented in three chapters. Chapter 4 introduces the surrogate selection and ISC chemical division processes. Regarding to surrogate selection, the aspects and features identified to describe SARA fractions of a crude oil and the structures and characteristics of the selected surrogates are presented. Related to the ISC chemical division process, the way in this thesis divided the stages of ISC into events is explained. Chapter 5 describes the development of low temperature oxidation pathways. It begins presenting a methodology diagram that explains the specific procedure to formulate LTO reaction pathways. Next, compound structures, summary tables and reaction schemes are presented. Finally, specific conclusions from the mentioned section are presented. In the same way as in the LTO case, Chapter 6 explains the development of thermal cracking pathways.

Chapter 7 presents the overall conclusions from this research and the future work derived from this research. Finally, an Appendix that contains extended reaction schemes of the proposed reaction pathways is presented. The reaction schemes describe the chemical routes followed by hydrocarbon

species with the related reaction energies.

Chapter 2

Fundamentals and Background

This section presents a description of the main concepts and research advances taken into account to develop this thesis. It introduces the ISC concept focused on the main aspects related to the chemistry involved in the process. The reaction schemes that have been developed for ISC are described. In addition, definitions for reactions and reaction mechanisms are presented, as well as a summary of the most accepted reaction mechanisms formulated for low temperature oxidation and thermal cracking. Finally, a brief background of the use of computational chemistry for modeling analogous processes that involve hydrocarbon molecules is presented.

2.1. In Situ Combustion (ISC)

In Situ Combustion (ISC) is an Enhanced Oil Recovery (EOR) technique designed to increase the recovery factor of heavy oils [1, 4, 44]. This technique has a large theoretical efficiency compared to other processes such as steam injection [1, 6] currently the most employed Enhanced Oil Recovery method [1, 45]. Only some drawbacks have been associated with the performance of this technique, such as: possible contamination of ground water sources or difficulties for controlling the combustion front, which could affect areas in the surroundings of reservoirs.

ISC is a thermal oil recovery technique that bases its operation on important physical-chemical phenomena [1, 4, 6, 46]. While some of those phenomena are well-known by the petroleum industry, particularly those associated with the flow through porous media, the chemical processes in ISC have not been largely explored or described, although they provide key information for a better understanding of the extraction process [11, 39]. Currently, however, some author's discussions focus on the question if it is better to describe this oil recovery technique as a thermal recovery method without emphasizing in the chemistry of the process or if it is critical to include a rigorous explanation about it [47, 48]. Those in the side to improve the chemical knowledge argue that a deeper chemical knowledge of the

ISC process would improve the performance of simulation tools [11] and the understanding of possible environmental consequences of the application of this technique to a reservoir.

ISC refers to the burning of fuel inside the reservoir [49] and is frequently associated with air injection in heavy oil reservoirs. During the process of oil recovery, air or oxygen enriched gas is injected into the reservoir; the reactive contact between the oil and gas produces heat which ignites the oil around and allows the formation of a combustion front [1, 6, 50]. Combustion reactions propagate along the reservoir facilitating the recovery of the unburned crude by a decrease in its viscosity [1,2]. The support of the combustion front is the formation of a carbon-rich residue, coke, that has been amply studied because it constitutes a typical product in any kind of process that involves crude oil, specially when it is being refined [51]. In the ISC case coke is the fuel for the process. Without coke formation, ISC is not sustainable [50]. Contrary in a refinery, coke formation constitutes a drawback that challenge the petroleum industry. It affects equipments performance in a negative form, it obstructs flow zones and deactivate catalysts, among others drawbacks associated to its production.

Figure 2.1 a) presents a diagram to explain ISC process, while Figure 2.1 b) shows the temperature profile of ISC zones related to the distance from the injection well in the reservoir. At the beginning of the process air is compressed and pumped into the reservoir in the injection well. The first zone is called upstream region. The combustion front previously moved through that region leaving a burned zone that, in theory, should not contain any remaining crude. In that section of the reservoir only heat transfer is relevant. The combustion zone is located downstream of the «upstream» region. Ideally, all oxygen is consumed in this zone. The reactive contact between oxygen and oil releases a large amount of energy in form of heat; therefore, this zone registers the maximum temperature, which is according to the fact that it provides the heat to the other zones of the process. The combustion zone separates the above mentioned upstream region to the downstream region, which is called the cracking-evaporating region. In the downstream region, the lack of oxygen combined with high temperatures promote the evaporation of light compounds and the cracking of heavy compounds producing lighter species and coke. Vaporized components and combustion gases follow in their way inside the reservoir. Eventually, those gases arrive to the oil bank, which is the place where the cold crude is immobile. That contact causes a heat transfer phenomenon that leads to gas condensation and an increase in the oil bank temperature that produces a reduction in the viscosity and enhances the mobility of the oil [1, 2, 6, 8]. The temperature maintains an almost constant value through this region.

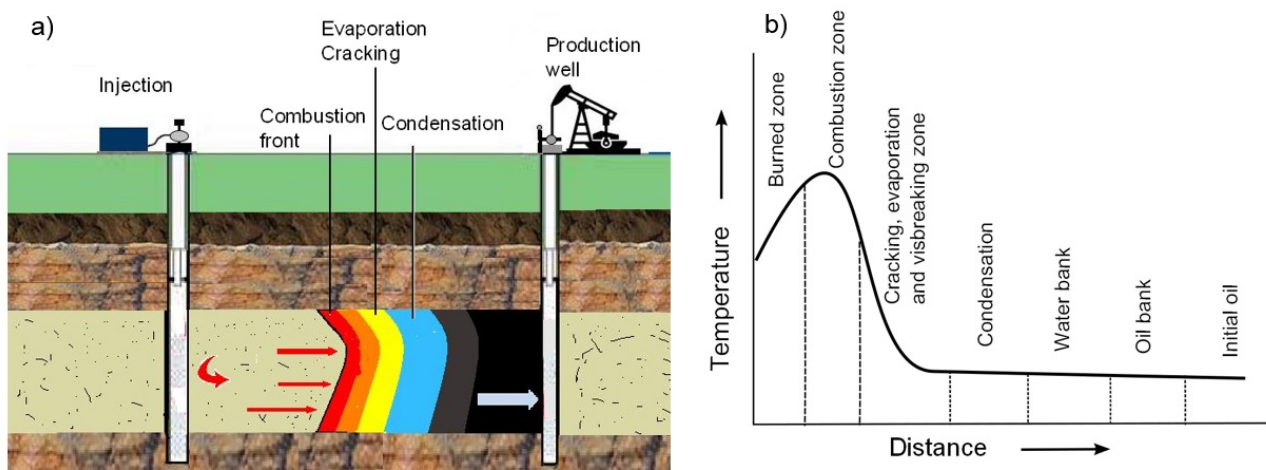


Figure 2.1: a) Scheme of the main phenomena involved in ISC. b) Temperature profile of ISC zones [1,2]

The chemistry related to the ISC process is one of the main difficulties associated to this technique. Most of the reaction schemes in the literature [6–8, 50, 52–56] have a modular structure. Focused on the chemistry of this process, several authors [4, 6–8, 50, 52–56] have proposed two types of reactions as responsible of the ISC chemical evolution: thermal cracking and oxidation. These reactions take place in two temperature ranges, up to and over 300°C . Taking this into account, ISC has been traditionally divided in three stages: low temperature oxidation, thermal cracking and high temperature oxidation [4, 6–8, 48]. The first two give rise to the formation of coke that reacts in the third stage to release energy in the form of heat. Other authors [1, 52, 57] have named these reactions in other ways such as: medium temperature reactions, fuel formation reactions or oil-mobilizing bond scission reactions. Given the complexity of crude oil, and thus the knowledge of its composition, all functional reaction models have been supported by the concept of pseudocomponents as starting point. Initial models [58] divided crude oil in two fractions: light and heavy oil. Other models have worked with a pseudocomponent formulation that includes maltenes, asphaltenes, coke and gases [1, 6, 8, 59, 60]. This approach has been preferred by some authors [8, 57] that consider a thorough chemical explanation of ISC as secondary. Contrary to this position that simplifies chemistry, recent studies [7, 13, 50, 55, 56] that aimed to obtain a better understanding of the ISC chemistry, proposed mechanisms with a higher number of pseudocomponents. In this case the authors have used complex groups of pseudocomponents such as Saturates, Aromatics, Resins, Asphaltenes (SARA fractions) and Coke. Moreover, they have included new fractions such as HMWG (high molecular weight gas) and some real compounds highly important in ISC such as carbon monoxide (CO), carbon dioxide (CO_2), methane (CH_4) [7].

2.1.1. Thermal cracking reactions

Thermal cracking reactions have been the most studied type of reactions involved in ISC. These reactions are commonly called Cracking reactions, but they have been named as Bond scission reactions, Medium temperature reactions, Pyrolysis reactions or fuel formation reactions [1].

Two different approaches have been employed to study these reactions. The chemical approach have identified three main characteristics for thermal cracking reactions. They occur mainly in gas phase (homogeneous reactions), require great amounts of energy to happen (endothermic reactions) and usually involve three types of process: dehydrogenation, cracking (bond rupture) and condensation [1]. In a dehydrogenation process, only hydrogen atoms are affected, they are removed from the molecule while carbon atoms are untouched [1]. During a cracking process, only the carbon-carbon bonds of the heavier molecules are broken, which results in a formation of hydrocarbon molecules with lower carbon number [1]. On the other hand, in condensation processes the number of carbon atoms in the molecules increases, which allows to obtain heavier hydrocarbons [1]. In conclusion, in a common process, short chain hydrocarbons undergo dehydrogenation and the larger molecules undergo cracking; therefore, it is possible to say that this process tends to establish a balance in the number of carbon atoms in the molecules [1,52]. Finally, those dehydrogenated molecules with a medium size recombine to form heavier molecules that after a prolonged heating or when the temperature is so high produce coke and volatile hydrocarbon fractions [1,6,52]. Some authors [55] have tried to explain with more detail these processes that involves radical formation; however, the proposed mechanisms for ISC do not offer rigorous chemical explanations.

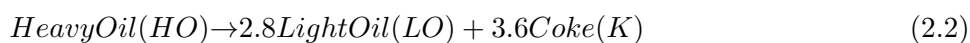
The previous description is one of the most accepted nowadays; however, other authors [52] have proposed a physical approach to study thermal cracking reactions. These works study and describe the reaction process from the physical phenomena involved in thermal cracking. From this approach, these reactions are seen as visbreaking reactions, term that refers to the changes in the viscosity of crude oil, due to the molecules cracking and it is commonly used in the petroleum industry [52].

Most of the reaction schemes proposed to explain ISC chemistry have been formulated based on experimental procedures [7,8,50,54–56]. The experiments carried out for mechanism formulation are usually tests where crude oil is heated under specific conditions of temperature and pressure. The process is controlled to determine in different times the advanced of the reaction by measuring the sample and products composition. Given that the presence of oxygen determine the nature of the reactions, the test environment is also controlled. Finally, by an analysis of sample evolution, reaction schemes that involve products and kinetic data for these reactions are formulated [7,8,50,53–56,59]. Reaction 2.1 [6] is the most simple chemical equation used to represent a thermal cracking reaction,

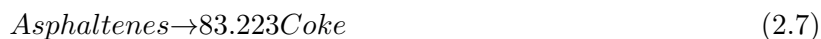
where coke ($C\downarrow$) and hydrogen are produced by the cracking of a hydrocarbon chain in liquid phase.



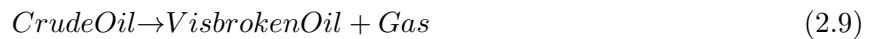
Reaction 2.2 [58] uses the most simple fractions of a crude, heavy and light oil, to explain the thermal cracking process. According to the reaction the cracking of heavy oil produces lighter compounds and coke. Stoichiometric coefficients presented in this and other models present below were determined by mass balance closure in experimental setups. This model raises that thermal cracking of a heavy oil mol produces 2.8 moles of light oil and 3.6 moles of coke.



Reactions 2.3 to 2.5 [59] constitute the first set of thermal cracking reactions schemes proposed, which some years later was modified by establishing their stoichiometric coefficients, giving raise to the formation of a new group integrated by reactions 2.6 to 2.8 [8]. This advance was an important input because stoichiometric coefficients represent mass balance and the coherence between reactants and products that are fundamental to employ simulation tools. Reactions 2.6 to 2.8 represent, nowadays, the most used model by those who prefer simple descriptions of ISC chemistry.

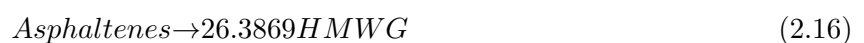


Other undetailed model is the one integrated by reactions 2.9 to 2.10 [52]. In this case the approach that takes into account visbreaking is involved. This model and some of the reactions presented above have in common the presence of the pseudocomponent named as gas. This pseudocomponent is commonly used by undetailed models to group several type of gases, whereas more detailed models attempt to extend the amount of specific chemical species related to this pseudocomponent.

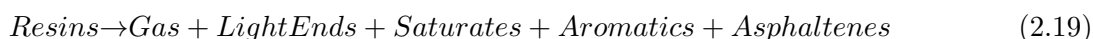


Some authors [54, 61] have built reactions pathways for explaining, among others, processes such as coke formation. Banerjee et al. [54] proposed a reaction pathway to explain coke formation that involves a higher variety of pseudocomponents. In this case, saturates were divided into paraffins and naphthenes, and other pseudocomponents that have not been largely explored like olefins and cycloolefins were used as well. This study also presented pseudocomponents defined by the authors such as lower hydrocarbons, large and small aromatics.

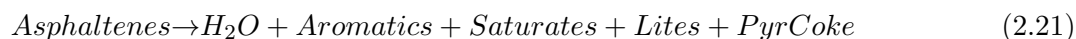
Reactions 2.6 and 2.7 [8] make part of an improved model that transforms 2.8 into six new reactions, reactions from 2.11 to 2.16 [7]. This reaction scheme attempted to get a better understanding, by being more specific about the chemical species grouped by the pseudocomponent gas. It involves real compounds such as hydrogen (H_2), carbon monoxide (CO), carbon dioxide (CO_2), methane (CH_4), high molecular weight gas ($HMWG$) and sulphydric acid (H_2S).



Given the widespread use of SARA fractions in research applied to the petroleum industry, the most recent reaction models [55] proposed for ISC take SARA fractions as reactants. The model proposed by Freitag and Exelby [55] is integrated by four reactions (2.17 to 2.20). It involves SARA fractions and pseudocomponents such as gas and one named by the authors as light ends. Stoichiometric coefficients for this model are not presented as they were determined as dependent on the composition of the crude oil.



Finally, attempting to synthesize the reaction model by Freitag and Exelby [55], other authors [62] reduced the four reactions to three and eliminate the presence of specific pseudocomponents in some of the reactions. Reactions 2.21 to 2.23 presents the reduced model, which exclude the thermal cracking process for saturates and deeply modify the chemical equation to explain the same process for the aromatic fraction. In addition, the authors assumed that the only gas produced by this process is water vapor (H_2O). In addition, this model introduced the pseudocomponents Lites and PyrCoke. Lites groups the hydrocarbons up to four carbon atoms that at environment conditions are gases, whereas, PyrCoke is used to refer to the carbon rich residue from the pyrolysis of hydrocarbons.



2.1.2. Low temperature oxidation reactions (LTO)

Contrary to the vast amount of studies related to cracking reactions, LTO reactions have not been largely explored probably due to their high complexity [11]. The occurrence of LTO reactions is the first reactive process in ISC. Main products from this type of reactions are oxygenated compounds and coke, which are consumed in the high-temperature oxidation stage to produce combustion gas. In spite of the requirement of LTO reactions to start the ISC process, this type of reactions are not highly desirable because they consume great amounts of crude oil at high rates [1]. In the ideal case, LTO reactions only produce the portion of coke required for the formation of the combustion front, which is fed by the coke formed in the thermal cracking stage. Nevertheless, given the tortuosity of a reservoir, oxygen may travel through the porous media, avoiding the combustion front and making contact with other zones in the downstream region [1, 6]. That contact may cause the formation of oxygenated compounds that could be extracted in the production well. A case that could have serious environmental implications and that have not been largely explored [46].

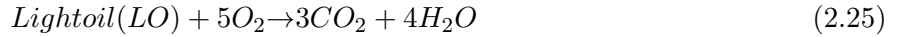
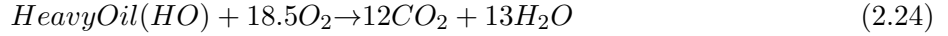
These reactions are heterogeneous (gas-liquid) and not complete combustion reactions, which means that their main products are not water and dioxide carbon (CO_2), although these species may be produced as well [1, 6, 48]. LTO reactions have been defined as oxygen-addition reactions. Their typical products are water and partially-oxygenated hydrocarbons such as carboxylic acids, aldehydes, ketones, alcohols and hydroperoxides [11, 48].

From a chemical point of view, LTO reactions have been defined as condensation reactions as during this process, low-molecular weight compounds become high-molecular weight products [1, 48]. Based on that, ISC reaction schemes propose that the low temperature oxidation of aromatic compounds produces resins that eventually form asphaltenes [8, 48, 53]. These are, clearly two opposite but complementary points of view. The first one supports the side that considers LTO reactions as inconvenient, as the content of asphaltenes grows increasing the viscosity of the crude oil, which would affect crude oil production and the technique performance [1, 4]. On the other hand, with a higher asphaltenes content, coke production would be higher, which contributes to maintain the combustion front [1]. Different authors [1, 53, 56, 63] have studied LTO effects and products based on experiments. The first proposed reactions proposed have not experienced important transformations through the last decades and are currently used. As for the thermal cracking case, researches that prefer these reactions look for undetailed models to save computational time when using simulation tools. In spite of that, other authors [13] have proposed new models that do not take into account the typical LTO reactions for ISC. New models change completely the typical vision that traditional models had.

Some of the reactions explained below are part of the reaction schemes that were explained in the

thermal-cracking-reactions section. In that case this section omits information previously given.

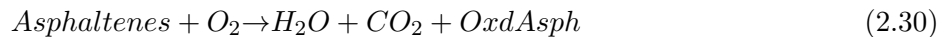
Reactions 2.24 and 2.25 [58] are one of the first proposed inputs in this research field. They describe the LTO process using the pseudocomponents Heavy and Light oil and, in spite of the low complexity of this crude oil division, this model involves real compounds such as carbon dioxide (CO_2) and water (H_2O).

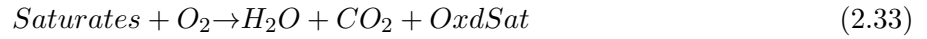
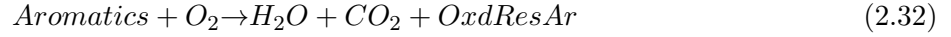


Reactions 2.26 and 2.27 [53] constitute the most important contribution in LTO reaction schemes. They are the typical LTO reactions that are currently used. Later experiments were carried out to determine the properties of these pseudocomponents and the stoichiometric coefficients for these reactions (reactions 2.28 and 2.29 [8]).



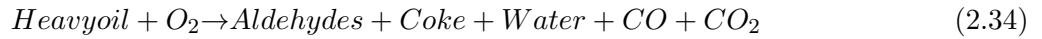
Some studies [56,62], following the objective to propose new reactions, have added other pseudocomponents and reactions to the typical LTO schemes. Reactions 2.30 and 2.33 [56] shows the only set of low temperature oxidation reactions that is based on the SARA fraction division. It is important to highlight that compounds such as carbon dioxide (CO_2) and water (H_2O) are included, which results coherent to the nature of these reactions. However, these reactions involve pseudocomponents such as, OxdAsph, OxdResAr and OxdSat, which constitute unknown species that have not been completely characterized by the authors. In addition, coke is not directly produced by these reactions, contrary to several authors [6,8,53] that identify coke as the main product from LTO reactions.





A more recent research [63] focused on developing new models taking into account intermediate species, which may be fundamental in the ISC performance. Reactions 2.34 to 2.37 [63] constitute the first reaction set that includes intermediate species and temperature subranges to explain low temperature oxidation chemistry. In the lowest temperature subrange $50 - 150^\circ\text{C}$ (reaction 2.34), heavy oil and oxygen form aldehydes, coke, water, CO and CO_2 . In the second subrange $150 - 200^\circ\text{C}$, aldehydes produced in the first subrange form alcohols, ketones and more water. Finally, in the remaining subranges $200 - 250^\circ\text{C}$ and $250 - 350^\circ\text{C}$, aldehydes and oxygen combine with ketones and alcohols, respectively. Those reactions produce hydroperoxides, carboxylic acids, ketones and water.

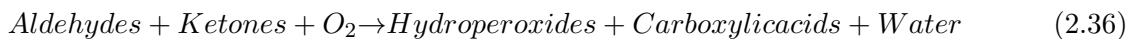
Subrange 1: $50 - 150^\circ\text{C}$



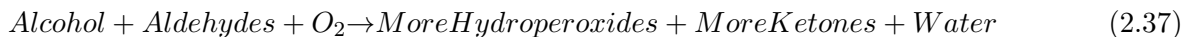
Subrange 2: $150 - 200^\circ\text{C}$



Subrange 3: $200 - 250^\circ\text{C}$



Subrange 4: $250 - 350^\circ\text{C}$

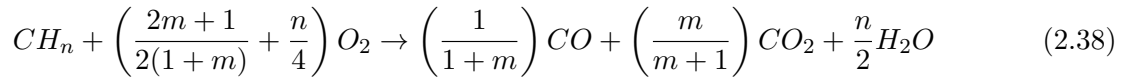


2.1.3. High temperature oxidation reactions (HTO)

High temperature oxidation reactions have been amply studied. Several reaction schemes and extended reaction mechanisms [40, 42] have been proposed for the combustion of coal. Although coke and coal are not the same, they share structural and chemical characteristics as carbon-rich materials.

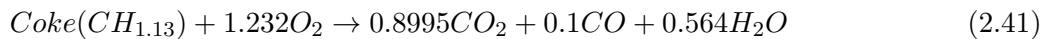
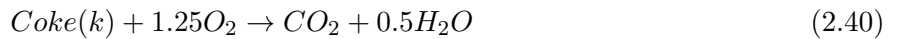
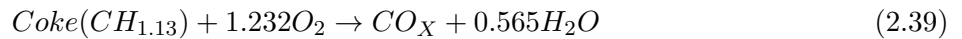
Most of the models proposed to explain the chemistry of HTO during ISC assume coke and oxygen as reactants. According to their nature, these reactions have been defined as a heterogeneous reactions in a gas-solid interface where main products are carbon dioxide (CO_2), carbon monoxide (CO) and water (H_2O) [1,6,8]. They occur in the temperature range from $300^\circ C$ to $800^\circ C$ [1,8]. HTO reactions are considered as exothermic, which means that energy is released when they occur. HTO is, according to ISC, where the energy released by combustion reactions reduces the viscosity of the crude to allow its extraction [1, 8].

HTO reactions keep a stoichiometric relation giving by the chemical equation 2.38. In this expression n is the atomic ratio of hydrogen to carbon and m is the mole percent ratio of produced CO_2 to CO that in the case of a complete combustion becomes zero [6].



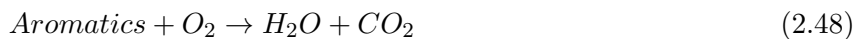
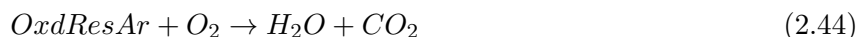
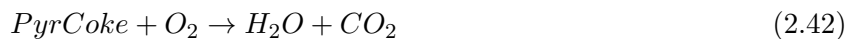
Given the heterogeneous nature of HTO reactions, several phenomena occur at the same time. Combustion is a surface-controlled reaction that may be divided in five processes. 1. Diffusion of oxygen from the bulk gas stream to the fuel surface. 2. Adsorption of the oxygen at the surface. 3. Chemical reaction. 4. Desorption of the combustion products. 5. Diffusion of the products away from the surface and into bulk gas stream [1]. The identification of the phenomenon responsible for the control over the process velocity is currently a controversial topic; however, diffusion and reaction steps have been identified as the most likely ones as they tend to be the slowest processes [1,6].

The conventional reaction schemes [8, 58] formulated to explain HTO chemistry have typically used a coke consumption reaction, which is represented by the reactions 2.39, 2.40 and 2.41. Reaction 2.39 introduces the pseudocomponent CO_X that was proposed by the author as a way for grouping the compounds CO and CO_2 .



Later models [50,62] that use SARA fractions as reactants indicate that seven reactions (reactions 2.42 to 2.48 [50]) occur at the conditions: presence of oxygen and temperatures in the range of $300^\circ C$ to $800^\circ C$). Although, most [6,8,58] reaction models for ISC assume that during the LTO stage all crude oil is transformed into heavier compounds and coke, leading them as the reactants in the HTO stage,

this model takes into account reactants such as, oxygenated compounds and hydrocarbons. All of the proposed reactions produce water (H_2O) and carbon dioxide (CO_2), i.e. complete combustion is assumed.



2.2. Reactions and reaction mechanism

Reactions are generally classified as two types: elementary and overall reactions [17]. An elementary reaction is defined as the one that occurs on a molecular level and it is represented exactly in the way it is described by the reaction equation [64]. An elementary reaction comes directly from a collision process; therefore, only one transition state is involved [64]. In addition, there are three kinds of elementary reactions: unimolecular, bimolecular and trimolecular, which is determined by the number of reactants involved in the reaction process [15, 64]. On the other hand, overall reaction is a group of many elementary reactions with a higher complexity [64]. Most of the reaction schemes presented in the last section explain ISC process based on elementary reactions; however, all ISC stages involve complex chemical processes where a great amount of reactions and final and intermediate species are involved.

Radical chain-reaction is an important concept in combustion reactions, all of these reactions imply the formation of intermediates or radical intermediates that produce other intermediates compounds

in following steps of the process [9, 15, 64]. In general, radical-chain reaction has four steps: initiation, propagation, branching and termination [64], all of them with specific purposes in order to achieve a final product. From a macroscopic point of view, the overall radical concentration is determined by a balance between initiation and termination reactions attempting to reduce the complexity in the process analysis [17], which is common when crude oil or other complex substances are involved.

A reaction mechanism is a group of reactions, elementary and/or overall reactions, which explains or represents the steps or stages that one or some reactants follow in a chemical process [64]. The design of a reaction mechanism is still a black art with majority being constructed with intuition and rules of thumb [17, 64]. Combustion chemistry is a science of cases, most of the things have been studied for some particular cases. Therefore, the use of analogies to develop better explanations for other cases is common and necessary [64].

Chemical transformations that hydrocarbon molecules undergo in several type of processes may be very different. Extended mechanisms for the thermal cracking or LTO processes involve thousands of species and reactions. Numerous researches [9] have studied in detail the chemistry of these processes and attempted to obtain a global description vision by the identification of *reaction pathways*, which are the different reaction routes that a compound may follow in a process. The identification of reaction pathways in a complex reactive process provides critical information about reactants, products, reaction probabilities, kinetic, etc.

2.2.1. Thermal-cracking reaction mechanisms for hydrocarbons

Several authors [21–37, 65] have studied the chemistry of processes that involve the thermal cracking of hydrocarbon molecules. Detail and extended mechanisms have been proposed for the thermal cracking hydrocarbon molecules from C_1 to C_{12} [22–30, 32, 33, 35–37, 65]. Those studies have determined that the chemical evolution of molecules in this process proceeds by the formation of free radicals, which implies that breaking of bonds is homolytic [35, 66, 67]. Three main stages have been identified in this process: initiation, propagation and termination.

- Initiation Stage [22–27, 29, 30, 32, 33, 35–37, 65]: it is usually called activation stage. During its occurrence three types of reactions take place, $C - C$ Cleavage, $C - H$ Cleavage and Reverse Radical Disproportionation (RRD). Initiation reactions have as reactants hydrocarbon molecules without dangling bonds, which undergo breaking in bonds or atom transfers in order to produce free-radical species. The final result of this stage is to produce active species that lead to the formation of new compounds. The energetic nature of this type of reactions is always endothermic, as it constantly occurs with reactions where bonds are broken or where the energetic level

of species is increased.

- Propagation Stage [22–27, 29, 30, 32, 33, 35–37, 65]: in this stage free radicals from initiation stage undergo reactions such as intermolecular and intramolecular H-abstraction, β -scission and isomerization. Reactants in this stage follow two types of routes: to a lower or to a higher energetic level. The energetic nature of the reactions involved determines the type of process that reactants experience. β -scission as endothermic reactions, produces species with higher energetic levels, whereas H-abstraction and isomerization reactions could be classified as endothermic as well as exothermic. The products from this stage are free radicals.
- Termination Stage [22–27, 29, 30, 32, 33, 35–37, 65]: during this stage evolved radicals from the propagation stage undergo reactions such as intermolecular and intramolecular addition and disproportionation. The overall outcome of this stage is the transformation of free radicals into molecules without dangling bonds by atom transfers and formation of new bonds. The energetic nature of these reactions is always exothermic because reactants have a higher energy level compared to products.

The effect of temperature and pressure conditions in these reactions have been analyzed. Some studies [22, 23, 27, 29, 30, 32, 33, 65] have determined that a temperature increase favors the occurrence of unimolecular reactions, whereas an increase in pressure intensifies the occurrence of bimolecular reactions. Most of the accepted mechanisms [21–37, 65] suggest that at least twelve reactions occur during thermal cracking of hydrocarbons.

- $C - C$ Cleavage: it has been classified as an unimolecular initiation reaction. Its reactants are hydrocarbon molecules without dangling bonds, whereas its products are free radicals, which constitute active species that lead to the formation of new molecules. By the addition of heat to the molecular system its energy increases, which causes $C - C$ bonds to break producing two dangling bonds. In two atoms that make part of one or two different molecules, which are called free radicals. the stability of free radicals depends on the bonds of the atoms that host dangling bonds. An atom with a dangling bond that is bonded to other three carbon atoms is classified as a tertiary free radical, whereas a host bonded to two C atoms is named as secondary and so on. Free radical stability decreases with a decreasing in its order, i.e. the number of carbon atoms bonded to the host, i.e. tertiary is the most stable followed by secondary and finalizing with primary.
- $C - H$ Cleavage: as in the $C - C$ cleavage case, this reaction has been classified as unimolecular initiation reaction. Its products are two free radicals and one of them is always a hydrogen free

radical, considered as the least stable free radical, because the hydrogen atom does not have electronic structural characteristics or bonds with other atoms in order to stabilize. Given that it involves the production of hydrogen-free radicals, this reaction usually requires higher energies to occur compared to $C - C$ breaking.

- Reverse Radical Disproportionation (RRD): it is a bimolecular initiation reaction with two unsaturated molecules as reactants. The presence of double or aromatic bonds implies an accumulation of electrons in determined zones of olefins and aromatic molecules. Although, those sites are not free radicals, the mentioned accumulation gives to those zones a reactive character that leads to a chemical interaction when those molecules make contact. In this process two types of species are identified, hydrogen donor and hydrogen acceptor. Donor species permits the abstraction of a hydrogen atom by the acceptor molecule. After this process, the donor molecule keeps the unsaturated bond or bonds and obtains a dangling bond. In the case of the acceptor molecule, it acquires a hydrogen atom that connects to an atom in an unsaturated bond, which produces a species with one dangling bond. The products from this reaction are two free radicals. One of them is usually stabilized by resonance from an unsaturated bond in the surroundings.
- Intermolecular H-abstraction: it has been classified as a bimolecular propagation reaction. Reactants are a hydrocarbon molecule without dangling bonds and a free radical. By the contact between the reactant species, the free radical abstracts a hydrogen atom from the hydrocarbon molecule, which forms two new species, a different hydrocarbon molecule without dangling bonds and a free radical. This reaction is exothermic if the new free radical produced has a higher order than the starting one. Some authors [21,22,28,34–37] affirm that these reactions only occur when the abstracting free radical has up to four carbon atoms, they established that, in the case of longer hydrocarbon chains, steric hindrance becomes an important factor.
- Intramolecular H-abstraction: as in the intermolecular H-abstraction case, this reaction consists in the transference of a hydrogen atom. In this case an atom with a dangling bond abstracts a hydrogen atom bonded to other atom in the same molecule. This reaction has been classified as propagation and termination reaction, depending on the nature of the final product. With a free radical as product, the reaction is considered as propagation, whereas if it produces a hydrocarbon species without dangling bonds the reaction is considered as termination. The last case is possible only when the free radical molecule is a biradical, i.e. it is produced by the breaking of a bond that makes part of a cycle. In the mentioned case, the product from this reaction is an olefin. This reaction has been considered as a particular case of isomerization reactions, because the molecule involved preserve all of its atoms and the only change occurs in

their arrangement.

- β -scission: the presence of a dangling bond in an molecule affects its geometric and electronic arrangements; however, a specific weakening effect has been identified in the bonds in β positions. This effect enables the breaking of a $C-C$ or $C-H$ bond in a free radical compound, producing an olefin and a free radical. This type of reactions has been largely studied, because they are considered as main responsible of ethylene ($CH_2 = CH_2$) production in several processes. As unimolecular reactions their occurrence increases with an increment in the process temperature. Their energetic nature is exothermic; however, their exothermicity level depends on the products and the type of bond broken. The rupture of a $C-H$ bond requires higher energy than a $C-C$ breaking, because the first case produces a hydrogen-free radical.
- Isomerization: they are characteristic of the propagation stage of a thermal cracking processes and have as reactants free radicals produced in the initiation stage. By an isomerization reaction one molecule is transformed in other one that contains the same atoms with a different rearrangement. Structural modifications induced by this type of reactions change the energy of free radical molecules. The energetic nature of isomerization reactions depends on the stability of the new free radical produced: if it is more stable than the reactants the transformation releases heat. The most studied case of these reactions is the one where a hydrogen atom is transferred from one carbon atom to another. Some authors [21, 22, 28, 34–36] have established that at least two carbon atoms must separate the donor and acceptor atoms, to give rise to the formation of a cyclic transition state with at least five members.
- Intermolecular addition: they constitute the most important reactions in the termination stage of a thermal cracking process. Their reactants are two free radicals that form a new bond producing a larger molecule. This transformation is exothermic because two free radicals with high energy produce a hydrocarbon molecule without dangling bonds, i.e. with lower energy level. This type of reactions is the main responsible for the growth of species. Given the constant addition of heat during a thermal cracking process, compounds produced by these reactions tend to suffer subsequent activation processes by bond breaking. The ruptures may occur in the bond formed or in any other bond. The energy released by bond formation is equal to the amount of energy required to carry out a breaking, a higher exothermicity in these reactions implies a higher probability for the new bond to stay without disturbance.

There is a specific case of intermolecular addition reactions that is not considered as a termination stage transformation. In which reactants are an olefin and a free radical. During this process, a new bond is formed between the atom with a dangling bond in the free radical and one of the

atoms in the unsaturated bond in the olefin; this interaction leads to the formation of a larger free radical. Although this reaction produces a radical species, its energetic nature is exothermic. This reaction have been seen as the contrary transformation to the β -scission reactions.

- **Intramolecular addition or cyclization:** there are two main cases for the formation of a cyclic molecule in a thermal cracking process. In the case of the intramolecular addition reaction the reactant is a biradical species. It is generally produced by breaking of a bond in a cyclic molecule, which leads to the formation of a molecule with two dangling bonds in different atoms. Eventually, with the energy increment and the constant molecular vibrations, the two unsaturated atoms meet and form a new bond producing a cyclic molecule. In the second case, the reactant molecule must contain one unsaturated bond and a dangling bond into two different atoms. As in the intramolecular case, the increasing energy of this molecule allows the formation of a bond producing a cyclic compound, with radical nature. Given the production of radical species, this type of reaction is considered as propagation.
- **Disproportion:** they are of common occurrence in the termination stage of a thermal cracking process and have as reactants two free radicals. As in other reaction cases previously explained, two types of compounds are distinguished in this reaction: donor and acceptor, both of them are free radicals. During this process the acceptor radical abstracts a hydrogen atom from the donor. It transforms the acceptor compound in a molecule without dangling bonds and the donor into an olefin, because, the hydrogen abstraction takes place in an atom that is located by the dangling donor bond. Given the formation of species with out dangling bonds from free radicals, the energetic nature of this reaction is exothermic.
- **Diels-Alder [22]:** the occurrence of this type of reactions has been largely explored because their products are six member rings, which are compounds of fundamental importance in organic chemistry. These reactions cannot be classified as initiation, propagation or termination because free radical species are not implied in this transformation. Their reactants are species with out dangling bonds, a diene and one olefin, which combine to produce a larger cyclic compound, a cyclohexane. These reactions have been identified as unavoidable steps in the routes that explain the aromatization of alkanes.

2.2.2. Low temperature oxidation mechanisms for hydrocarbons

Several authors [9–20] have studied the chemistry of the low temperature oxidation (LTO) of hydrocarbon molecules. Detailed mechanisms have been proposed for molecules that contains up to tens of carbon atoms [9, 12, 14, 15, 37]. Normal saturates and polycyclic aromatic compounds have been the

most explored molecules, given their high content in most fuels. In the case of the polycyclic aromatic compounds, several studies [68, 69] have attempted to understand their chemical evolution during a combustion process that lead to the formation of soot, which constitutes a drawback particularly in diesel and gasoline combustion processes. Most of the authors [9, 11, 12, 14, 15, 37] have determined that a LTO process proceeds by the abstraction of hydrogen atoms from hydrocarbon molecules, which gives rise to the production of free radicals, activated species with high reactivity. Contrary to the thermal cracking process, reaction stages have not been clearly defined for LTO. However, the reactions in this process could be classified as initiation, propagation or termination, according to their reactants and products.

Six reactions have been identified as the main responsible for the chemical evolution of species during the LTO process [9, 12, 14, 15].

- Intermolecular H-abstraction: it has been recognized as the main initiation reaction during a LTO process, with hydrocarbon and O_2 molecules as reactants. The abstracting molecule, which is also called oxidizing agent, is generally oxygen (O_2). However, other oxidizing agents such as $\bullet OH$ and $HO_2\bullet$ may carry out the abstraction process. Actually, the presence of $\bullet OH$ radicals increases dramatically the oxidation rate in this process, because an H-abstraction reaction by this molecule produces water, a compound with high stability, which is a final product in an oxidation process. This reaction is the main responsible for the formation of $\bullet R$ free radicals, which constitute key compounds in the evolution of an oxidation process due to the electrophilic character of oxidizing agents, which means that they constantly look for sites with high-electron density or electron availability. The energetic nature of this reaction is highly dependent on its reactants, an initiation process by O_2 is usually endothermic, whereas one with $\bullet OH$ as abstracting compound is usually exothermic.
- Intramolecular H-abstraction: during the chemical evolution of species in a LTO process, it is common to find $ROO\bullet$ radicals. The presence of an $O - O$ bond and the radical nature of one of those oxygen atoms allow to this type of radicals to undergo internal H-abstraction reaction. The abstraction of a hydrogen atom from one molecule site to the radical oxygen atom, favors the formation of a hydroperoxide molecule that contains a dangling bond in one of its carbon atoms, i.e. a $\bullet QOOH$ radical. The presence of this type of radicals has been identified as a requirement for the formation of cyclic ethers. The reaction energies for these transformations are highly dependent on the reactants and the order of the produced radicals.
- β -scission: these reactions and their characteristics were previously described in the section that explained thermal cracking reaction mechanisms. Given the low-temperature range of this

process, the occurrence of β -scission reactions is not common. Some studies, however, have identified them as the only route that conducts to the formation of lighter hydrocarbons during an oxidation process. This transformation has two important molecules as products, one olefin and a $\bullet R$ radical. As it was previously explained, $\bullet R$ radicals are key compounds in the development of an oxidation process, as high reactive species. In addition, the presence of an double bond in an olefin constitutes a particular oxidation case. These molecules present some particularities in their oxidation process, such as the possibility of being activated by intermolecular addition reactions and the formation of radicals stabilized by resonance, which seriously affect oxidation rates. The energetic nature of these reactions is always endothermic.

- Intermolecular addition: this type of chemical transformation could be classified as propagation or termination reaction during an oxidation process. When the addition takes place between two radical species, such as two $\bullet R$ radicals, the product is a heavier hydrocarbon and the reaction is considered as a termination. This type of intermolecular addition is always an exothermic reaction. On the other hand, with $\bullet R$ radical and O_2 molecules as reactants, as it is usually the case in an oxidation process, a hydroperoxyl radical is the product. Indeed, given the production of radical species the reaction is classified as a propagation one. The addition of $\bullet R$ radical and O_2 molecules is considered as the first step in the route for the production of oxygenated compounds. The produced $ROO\bullet$ radical may proceed by two routes in order to obtain a hydrogen atom to saturate its dangling bond: abstract it from other compounds such as a hydrocarbon molecule or a $HO_2\bullet$ radical or obtain it from its own structure. The registered energies for these reactions are generally exothermic.
- Intramolecular addition: as in the intermolecular addition case, this reaction may be classified as a propagation or termination one. Reactants for this transformation could be $RO\bullet$ or $\bullet QOOH$ radicals. In the case of the $RO\bullet$ radical, the oxygen with the dangling bond forms a new bond with the same carbon atom, which leads to the formation of a $C = O$ bond and the cleavage of one of the previous $C - C$ or $C - H$ bonds. Depending on the type of bonds of the affected carbon atom and the one that undergoes breaking, this reaction may produce ketones or aldehydes. In the case for $\bullet QOOH$ radical, the oxygen atom bonded to the Q chain forms a new bond with the dangling bond in the molecular structure leading to the formation of a cyclic ether and an $\bullet OH$ radical.
- $O - O$ Cleavage: this chemical transformation is one of the most common reactions in an oxidation process and is defined as initiation. Although reactants are not hydrocarbon molecules, this reaction transforms peroxide molecules $ROOH$ or $ROOR$ into $RO\bullet$ and $\bullet OH$ radicals, its main

result is to produce activated species as the reactions in the initiation stage of a reactive process always do. The $O - O$ bond is one of the weakest in the organic chemistry, its bond dissociation energy is much lower than the one associated to $C - C$, $C - H$ or $C - O$ bonds. Taking this into account, hydroperoxide molecules are considered as less stable than other oxidation products such as ethers and alcohols. In the case of the oxidation processes with O_2 as oxidizing agent, these reactions constitute the only option for the production of $\bullet OH$ radicals that become new oxidizing agents with important implications in reaction rates. The energetic nature of these reactions is always endothermic.

Table 2.1 presents the types of free radicals produced in a LTO process, the reactions from which they originate and the reaction routes that they follow.

Table 2.1: LTO free radicals, production reactions and reaction routes

Free radical	Production reactions	Reaction routes
$\bullet R$	H-abstraction or β -scission	β -scission, Intermolecular H-abstraction or Intermolecular addition of O_2 or $\bullet R$
$ROO\bullet$	Intermolecular addition of O_2	Intramolecular H-abstraction or Intermolecular H-abstraction
$RO\bullet$	O-O Cleavage	Intramolecular addition, Intermolecular addition of $\bullet R$ or Intermolecular H-abstraction
$\bullet QOOH$	Intramolecular H-abstraction	Intramolecular addition or Intermolecular addition of O_2 or $\bullet OH$
$HOOQOO\bullet$	Intermolecular addition of O_2	Intramolecular H-abstraction or Intermolecular H-abstraction
$\bullet U(OOH)_2$	Intramolecular H-abstraction	Intramolecular addition or Intermolecular addition of O_2 or $\bullet OH$
$\bullet OH$	O-O Cleavage	Intermolecular H-abstraction Intermolecular addition
$HO_2\bullet$	Intermolecular H-abstraction	Intermolecular H-abstraction

Clearly, in a LTO process different reaction routes may be followed by several compounds. Some

authors [9, 12, 14, 15] have developed reaction schemes that explain in detail, species and reactions involved in the low-temperature oxidation of hydrocarbon molecules. Those studies [9, 12, 14, 15] explain generalities, reaction pathways and kinetic data for the chemical evolution of many types of compounds: saturates, aromatics, olefins, among others. Battin-Leclerc [9] applied LTO reaction pathways to complex hydrocarbon mixtures such as gasoline and diesel.

2.3. Computational chemistry to model hydrocarbon species

Quantum chemistry is the branch of chemistry that bases its fundamentals in quantum mechanics. Quantum mechanics is a branch of physics, which proposes that the solution of the *Schrödinger* equation is a wavefunction (Ψ) may be obtained, allowing to calculate important information related to molecular systems [70, 71]. Unfortunately, it has been established that it is not viable to solve this equation, except in the case of small molecular systems [71, 72]. Taking this into consideration, different of approximations have been proposed to consider the information that could be obtained through Ψ , such as semi-empirical, *ab initio* and Density Functional Theory (DFT). Those have been implemented in a variety of computational packages.

Semi-empirical methods adopt correlations and parameters obtained from experimental data in order to facilitate calculation processes [70, 71]. They provide reasonable qualitative descriptions of molecular systems [71] with low computational cost requirements. On the other hand, *ab initio* methods base calculations only in quantum mechanics laws with mathematically-tested approximations [71, 72], which provides high quality quantitative predictions that require higher computational costs [71].

Density Functional Theory (DFT) explains the electronic states of atoms and molecules in terms of the three-dimensional electronic density of the system [71]. It constitutes a great simplification in wavefunction theory, which consists on 3N-dimensional antisymmetric wavefunction for a system with N electrons [71, 73]. Based on this, it is possible to affirm the important advantage of working with this method that does not calculate the wavefunction, since it uses the electronic density, which is a physical observable property of the compounds. The most-employed functionals are called generalized-gradient approximations (GGAs), including *BP86*, where *B* denotes Becke's 1988 exchange functional and *P86* denotes Perdew's 1986 correlation functional; *BLYP*, where *LYP* denotes Lee-Yang-Parr correlation functional; *PW91*, from Perdew and Wang in 1991 [71]. The most popular hybrid functional particularly for hydrocarbon molecules is *B3LYP*, which couples Beckes three-parameter exchange functional (*B3*) with Lee-Yang-Parr correlation functional (*LYP*) [71–73].

DFT methods have been, so far, the most used to model hydrocarbon molecules and their reaction processes, particularly when those molecules contain more than 20 carbon atoms [74–81]. Indeed,

when the size of a molecular system increases, the computational modeling cost raises. Several studies [75, 80, 82, 83] have employed DFT methods to obtain optimized geometries, frequencies, energies, parameters that constitute key information in order to analyze reaction processes. *B3LYP* has been the most employed functional and the preferred one to obtain optimized geometries [80, 82, 83]. Many authors [75, 80, 82, 83] have used this functional employing several basis sets (4–31G, 4–31G*, 6–31G*, 6–311G**, among others) to model hydrocarbon molecules up to hundreds of carbon atoms and reactions that involve them, such as, bond cleavage, isomerization, intermolecular additions, hydrogen abstractions, etc. [75, 80, 82, 83]. The Basis Set is a mathematical representation of the molecular orbitals within a molecule [71, 74]. A larger Basis Set imposes fewer constraints on electrons and a more accurate approximation to molecular orbitals [71]. Standard basis sets for electronic structure calculations use linear combinations of Gaussian functions to form the orbitals [71]. The use of a higher basis set provides more accurate results but, it also requires higher computational costs [80]. In general, good agreement has been found between DFT calculation values and experimental data for many compounds [74–81].

In the last decade, several computational chemistry studies [75, 77–79, 81] have focused on the study of DFT methods and tested the performance of the functional *B3LYP*, by comparing its results with those by many other functionals and even other calculation methods. The *B3LYP* performance has been compared to *MP2*, *BP86*, *SVWN5*, *G3*, *MWB1K*, *MPW1K*, *B1B95*, *HF*, and recently developed functionals such as the *M06*–class [75–77]. These studies carry out strict analysis of the results provided by these functionals and methods for molecules with up to 12 carbon atoms. They have found deviations to experimental values from 2 to 10 kcal/mol on reaction energies results for many types of reactions, when using the *B3LYP* functional [75]. In addition, many authors [74–81] have defined *B3LYP* as a good functional for simulating hydrocarbon compounds when transition states and weak molecular interactions are not implied [77, 78]. Based on that and in spite of some authors [75] that consider the use of this functional as a shortcoming that lead to obtain inaccurate results, the mentioned functional is currently the most used one for modeling hydrocarbon species that contain more than 20 carbon atoms [78].

Chapter 3

Methodology

This section presents the procedure followed to propose reaction pathways for the thermal cracking and low temperature oxidation (LTO) stages of ISC.

Main studies on ISC chemistry [4, 7, 8, 39, 50, 55, 56] have proposed condensed reaction schemes based on experimental results. On the other hand, works on mechanistic studies have proposed detailed reaction mechanisms for molecules up to ten carbon atoms approximately [9, 12, 14, 15], using tools such as computational chemistry, software for automatic generation and experiments. With the overall objective of propose reaction pathways that describe the chemical transformations that a heavy crude oil undergoes during ISC, the mentioned procedures did not constitute viable options. The application of an experimental ISC methodology would not give enough information to describe the chemistry of this process in detail. On the other hand, following a mechanistic straight methodology did not constitute an option, given the large variety of species in crude oil and their sizes. Therefore, it was necessary to propose a new methodology by mixing attributes from each of these options. This methodology implied the selection of surrogates and the study of the main reaction schemes proposed for ISC and the typical reaction mechanisms proposed for thermal cracking and LTO processes. That process enabled to identify reactants and reactions in order to apply electronic structure calculations that allowed to identify the reaction routes that these compounds follow and the construction of detailed reaction schemes.

3.1. Surrogate selection

The use of pseudocomponents in research fields related to petroleum is almost mandatory. A division by pseudocomponents is a classification made on a group of compounds according to specific structural or reactive characteristics. Most of ISC studies presented before the 90s [1, 6, 8, 59, 60], used maltenes and asphaltenes as the set of pseudocomponents to present crude oil. From 2000 and beyond [7, 13, 50,

55,56], most of the authors have reported experimental studies dividing crude oil in SARA (saturates, aromatics, resins and asphaltenes) fractions. Taking this into account, this study selected SARA fractions as the group of pseudocomponents for representing crude oil and through a literature review identified the main characteristics of SARA fractions.

Dividing crude by fractions allowed the selection of surrogates, which is the first step in developing a reaction pathway. As surrogate is a real compound that represents specific structural characteristics of a crude oil fraction. Based on that and by a literature review, it was possible to identify representative species of crude oil fractions. The selection of surrogate compounds allows to describe the chemical evolution of crude oil fractions during ISC stages with real compounds one of the most important goals of this research.

In order to determine saturate and aromatic fraction surrogates, different studies [84–92] about crude oil composition were considered. Two criteria were taken into account to select a specific compound: the presence and concentration in experiments. These two characteristics and the evaluation of the most representative characteristics of SARA fractions, determined the selection of two saturated and two aromatic compounds. In the case of the resin and asphaltene fractions, it has been established that their structures are highly dependent on the specific crude oil [85], and therefore, other criteria were used to make a choice.

This thesis is part of the research program entitled «Herramientas tecnológicas para incrementar el factor de recobro de crudos pesados». It is integrated by other six graduate thesis with different theoretical and experimental approaches. This program adopted a specific crude as reference in order to assemble a global knowledge and compare the results from the different approaches. The selected crude was Castilla oil that is a heavy Colombian crude oil. Based on that, the study published by Navarro et al. [85] was the main source to determine resin and asphaltene surrogates. That study proposes resin and asphaltene structures suggested for Castilla oil, built by theoretical and experimental analysis, using characterization techniques such as Nuclear Magnetic Resonance (NMR), X-ray Diffraction (XRD) and elemental analysis.

3.2. ISC chemistry study and ISC chemical division

Most of the methodologies developed for the formulation of reaction mechanisms [9, 12, 14, 15, 37], demand previous knowledge of the reactants and products of the process. This importance stems from the fact that having start and end points is of great importance in order to trace a route to make the connection. In addition, chemical evolution of species not only depends on their chemical structures and characteristics, it is also related to process conditions, i.e. temperature, pressure and the presence of

other compounds, which condition the chemical response of any species. Based on that, by a literature review in ISC, it was possible to identify the main recognized products and environment conditions of the thermal cracking and LTO stages. Although the chemistry of the transformations during ISC process has not been described in detail, it was possible to recognize a variety of experimental studies [1,53,56,63] that characterized the different stages of the process by an analysis of their products and conditions. From this review, the division of the ISC process by thermal cracking, LTO and HTO stages was adopted. However, attempting to introduce a chemical approach to the process, some events were added to the description of the evolution in every stage. Those were determined by the exploration of the most-accepted extended reaction mechanisms proposed for hydrocarbons [9–20].

3.3. Study of typical reaction mechanisms

Connecting reactants and products, demands identification of the type of reaction routes that could be explored. Routes in the context of this research are mainly sets of reactions, that describe step by step each chemical transformation. A literature review on mechanistic studies provided the tools to identify the type of possible reactions that take place during thermal cracking and LTO.

3.3.1. Thermal cracking

The conducted study allowed to determine two facts: i) the thermal cracking process at ISC conditions proceeds by free-radical production due to homolytic breaking of bonds [35,66,67] ii) there are at least twelve different types of reactions that describe the chemical evolution of hydrocarbons during thermal cracking [21–37,65] in ISC. Unimolecular ($C-C$ and $C-H$ cleavage) and bimolecular (RRD) initiation reactions, intramolecular and intermolecular H-transfers, β -scission, isomerization, intramolecular and intermolecular addition, disproportion and Diels-Alder [22]. All of them were already described in Chapter 2.

3.3.2. Low temperature oxidation

The studies considered in the area of mechanistic studies [9–20] indicate that at ISC low temperature oxidation conditions, the oxidation process proceeds by the interaction of oxygen molecules with the sites in hydrocarbon molecules where the electronic density is higher. In most of the cases oxygen (O_2) abstracts a hydrogen atom leading to the formation of a new free radical that constitutes a reactive site. At least seven different types of reactions occur during LTO [9,12,14,15]: intermolecular and intramolecular H-abstraction, β -scission, disproportion, intermolecular addition and O-O cleavage.

3.4. Computational methodology

Quantum chemistry calculations were the main tool used to propose the reaction pathways. The calculations presented in this thesis were carried out by the use of two versions of the software *Gaussian*. *Gaussian 09, Revision D.01* [38] was provided by the Computational Modeling Group *CoMo* (<https://como.cheng.cam.ac.uk/>) in the head of Prof. Markus Kraft during a research internship performed in The University of Cambridge. *Gaussian 09, Revision B.01* [93] was provided by the Quirema research group. QUIREMA (<http://quirema-udea.wix.com/quirema>) also provided *GaussView 5.0.8* [94] as visualizer software, which was used to build molecules and visualize simulation results, such as, surfaces and optimized structures. *Gaussian* was employed to calculate molecule energies and structures, reaction energies, bond orders, atom charges, Mulliken atomic spin densities, Topological Fukui and Scans.

The use of a software for quantum chemistry calculations require the definition of the «Molecular system» and the «Model chemistry», which constitute the inputs for any computational package [71,74]. «Molecular system» groups aspects related to the particular molecule such as, geometry, charge and multiplicity [71,74]. «Model chemistry» integrates the parameters associated to the theoretical, i.e. Method and Basis set [71,74].

3.4.1. Model chemistry definition

As this thesis is, in the refereed literature, the first that applies computational chemistry tools to ISC, it was necessary to refer to the computational chemistry literature [74–81] to identify the set of theoretical parameters, the Method and the Basis Set, most applied when modelling molecules in crude oil. Several studies [74–81] reported accurate results when compared to experimental results and reasonable computational cost by the use of the DFT method with the hybrid functional and basis set *B3LYP/6 – 31 + G(d)*, respectively.

3.4.2. Geometry optimizations

The first step in a computational chemistry study requires an optimization of the molecular geometry [71,72]. This type of calculations allows to obtain a structure with the lowest energy level in close proximity to the starting structure [71,72]. The software assumes the molecule in a vacuum atmosphere at 0°C. The calculation process makes continuous changes in the molecule structure, calculating its energy until the difference in the energy values obtained from one step to the next one reaches a tolerance value.

The selected surrogates, reactants and intermediate species proposed during reaction pathways were

optimized with the method and basis set described above. The optimization calculations gives as result the energy of the obtain molecules, which allowed to calculate the reaction energies presented in this thesis. These reaction energies are the difference between products and reactants energies that provide an idea about energetic nature of reactions. However, it is important to clarify that they do not constitute reaction enthalpies. The calculation of reaction enthalpies would require the implementation of frequency calculations, which would allow to correct the energy values at the temperature of process conditions. Nevertheless, it becomes an unfeasible task due to the high computational cost that the frequencies calculations demand even for short molecular systems. The implementation of that type of calculations for large molecules, as the ones studied by this thesis, is probably impossible with the computational resources available. In spite of this, the consideration of reaction energies could be considered as a good approximation since they constitute differences between products and reactants energies.

3.4.3. Natural bond orbital (NBO) calculations

Full NBO energy calculations were carried out for the optimized structures obtained by geometry optimization calculations. NBO calculations are generally regarded as single point calculations, because no changes are done in the source structure. But, the simulation calculates energy, electron distribution, charges, bond orders, among other parameters, for the specified structure.

These calculations provided essential information to study breaking patterns, reactivity sites and electron distributions. Breaking patterns were studied for the selected surrogates by bond orders (through Wiberg Index). Bond order values gave a description of the nature of chemical bonds that allows the identification of the sites that tend to break when the molecule's energy is increases. During the development of thermal cracking and LTO pathways, bond orders were also calculated for other intermediate species in order to evaluate the state of particular bonds that undergo strengthening or weakening processes. Reactivity sites were determined by the use of atomic charges obtained by NBO calculations and the condensed Fukui function [95]. This function provides a quantitative measure of electron accumulation in specific atoms, which leads to identify the sites that tend to undergo an electrophilic attack. Calculation of electron distribution provided the Mulliken Atomic Spin density. This parameter was used to identify sites with higher electron density, mainly in the cases of species with dangling bonds and aromatic character.

3.4.4. Topological Fukui calculations

During the first step of the LTO stage oxygen molecules interact with hydrocarbon species. Oxygen is an electrophilic compound, which implies that it constantly looks for regions with high electron

densities. Based on that, in order to identify the most likely places in the surrogate molecules that undergo an electrophilic attack, the electrophilic topological Fukui function was calculated [95].

The first step to calculate a Topological Fukui was to run single point calculations, modeling the optimized structures as cation and neutral systems. Next, it was important to save chk files during the *Gaussian* calculation process and converting them to fchk format [95]. The formatted files allowed, by the use of the Cubegen *Gaussian* application, to form Cube files that contained the electron density information for each molecule. These cube files were processed using the Cubeman *Gaussian* application, in order to subtract the density of the cation system from the density of the neutral one. The final result from this calculation process was a cube file that contained the difference between those densities and that was explored using *GaussView 5.0.8*. The visualizer software allowed to produce isovalue density surfaces that made evident the most likely places that can undergo an electrophilic attack.

The Topological Fukui calculation was carried out for the saturate and aromatic surrogates. In the case of resin and asphaltene molecules, the application of this methodology became unfeasible due to the great sizes of the related chk files, which makes saving them hardly possible. In addition, as it was previously explained, this type of calculations produce surface graphics, which are for analyzing molecular systems with few atoms but that in the case of molecules with hundreds of atoms as those selected to represent resin and asphaltene fractions, render the analysis impossible.

3.4.5. Condensed Fukui function calculations

Given the qualitative nature of the results provided by Topological Fukui calculations and its limitations for modeling large molecules, condensed Fukui calculations were implemented. This process allows a quantitative analysis of the reactivity of every atom in the selected surrogates.

Lu et al. [95] have studied ways to quantify the character of reactive sites by the use of the atomic population number, which is used to represent the electron density distribution around an atom. The authors [95] have expressed the Fukui function for electrophilic attack as equation 3.1 [95]. In this expression q_{N-1}^A represents the charge for an atom A when the molecular system has N-1 electrons, i.e. as cation. In the same way, q_N^A is the charge for the atom A when the molecular system is neutral, i.e. it has N electrons.

$$f_A^- = q_{N-1}^A - q_N^A \quad (3.1)$$

This equation demands the calculation of charges for every atom in the surrogates when modeled as cation and neutral molecules; therefore, full NBO calculations were carried out for the optimized

structures with charges 0 and +1. These single point calculations present a summary of the Natural Population Analysis which, among other data, provides the charges of every atom in the molecular systems, required to calculate the electrophilic Fukui function. Results from this function quantify the tendency of a specific atom to undergo electrophilic attack, the higher its value the higher the possibility [95].

3.4.6. Scans

Activation energy is the minimum amount of energy required for the occurrence of a specific reaction. Some computational and experimental procedures have been implemented for calculating this and other kinetic reaction parameters, such as frequency factor. This thesis presents activation energy graphics calculated for some specific reactions. Only few reactions were objective of these calculations, because of the computational cost that they imply. Results from this type of calculations were mainly used to study possible reduction criteria that may be applied to some of the proposed pathways, where reactions exceed hundreds.

Approximation to activation energy values were obtained by relaxed-scan calculations, which study the energy of a molecular system in function of variations in structural characteristics, such as bond angles, bond lengths or dihedral angles. The thermal cracking initiation reactions were analyzed by this calculation process. These reactions imply breaking of $C - C$ or $C - H$ bonds, and therefore, bond length was the structural characteristic disturbed. Having the optimized structures as starting point, specific bonds were extended with elongation distances defined for each case. This was carried out step by step, optimizing in every step the molecular structure.

The main result from this type of calculations is the set of optimized structures and a plot that represents the energy behavior as function of the applied variations. The data provided by this type of plots is used to estimate the activation energy.

3.5. Reaction pathways

The development of the reaction pathways considered the reactants, products, routes and support tools previously described. A particular consideration was taken for the products of LTO that based on the most-accepted ISC descriptions [1, 6, 8], were assumed to undergo complete oxidation in the combustion front. This implies that the LTO products are transformed into combustion gas, this only affects the oil bank through heat release. Furthermore, both processes, LTO and thermal cracking, start with the same reactants as this facilitates the comparison of the chemical evolution of the selected species.

Based on the relatively large time and length scales in ISC, it seems reasonable to assume that every crude oil fraction is exposed to the same physical and reactive processes. In fact, several reactions may occur among different SARA fractions. In spite of that, this thesis assumed that the reaction pathways are independent for each SARA fraction. A simplification justified by several reasons. In the case of LTO, most interactions occur between hydrocarbon and oxygen molecules [11]. Interactions among hydrocarbon molecules are only possible as intermolecular addition reactions between $\bullet R$ radicals that have as products new hydrocarbon molecules. These molecules would be part of one of the SARA fractions; therefore, the analysis for the surrogate molecules would be applicable to them, which makes a deep analysis of their chemical evolution impractical.

In the case of the thermal cracking process, some authors [96] have studied the possible effects of interactions among SARA fractions, identifying them as negligible. In addition, during the formulation of thermal cracking reaction pathways a great amount of species were involved, even when neglecting interactions among SARA fractions. Considering interactions would greatly increase the number of reactions and species in the process, turning the development of a reaction pathway a hardly possible task.

Taking into account that the small molecules such as those present in the saturate and aromatic fractions are part of the large molecules present in the resin and asphaltenic fractions, the results obtained for the step by step analysis of the former were used to understand the behavior of the latter in an attempt to describe in a practical way the complex reaction processes associated to resins and asphaltenes. The fact that [67] simple changes in bonds and other structural characteristics in molecules of large size only affects their structures in the close surroundings of the modification supports this approximation.

3.5.1. Low temperature oxidation

The development of reaction pathways for LTO considered a literature review of the most-accepted reaction mechanisms [9–20] proposed for this process. Several studies [9,12–15,17] established the steps that follow when hydrocarbon molecules interact with oxygen at temperatures from 50°C to 350°C.

- Initiation: considers two groups of reactions: i) H-abstraction and intermolecular addition and ii) $O-O$ cleavage. The first group of initiation reactions apply to surrogate compounds. Condensed Fukui calculations indicated the pathway that every molecule undergoes in this regime. The main products from these reactions were $\bullet R$ and hydroperoxyl ($HO_2\bullet$) radicals, although $ROO\bullet$ radicals were also produced. $O-O$ cleavage reactions apply to peroxide molecules ($ROOR$ and $ROOH$), that produce hydroxyl ($\bullet OH$) and alkoxy ($RO\bullet$) radicals. This is an initiation step as

it produces radical species from compounds without dangling bonds. The information required to study this sort of reactions was provided by NBO calculations (Wiberg Index) through the analysis of bond orders .

To analyze the chemical evolution of olefins, an intermediate product in various ISC processes a terminal olefin with seven carbon atoms was selected, 1-heptene. This selection responds to the fact that β -scission reactions are considered [9] the main responsible for olefin formation during LTO and always produce molecules with double bonds at the end of hydrocarbon chains, i.e. terminal olefins. The number of carbon atoms was the same of the molecule selected as normal alkane in the saturate fraction, n-heptane as this facilitates the analysis of the reaction pathway.

- Propagation: it involves the products of the initiation stage in reactions such as β -scission, intermolecular and intramolecular H-abstraction and intermolecular addition. Several interactions may occur in these steps; however, only those that produce species with dangling bonds, i.e. radical species, could be considered as part of propagation. Interactions of radicals with not radical species, such as surrogate compounds or oxygen molecules, which produce other radical species were also included in the propagation stage. β -scission and intermolecular H-abstraction reactions were considered in the production of through olefins, the formation of double bonds in $\bullet R$ radicals and the interaction between $\bullet R$ radicals and oxygen (O_2), respectively. H-abstraction reactions also produced hydroperoxyl radicals.

Among the variety of reactions in these steps, the most important reaction was the intermolecular addition of $\bullet R$ radicals and oxygen (O_2) molecules, which produces peroxy ($ROO\bullet$) radicals. This reaction has been considered [9] as the first step in the formation of oxygenated compounds. Depending on the structural characteristics of the $ROO\bullet$ radicals, they could undergo intramolecular H-abstraction reactions, with $\bullet QOOH$ radicals as product. This reaction route, intramolecular H-abstraction was fundamental in the study of the production of cyclic ethers.

- Termination: intermolecular addition reactions constituted the only transformations involved in this event that considered the products of the initiation and propagation events as reactants. In these reactions radicals form species with larger size and without dangling bonds. Several types of radical species are present in the reactive media of a LTO process and tens of interactions are likely to occur among them. The process followed to propose a reaction pathway took into account all possible interactions among radical species, except those that involve two $\bullet R$ radical species. Two reasons justified this approach: i) the main products from these reactions are saturate, aromatic, resin or even asphaltene compounds, and therefore, the conclusions or finds

made for the surrogate structures are applicable to those species. ii) the main source for these reactions are $\bullet R$ radicals formed during initiation steps. The process for the formation of this type of radicals is influenced by oxygen concentration, the higher the concentration of O_2 the higher the yield of radicals. However, oxygen concentration is considered low during ISC process because the high presence of aromatic structures in crude oil consumes great amounts of this compound acting as oxidation inhibitors [11]. Consequently, the low expected concentration of $\bullet R$ radicals allows to assume this type of reactions as negligible.

3.5.2. Thermal cracking

The development of thermal cracking pathways was based on the study of the most accepted thermal cracking reaction mechanisms [21–37,65] proposed for hydrocarbon molecules. Those mechanisms have established the steps that these compounds follow when their energy is increased by a heating process, as the one in ISC, at temperatures varying from 200°C to 900°C approximately. Contrary to the LTO case, thermal cracking processes have been clearly divided by stages: initiation, propagation and termination. The reaction pathways proposed make use of this division.

During the study of the thermal cracking reactions great amount of species were involved, mainly in propagation and termination stages. Therefore, in order to describe the process in a practical way, this study used the strategy of dividing the produced species by groups with common structural characteristics. It facilitated to study the evolution of high importance species in detail and extend the finds to molecules with similar characteristics, allowing to obtain global conclusions.

- Initiation: two main types of reactions were considered in this event, unimolecular and bimolecular initiation reactions. In the case of unimolecular reactions, the reactive process takes places when the energy of the molecular system is increased, with two free radical species ($\bullet R$) as products. The production of only one radical compound by this process is also possible, when the starting structure is a cyclic molecule that undergo breaking in one of the bonds that make part of the cyclic structure. In the case of small molecules, and based on the appreciations of some authors [21–25,27–29,32,33,36,37,65], this study considered $C - C$ and $C - H$ cleavage as initiation reactions. On the other hand, in the case of resin and asphaltene structures, given the complexity of their structures and variety of researches in ISC thermal cracking [1,4,6] that have identified $C - C$ breaking as the main responsible for the activation of these molecules, those were the only initiation reactions considered. In addition, breaking of $C = C$ (both double as resonant) bonds was not considered, because several studies [22,27,29] report the occurrence of this reaction at temperatures above 900°C.

Full NBO calculations provided the information required for the study of unimolecular initiation reactions. Particularly the bond order of the surrogate structures gave a description of bonds nature, allowing the identification of the sites that tend to break. Bond orders depend on the bond nature and therefore, results for the order of $C - C$ or $C - H$ vary in certain range, which makes difficult the analysis of bond strength solely based on the bond order. In the light of this, during the study of both types of bond breaking for small molecules, a free-radical-formation study was developed. This study calculated reaction energies of every possible unimolecular initiation reaction and provided with another parameter that complemented the information of bond order to make a better evaluation of the weakest bond. A free-radical formation study, such as the one described above was not required for the resins and asphaltenes because the $C - C$ cleavage was the only initiation reaction considered for these fractions.

Bimolecular reactions were also considered for the initiation event. Bimolecular initiation reactions or reverse radical disproportionation (RRD), involve the interaction of two molecules with double bonds; therefore, this type of reactions was considered when unsaturated compounds interact, i.e. two olefins, two aromatics or one olefin and one aromatic. RRD has as main products two $\bullet R$ radicals, one of them commonly stabilized by resonance.

Two types of molecules are identified in an RRD reaction, donor and acceptor. The donor molecule allows the abstraction of a hydrogen atom by an acceptor molecule. Afterwards, the donor molecule keeps an unsaturated bond and produces a dangling bond, while the acceptor molecule acquires a hydrogen atom that forms a bond with one of the atoms in an unsaturated bond, producing a radical molecule.

During an RRD process, both reactants may act as acceptor and donor molecules. Species that act as donor molecules experiment the abstraction of a hydrogen atom, i.e. the breaking of a $C - H$ bond; therefore, the compound with the lowest bond dissociation energy is likely the one that acts as donor. Considering this, some of the required information for studying these reactions was provided by the free-radical-formation study. The analysis of the results allowed the identification of the most stable free radicals from C-H cleavage, which become the species that likely act as donor in an RRD reaction.

In the case of acceptor molecules, during the reaction process they form a new bond with the hydrogen atom abstracted from the donor molecule. With an olefin compound as acceptor, there are two possible atoms to form a bond with the new hydrogen, whereas, in the case of aromatic compounds, double or resonant bonds make part of many sites in the molecule, which increases the amount of possible atoms that may undergo the addition process. This highly increases

the complexity of the analysis for these reactions, forcing the evaluation of all possible sites in the acceptor molecule structure. Taking this into account, every possible atom in the acceptor molecule structures was tested, in order to determine the most stable places to form the new bond. Reaction energies for every possible addition were calculated to determine addition sites. The addition of new atoms to aromatic structures generates changes in the geometry and electron distribution of the molecules, with radical species as products. Given the aromatic character of these molecules, the localization of dangling bonds in their molecular structures is not evident and, therefore, the calculation of electronic atomic spin density became imperative. This information was provided by full NBO calculations by the analysis of Mulliken Atomic Spin Densities. Those parameters allowed to identify specific atoms with higher electron densities, which constitute the most likely locations for dangling bonds.

- Propagation: the products from initiation reactions were the reactants for this event. During the formulation of propagation, intermolecular H-transfer, β -scission and isomerization reactions were studied. In the case of intermolecular H-transfer reactions, they describe the interaction between a radical and a saturated molecule, i.e. without dangling bonds, to produce two new species with the same nature, radical and saturation. This study only considered intermolecular H-transfer reactions with exothermic reaction energies, because products from an endothermic intermolecular H-transfer reaction are less stable, which implies lower possibilities to be produced and shorter lifetimes.

β -scission are unimolecular reactions, where the presence of a dangling bond leads to breaking of a $C - C$ or a $C - H$ bond to form a double bond. They have as products two species, a terminal olefin and a free radical. These reactions were largely explored.

Contrary to the β -scission case, isomerization reactions were only applied to molecules with the structural characteristics described by some authors [21, 22, 28, 34–36]. Molecules had to contain at least four carbon atoms in chain, which implied that most of the aromatic or cyclic molecules were not allowed to undergo these reactions, unless they had alkyl substituents with at least four carbon atoms. In addition, for the same reasons explained above for the H-transfer reactions case, only isomerization reactions with exothermic character were taken into account. Based on these specifications, isomerization reactions were mainly applied to saturate compounds, not only the ones from saturate fraction, saturate compounds produced from other fractions were also analyzed.

- Other intermediate formation and termination events: the products of propagation reactions were the reactants for these events. This set grouped saturates, olefins and free radical compounds.

Given the presence of many types of compounds, several reactions take place. The interaction among stable compounds such as saturates and olefins does not produce any reaction; however, combining saturates with radicals, olefins with radicals and radicals with radicals produced different type of species. In addition, radical molecules could undergo transformations without any other participant, by β -scission and isomerization reactions.

The termination reactions were those that produced new hydrocarbon species without dangling bonds. Disproportion and intermolecular addition reactions between free radicals met the requirements to be classified as termination reactions. They constituted two different routes. In the first one, compounds interact keeping their initial sizes and changing structural characteristics like bonds and atomic distribution; in the second one, intermolecular addition, larger species are produced by the addition of both reactants. In the case of disproportion, products were saturate and olefin compounds, whereas, intermolecular addition produced larger hydrocarbons.

The event «Other intermediate formation» has not been defined by the studied mechanisms as a thermal cracking mechanism stage. The author proposed this event for explaining the routes followed by some compounds produced by the propagation event, and that did not produce final products. This event was integrated by a variety of reactions studied for initiation, propagation and termination events. Species without dangling bonds, saturates and olefins underwent bond breaking, which implies $C - C$ and $C - H$ cleavage reactions. On the other hand, radical species tended to experiment typical propagation reactions, β -scission and isomerization. In the case of bimolecular reactions, combination of the different species produced a variety of compounds. Two olefins interacting led to the occurrence of an RRD reaction, producing two new radicals. The union of an olefin with a radical gave rise to a radical-addition reaction, producing a larger radical. Finally, one saturate and a radical interacted by an intermolecular H-transfer reaction, producing two new species with the same nature.

3.5.3. Construction of reactive schemes

To have a global vision of the chemical processes involved in LTO and thermal cracking during ISC, reaction schemes were developed. The schemes are available in the Appendix and were built by using the free software MarvinSketch 15.2.2, 2015, ChemAxon [97]. This software was used for drawing and calculating the elemental composition of the molecular structures.

3.6. Thematic DataBase

Several amount of species were involved in the formulation of thermal cracking pathways, mainly for the saturate and aromatic fractions. Hence, a thematic database was developed in order to count on an inventory of species and reactions. The database includes an algorithm that reads .txt files that contain species and reactions and allows to obtain more condensed reaction pathways with different level of complexity depending on the application of the reaction scheme.

3.7. Validation

Intermediate species, products and reaction energies obtained from this study were compared in as much as possible with the experimental data available in the scientific literature. This was carried out as validation of the proposed reaction pathways.

Chapter 4

Surrogate selection and stages associated to the chemical processes in ISC

This chapter presents the results from the surrogate selection and addresses the current division of ISC according to the chemical processes. In the surrogate selection section, the criteria and selected structures to represent crude oil are explained. In the case of the analysis of the stages in ISC an analysis was carried out based on the chemical concepts presented in the Fundamentals and Background chapter. The thermal cracking and LTO processes of ISC were divided into several events such as initiation, propagation and termination.

4.1. Surrogate selection

Heavy petroleum is an extremely complex substance that contains hundreds of different hydrocarbon compounds mainly formed by carbon and hydrogen atoms, although, it may also contain elements such as nitrogen, sulfur or metals like nickel, vanadium and iron [84]. Several authors [84–88] have studied the composition of complex hydrocarbon mixtures such as crude oil, gasoline or diesel. Methods such as elemental analysis, small-angle neutron scattering, several fluorescence measurements and nuclear magnetic resonance (NMR) have been implemented for studying the molecular characteristics, at least in average, of petroleum compounds, whereas, detailed description of individual constituents has not been largely explored [84]. The analysis of crude oil composition has been based on dividing the material into fractions. The most used division is the one that classifies crude oil compounds by their polarity and solubility, resulting in four fractions, saturates, aromatics, resins and asphaltenes [84,86]

that are described below.

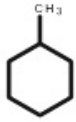
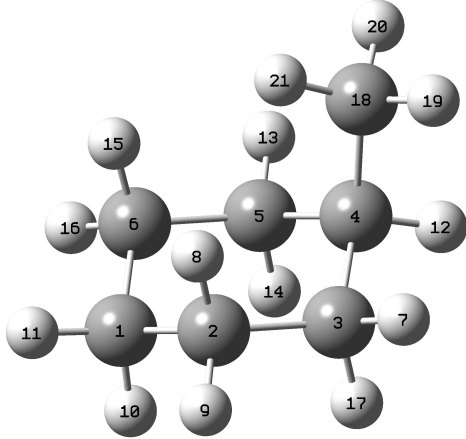

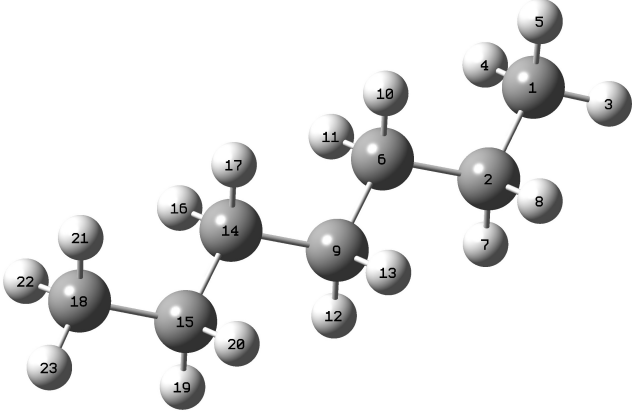
- **Saturates:** aliphatic hydrocarbons generally known as alkanes or paraffins. All bonds in their chemical structures are simple, which implies that every carbon atom forms four bonds with *sp*³ hybridization. Saturates group normal paraffins, iso-paraffins and cycloparaffins (naphthenes). This fraction usually constitutes the most abundant group of hydrocarbons in many crude oils [90,98]. It has been found that most of heavy crude oils are rich in normal paraffins and naphthenes, whereas, iso-paraffins are less abundant [90]. Naphthenes with high molecular weights are common in heavy crude oils and are typically composed by five and six member rings, being the six member ones more common [89].
- **Aromatics:** hydrocarbons with ring molecular structures that alternate single and double bonds, which confers special electronic and structural attributes. Aromatics are usually the second group with higher content in heavy crude oils [91, 98]. They have been classified as mono, di and polyaromatic, depending on the number of condensed aromatic rings. Compounds such as benzene, toluene, xylene, mesitylene and naphthalene have been detected and measured in petroleum by experimental techniques [87, 91]. Benzene constitutes the basic unit for aromatic molecules. Molecules denominated as poly-aromatic hydrocarbons (PAH) are formed by sets of condensed benzene rings and are highly stable to thermal degradation processes [87, 91]. The presence of sulfur atoms have been measured in several crude oils and it has been established that at least benzothiophene and dibenzothiophene could make part of petroleum [87].
- **Resins:** hydrocarbons soluble on petroleum or excess of pentane and heptane [91,98]. Their basic structural elements are units of condensed aromatic rings with alkyl substituents [91,92]. These compounds usually contain five or six membered naphthenic or aromatic rings [91, 92]. Resin molecules include heteroatoms such as nitrogen, sulfur or oxygen that confer polarity to some parts of their structures, and therefore to the molecule [91, 92].
- **Asphaltenes:** polar, aromatic, high-molecular-weight, high-boiling-point and low-API-gravity fractions of crude oil [99]. They have been identified as insoluble in alkanes and crude oil and soluble in aromatic solvents such as benzene or toluene [99]. These compounds consist of highly condensed polyaromatic nuclei that are bonded to cyclic or chain substituents. Aromatic nuclei usually host heteroatoms such as oxygen, nitrogen, sulfur or even metals [99]. Asphaltene structures have been classified depending on their configuration as archipelago and continental according to their number of large condensed aromatic ring units. A continental structure contains one condensed aromatic unit whereas an archipelago configuration may contain two

or more [92, 99]. As the heaviest fraction of crude oil, these compounds are usually present on refining residues.

Based on the characteristics identified for SARA fractions and several studies on crude oil composition, six compounds were selected as surrogates to represent a heavy Colombian crude oil. Two molecules were chosen as saturates, a naphthene and a normal alkane. For the aromatic fraction two structures were selected, a monocyclic and a bicyclic that includes a sulfur atom. In the case of resin and asphaltene fractions, one structure was selected to represent each of them as explained below. It is important to highlight that small molecules, such as those selected to represent the saturate and aromatic fractions are part of the resin and asphaltene structures, which is useful in order to extrapolate most of the results from detailed chemical analysis of simple molecules to the more complex structures such as those selected to represent the resin and asphaltene fractions. A more detailed explanation of the criteria used to select the surrogates follows.

- Methylcyclohexane (Cyclic Saturate): a naphthene hydrocarbon that consists of a six-member ring with a methyl substituent. Its molecular formula is C_7H_{14} . This compound has been detected and measured in some heavy crude oils with APIs between 10 and 20, with a V/V percentage of 1.6, the highest among the naphthenic compounds followed by methylcyclopentane with 0.87 [88]. Table 4.1 shows the 2D and 3D structures for this compound which for simplicity is called from now on Cyclic Saturate (CS). The 3D structure that derived from an optimization calculation indicates that the chair conformation with the methyl group in axial position presents the lowest energy.
- n-Heptane (Normal Saturate): a linear paraffin composed by seven carbon and sixteen hydrogen atoms (C_7H_{16}). Some studies [88] have detected and measured up to 2.3 V/V percentage of this compound in crude oils, the highest among the normal alkanes. As a normal paraffin with a reasonable length, n-heptane allows to study every type of thermal cracking and oxidation reactions given its structural characteristics. Therefore, most of the conclusions found for n-heptane would be applicable to longer linear alkanes. Table 4.1 shows the 2D and 3D optimized structures for this compound, which is called from now on Normal Saturate (NS).


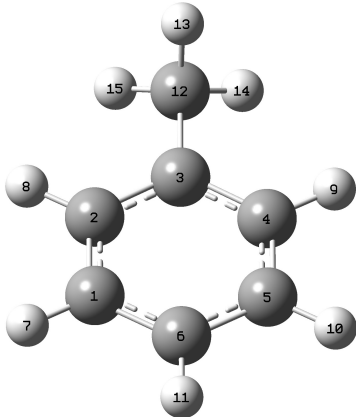

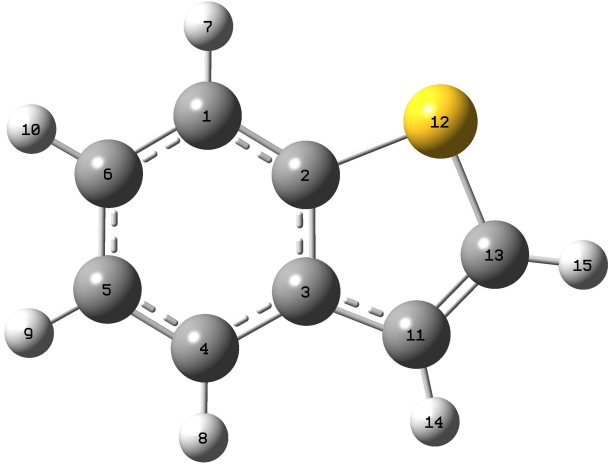
Table 4.1: Molecular structures in 2D and 3D of saturate surrogates

Name	2D Structure	3D Structure
Cyclic Saturate (CS)		
Normal Saturate (NS)		

- Toluene (Monocyclic Aromatic): monocyclic compound that consists of a six member aromatic ring with a methyl substituent (C_7H_8). Its concentration in crude oils has been reported as high as a V/V percentage of 0.51, the highest among the aromatic compounds [88]. As the basic unit for aromatic molecules, benzene become an important option to represent an aromatic fraction; however, most of the aromatic molecules in crude oil in minor and larger structures (resin and asphaltene) contained aromatic nuclei integrated by benzene with alkyl substituents, making the selection of toluene reasonable. Table 4.2 presents the 2D and 3D optimized structures for this molecule that is referred from now on as Monocyclic Aromatic (MA).
- Benzothiophene (Polycyclic Aromatic): polycyclic aromatic compound that contains six and five-member aromatic rings. The second ring includes a sulfur atom (C_8H_6S). The refereed literature did not present an exact measure of the concentration of this species in crude oil; however, some authors have detected its presence by experimental techniques [87]. In addition, the structures

selected for resin and asphaltene fractions contained five member aromatic rings with sulfur atoms. The 2D and 3D optimized structures for this compound are presented in Table 4.2. The 3D optimized structure shows the presence of one double and several resonant bonds. In this research Benzothiophene was labeled as Polycyclic Aromatic (PA).

Table 4.2: Molecular structures in 2D and 3D of aromatic surrogates

Name	2D Structure	3D Structure
Monocyclic Aromatic (MA)		
Polycyclic Aromatic (PA)		

- Castilla Resin: Navarro et al. [85] carried out an experimental characterization of Castilla resins and asphaltenes by experiments with the solvent Apiasol, which separated Castilla oil into two fractions. Those fractions underwent experimental procedures that determined the presence of two different types of resins named as Resins I and II. Resins I were defined as those in the insoluble fraction that form aggregates with asphaltene molecules. On the other hand, Resins II were identified as those in the soluble fraction, i.e. the resins that make part of the fraction crude oil typically defined as maltenes, which contains saturates, aromatics and resins. The

authors [85] proposed molecular structures based on, the results of characterization techniques such as Nuclear Magnetic Resonance (NMR), X-ray Diffraction (XRD), elemental analysis, among others. The mentioned study also determined percentages of these resin compounds in Castilla oil. The percentage (W/W) of Resin I content was determined as 2.8, whereas that for Resin II it was 16.5. In spite of this higher concentration of Resin II, the structure proposed for Resin I was selected as surrogate compound for the analysis in this thesis as it presents a continental structure with high aromaticity, the presence of various functional groups and structural characteristics that are common to asphaltenes. The structure proposed for Resin II was discarded because it presents an archipelago form with low aromaticity. This type of structures tends to form lower molecular weight species by processes such as thermal cracking, which lead to new saturate and aromatic compounds, similar to those already taken into account above. In conclusion, based on the possible behaviors of these structures under the chemical processes in ISC, it was considered that the study of the evolution of Resin I could be more interesting than that of Resin II.

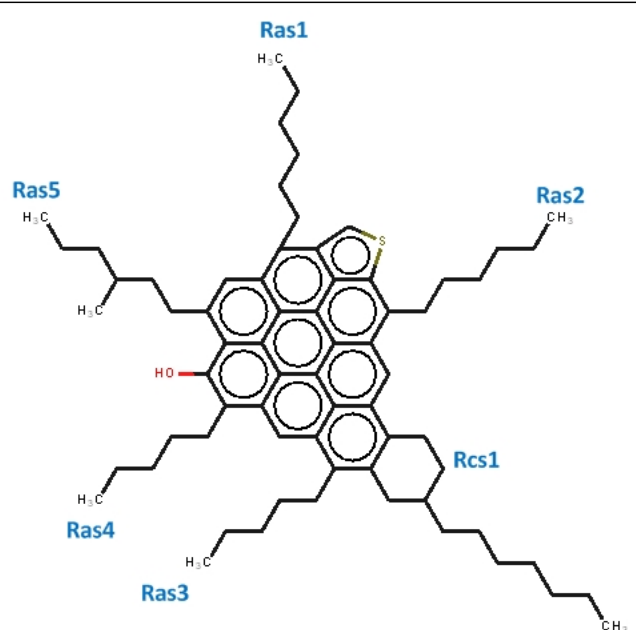
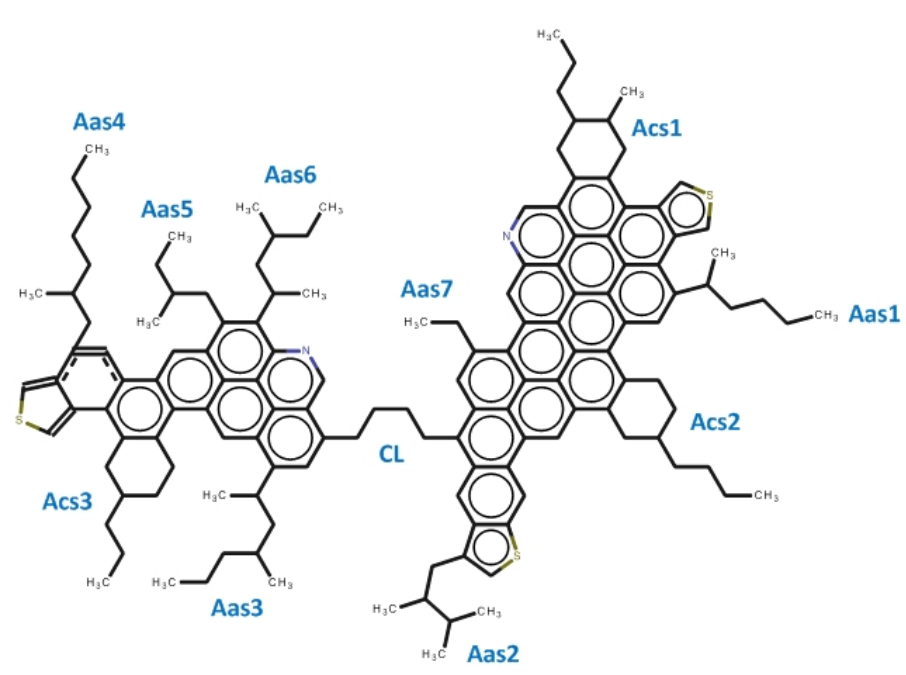
Based on the explained reasons, the Resin I structure was selected as surrogate and is named in this research as Castilla Resin (CR). Table 4.3 presents the CR structure, which contains five alkyl and one cyclic substituent and a large aromatic nucleus integrated by nine condensed aromatic rings, one alkoxy group and one sulfur atom. The molecular formula of this structure is $C_{68}H_{90}OS$ with molecular weight of 955.53 g/mol. The hydrogen-carbon ratio, which is a parameter commonly used to characterize hydrocarbon structures is $H/C = 1.32$ for this molecule.

- Castilla Asphaltene: the asphaltene structure proposed by Navarro et al. [85] was selected as surrogate for the asphaltene fraction. This structure was named in this research as Castilla Asphaltene (CA) and it is presented in Table 4.3. This compound has an archipelago structure integrated by two large aromatic nuclei, which were defined as left and right nucleus. The left nucleus is integrated by eight aromatic rings that contain sulfur and nitrogen atoms, one cyclic and four branched alkyl substituents. The right nucleus is formed by 15 condensed aromatic rings also with the presence of sulfur and nitrogen atoms, two cyclic and three branched alkyl substituents. The molecular formula for this compound is $C_{143}H_{162}N_2S_3$ with 2005.06 g/mol as molecular weight. The author is aware that most recently developed structures for representing asphaltene structures are smaller than the one selected and that archipelago structures have not been lately proposed, however in order to represent a heavy Colombian crude oil, Navarro et al. [85] work was the only that analyzed that specific case.

Regarding the presented structures for resin and asphaltene fractions, it is important to clarify

that the resonance illustrated by the structures is not exactly in that way in all the molecule states. The resonance could be broken in some areas of the structure, however, that only could be observed in the 3D structures obtained by electronic structure calculations.

Table 4.3: Molecular structures in 2D of resins and asphaltene surrogates

Name	2D Structure
Castilla Resin (CR)	
Castilla Asphaltene (AR)	

Tables 4.1 to 4.3 present the structures for the surrogates selected by this research. In the case of saturate (Table 4.1) and aromatic (Table 4.2) surrogates, the 3D optimized structures show the labels

for the atoms implied. This numeration does not depend on the atom nature, i.e. carbon, hydrogen or sulfur atom. On the other hand, for resin and asphaltene (Table 4.3) surrogates, given the great amount of atoms involved, the way to label these molecules was to identify zones such as large aromatic nuclei or alkyl substituents. Based on this, the 2D structures presented for these compounds show the nomenclature applied to these molecules. The convention begins with «R» (resin) or «A» (asphaltene) and may contain «as» (alkyl substituent) and «cs» (cyclic substituent). In the case of the asphaltene structure the label CR (cross linking) was included to refer to the alkyl chain that links the two large aromatic groups. These labels and conventions apply to all the chapters in this thesis.

4.2. Stages associated to the chemical processes in ISC

Based on the literature review carried out by this research, it was possible to identify the traditional division that most of the studies [1, 6, 8] have proposed for ISC: thermal cracking, low temperature and high temperature oxidation stages. Clearly, several authors [6–8, 50, 52–56] have characterized these ISC stages and have proposed overall reaction schemes to represent them, but only Khansari et al. [13] have proposed a subdivision by temperature ranges and only for the LTO stage of the process. Given the extended use of this division, this research adopted it; however, in order to expand the chemical knowledge of the ISC process, events that subdivided the ISC stages were included. The study of several studies [9–37, 65] on hydrocarbon chemistry identified events that condition the evolution of hydrocarbon species during the LTO and thermal cracking process, initiation, propagation and termination. Those were included in the reaction pathways proposed by this study. Indeed, they constituted a cornerstone in these reaction models as they allowed the determination of the reactions that take place. In addition to these events that have been already defined by several thermal cracking studies [?, 21–36, 65] in hydrocarbons chemistry, the author proposed a new event named «Other intermediate formation» as this event characterizes the particular dynamic that a chemistry process may experiment inside a reservoir. Typical chemistry studies assume that most of molecules undergo all chemical processes at the same time. This seems a good approximation in systems of low size but not for a reservoir system. It is not possible that all crude oil molecules undergo, for example, a bond breaking process almost at the same time. Material inside the reservoir does not experiment an uniform heating and, moreover, there is crude oil flow, which implies the constant mixture of radical and no radical species leading to the occurrence of many types of reactions.

Following chapters 5 and 6, explain reactions and species involved in the LTO and thermal cracking pathways. The formulation of those pathways was based on the stage and event divisions explained above.

Chapter 5

LTO reaction pathways

This chapter presents a diagram that explains the methodology, the main results and conclusions obtained from the formulation of the LTO reaction pathways, which was divided, as discussed above, in three events: initiation, propagation and termination. These reaction pathways were developed in detail for saturate and aromatic surrogates. In the case of resin and asphaltene compounds, only the probable chemical evolution of some structure sites was analyzed.

5.1. Methodology

Figure 5.1 presents the diagram that explains the process employed for the formulation of LTO reaction pathways. The chapter 3, which presented the methodology, offers a deeper explanation about the steps condensed in the diagram. In the Step 1, the surrogate structures are optimized to obtain ground state structures. The Step 2 considers the performance of NBO simulations to calculate electrophilic topological and electrophilic condensed Fukui functions. Those results are analyzed during the Step 3 to determine the most reactive sites. In the Step 4, with surrogate structures as reactants, initiation reactions are considered obtaining several radicals. The Step 5 takes into account radicals produced in the Step 4 to apply reactions classified as propagation producing alkenes and peroxy radicals. Step 6 involves the radicals produced during the Step 5 as reactants for the reactions in the termination event producing several oxygenated compounds. In addition, all species considered during the Steps 4 to 6 are simulated in Step a to obtain optimized structures that allows to calculate reaction energies (Step b). Finally, all reaction energies calculated in the Step b and the chemical structures considered during the Steps 1 to 6, feed the Step 7 that involves to construction of reaction schemes.

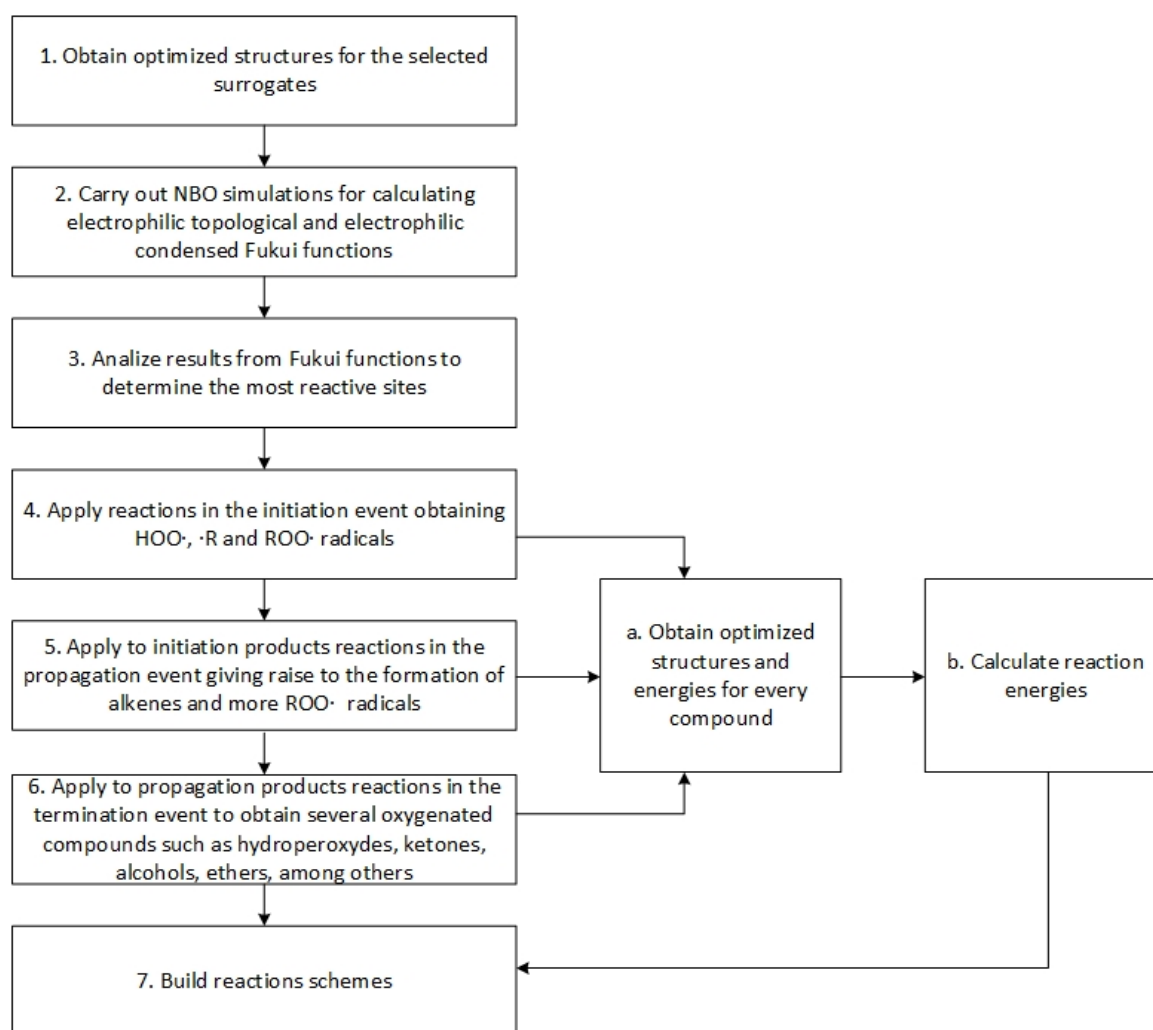


Figure 5.1: Methodology diagram for the formulation of the LTO reaction pathways

5.2. Results for saturate and aromatic surrogates

5.2.1. Initiation

The reactants for this event were the surrogate compounds. A study of the most accepted reaction mechanisms proposed for the LTO of hydrocarbon molecules determined an intermolecular hydrogen abstraction as the typical initiation step in this process. Given the presence of several hydrogen atoms in the reactant molecules, electrophilic topological and electrophilic condensed Fukui functions were calculated in order to identify the most reactive sites. Main result for the topological function calculations were contours that indicated reactive places, whereas, for the condensed function the result were values that indicated quantitatively the reactive character of atoms or molecule parts. A higher value a higher probability for that place to undergo an attack by an oxidant agent. Negative values indeed indicated a low electron density, and therefore a low probability for oxidant agent to

interact with the place.

Figures 5.2 to 5.5 show contours for electrophilic topological Fukui function for the CS, NS, MA and PA molecules. In order to compare the reactivity of different bonds, the figures present contours at an isovalue of 0.007 that indicate the places where an electrophilic attack is more probable. The larger the contour the higher the probability for oxygen to interact with atoms in that site of the molecule. From Figure 5.2 it was possible to determine that in CS, the hydrogen atoms 11 and 12 have the highest probability of being subtracted. Isocontours associated to bonds between atoms 2-3 and 5-6 cannot be considered as reactive places given the nature of the initiation reactions associated to LTO that affect the molecules by the addition and abstraction, which do not occur to bonds. Given the similarities between the isocontours of atoms 11 and 12 electrophilic condensed Fukui function (ECFF) results were necessary to determine, in a more quantitatively manner, the reactivity character associated to atoms 11 and 12. Table 5.1 presents ECFF results for the CS surrogate. Clearly, a value of 0.14 for the Hydrogen atom 12 compared to a value of 0.11 for 11, indicates that atom 12 is where hydrogen abstraction may take place. The rest of the values presented by the Table 5.1 have an average 0.04, much lower than 0.14.

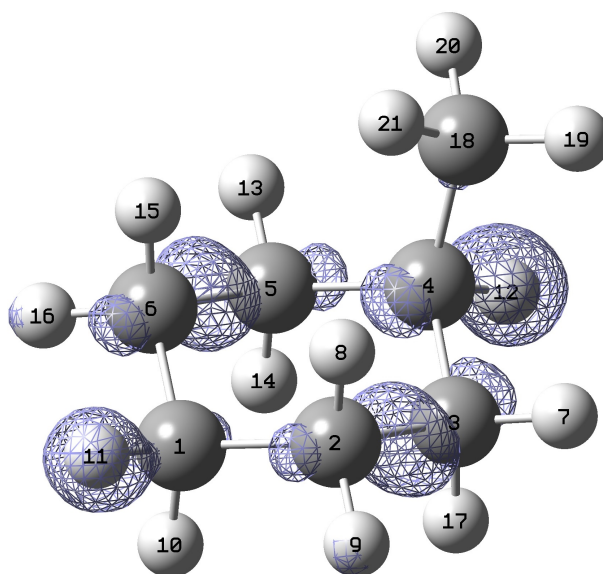


Figure 5.2: Contours of electrophilic topological Fukui function for Cyclic Saturate (CS)

Table 5.1: Results of electrophilic condensed Fukui function for Cyclic Saturate (CS)

Element	Atom number	Electrophilic condensed function
C	1	0.01
	2	0.04
	3	0.03
	4	0.03
	5	0.03
	6	0.04
	18	-0.01
H	7	0.06
	8	0.04
	9	0.06
	10	0.04
	11	0.11
	12	0.14
	13	0.06
	14	0.04
	15	0.04
	16	0.06
	17	0.04
	19	0.04
	20	0.04
	21	0.04

In the case of NS, Figure 5.3 shows that atoms 3 and 23 are the most likely hydrogens to undergo an electrophilic attack. Based on the ECFF results in Table 5.2, hydrogens 3 and 23 have an identical value of 0.08, as it was expected given the symmetry of the molecule. Taking this into account, there was no difference between the intermolecular H abstraction in both sites, and therefore, only the abstraction of *H* atom 3 was analyzed. The average value for the rest of the atoms in NS is 0.04 that is much lower than the value registered for the selected hydrogen atom.

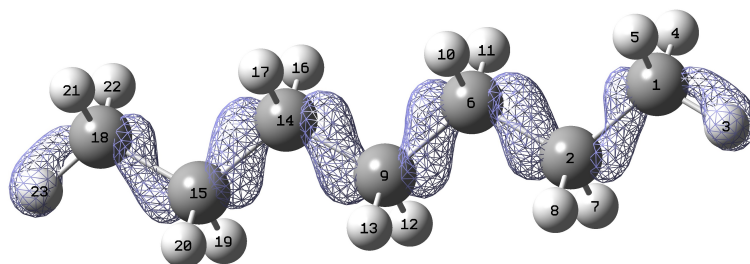


Figure 5.3: Contours of electrophilic topological Fukui function for Normal Saturate (NS)

Table 5.2: Results of electrophilic condensed Fukui function for Normal Saturate (NS)

Element	Atom number	Electrophilic condensed function
C	1	0.03
	2	0.04
	6	0.05
	9	0.05
	14	0.05
	15	0.04
	18	0.03
H	3	0.08
	4	0.03
	5	0.03
	7	0.04
	8	0.04
	10	0.04
	11	0.04
	12	0.04
	13	0.04
	16	0.04
	17	0.04
	19	0.04
	20	0.04
	21	0.03
	22	0.03
	23	0.08

Figure 5.4 presents electrophilic topological Fukui function contours for MA that identify two zones with higher reactive character: the pi bond and the hydrogen atom 13. The reactive character of pi bond is represented by the clouds that cover the aromatic part of the MA structure. Given the uniform electron density in pi orbitals, oxygen may interact with them in order to form a bond, altering the aromaticity of the molecule. Although the contours in Figure 5.4 almost cover entirely the aromatic part of the MA molecule, according to the ECFF results presented in Table 5.3, atoms 3 and 6 have the highest reactivities with values of 0.22 and 0.23 respectively.

Given the high reactive character in carbon atoms 3 and 6, initiation reactions by the formation of bonds between each of those atoms and oxygen molecules were evaluated. Oxygen was bonded to each of the carbon atoms; however, optimization calculations always found the isolated structures to be more stable despite their high reactive character, it was not possible to obtain stable structures from addition reactions of oxygen to carbons 3 and 6. The possible explanation for these results is that the formation of bonds in those sites would alter the molecule aromaticity, which requires high reaction energies. In addition, both reactants are species without dangling bonds, this hinders the process for the formation of new bonds. This does not reduce the reliability of ECFF results for determining reactive sites, in the case of pi bonds zone it indicated the site with higher electron density; however, the reaction could not occur given the stability of the aromatic ring.

According to the ECFF results in Table 5.3, another possible electrophilic attack is the one that may take place in the hydrogen atom 13. The average value of ECFF for hydrogen molecules in MA is 0.05. The hydrogen 13 presented the highest value, 0.07. This result is explained by the presence of pi bonds that have an effect over the 13 atom because of its position. Compared to atoms 14 and 15, 13 is significantly displaced from the molecule plane, which in addition to the possibility to form a radical stabilized by resonance, facilitates the abstraction of hydrogen 13.

Compounds such as the surrogate MA make part of the species typically classified as oxidation inhibitors. Given the possibility to obtain radicals highly stabilized by resonance, the H-intermolecular abstractions for these compounds require lower energies than those for saturate compounds. This suggests that oxygen consumption by monocyclic aromatic compounds consume more oxygen than their saturate counterpart.

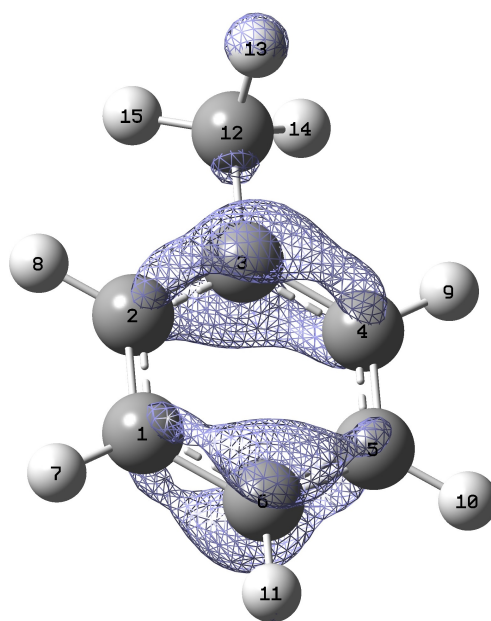


Figure 5.4: Contours of electrophilic topological Fukui function for Monocyclic Aromatic (MA)

Table 5.3: Results of electrophilic condensed Fukui function for Monocyclic Aromatic (MA)

Element	Atom number	Electrophilic condensed function
C	1	0.04
	2	0.06
	3	0.22
	4	0.06
	5	0.03
	6	0.23
	12	-0.04
H	7	0.05
	8	0.05
	9	0.05
	10	0.05
	11	0.04
	13	0.07
	14	0.05
	15	0.05

The analysis for PA surrogate presented some similarities with the MA case. From Figure 5.5 it was

possible to identify two main nucleophilic regions, contours associated to the pi bonds from both aromatic rings and a contour because of the sulfur atom (12). Similar to the procedure followed for MA, based on the ECFF results for PA (Table 5.4), the addition reactions to the carbon atoms with the highest values, 1, 4 and 11, were evaluated. As in the MA case, molecular structures produced by these reactions were not stable and, therefore, were not considered in the analysis.

Taking into account the results in Table 5.4 and with the carbon atoms in the cycles discarded as possible sites for addition, values for the remaining atoms were analyzed. Typical reaction mechanisms have identified the hydrogen abstraction reactions as responsible of the start of the LTO process; however, all hydrogen atoms in this molecule presented ECFF values of 0.04, which are very low compared to the sulfur atom value of 0.26. Based on this result, the author considered an addition reaction between oxygen and PA as the initiation step for the oxidation process of this surrogate molecule.

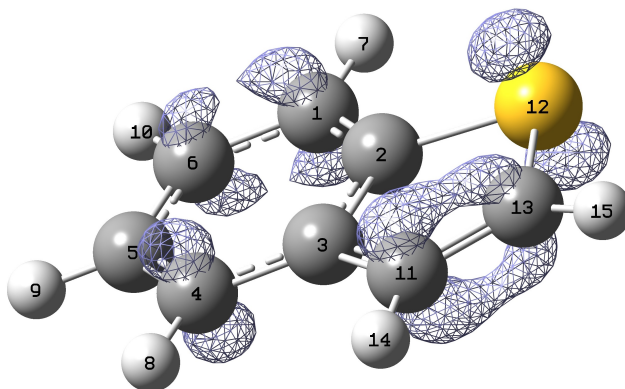


Figure 5.5: Contours of electrophilic topological Fukui function for Polycyclic Aromatic (PA)

Table 5.4: Results of electrophilic condensed Fukui function for Polycyclic Aromatic (PA)

Element	Atom number	Electrophilic condensed function
C	1	0.12
	2	-0.03
	3	-0.02
	4	0.14
	5	0.03
	6	0.08
	11	0.14
	13	0.05
S	12	0.26
H	7	0.04
	8	0.04
	9	0.04
	10	0.04
	14	0.04
	15	0.04

In the case of the olefin surrogate, 1-heptene, which was specially selected to explain how this type of compounds acts in the initiation events of the LTO process, it was determined that the process proceeded by the addition of an oxidant agent to one of the carbon atoms in the double bond. Given the good agreement found between the results of ECFF and topological Fukui function for all the surrogates and the consideration of ECFF always as decisive criteria in all cases, for the olefin selected only the ECFF was calculated. Based on that the Figure 5.6 that shows the molecular structure for the olefin selected does not present any contours. Considering the ECFF results presented by Table 5.5, it was possible to define that the carbon atom 14, the highest value was the place for the addition of the oxidant agent.

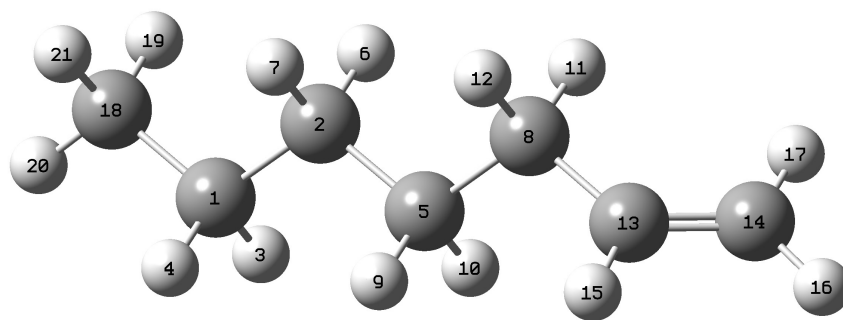


Figure 5.6: Molecular structure of the olefin surrogate

Table 5.5: Results of electrophilic condensed Fukui function for the olefin surrogate 1-heptene

Element	Atom number	Electrophilic condensed function
C	1	0.009
	2	0.014
	5	0.017
	8	-0.033
	13	0.217
	14	0.304
	18	0.009
H	3	0.019
	4	0.022
	6	0.025
	7	0.025
	9	0.033
	10	0.030
	11	0.037
	12	0.075
	15	0.044
	16	0.038
	17	0.035
	19	0.018
	20	0.042
	21	0.018

The products obtained from the reactions in the initiation event were $\bullet R$, peroxy ($ROO\bullet$) and hydroperoxy ($HOO\bullet$) radicals. Figure 5.7 shows the structures of these species and Table 5.6 summarizes the reactants, products and energies from this event. For the three surrogates that underwent the initiation process by intermolecular H-abstraction, CS, NS and MA, the reaction energies calculated were 9.85, 19.54 and 6.13 kcal/mol respectively. As it was expected, the lowest value was registered for the most stable free radical formed, the one stabilized by resonance, i.e. the radical from the MA surrogate (Figure 5.7 c). On the other hand, the highest energy value obtained was for the most unstable radical that originated from the NS molecule (Figure 5.7 b).

In the cases of PA and olefin surrogates, where initiation reactions were intermolecular additions, the reaction energies calculated were 17.88 and -2.27 kcal/mol respectively. The first one was considered high when compared to the rest of the species because of the changes in the aromaticity of the structure, which were caused by the formation of a bond between oxygen and sulfur atoms (Figure 5.7 d). In the case of the olefin surrogate, the energy value obtained was considerably lower than in the other cases. This result is explained because of the addition of a hydrogen atom in this molecule that formed a biradical that was stabilized by the formation of a cyclic ether (Figure 5.7 e).

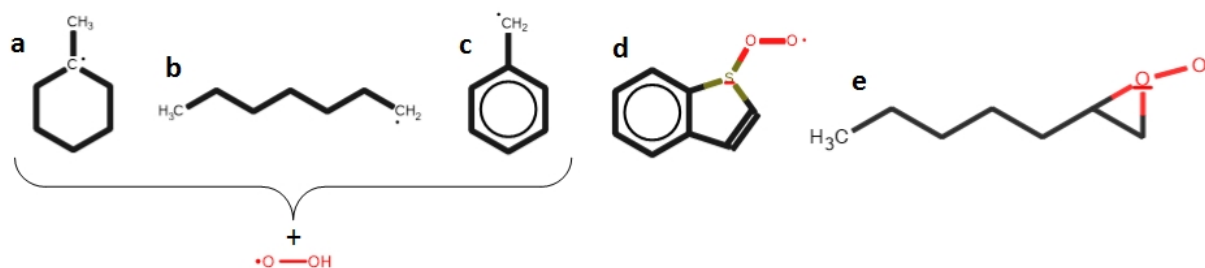


Figure 5.7: LTO Initiation products. a) $\bullet R$ radical from CS. b) $\bullet R$ radical from NS. c) $\bullet R$ radical from MA. d) $ROO\bullet$ radical from PA. e) $ROO\bullet$ radical from Olefin

Table 5.6: Summary of LTO initiation event with O_2 as oxidant agent

Route	Surrogate	Reaction energy (kcal/mol)	Products
Intermolecular H-abstraction	CS	9.85	Tertiary free and hydroperoxyl radicals
	NS	19.54	Primary free and hydroperoxyl radicals
	MA	6.13	Primary free radical stabilized by resonance and hydroperoxyl radical
Intermolecular addition	PA	17.88	Peroxyl radical
	Olefin	-2.27	Cyclic ether radical

During the LTO stage of ISC, the main and starting oxidant agent is molecular oxygen, given its presence in the gas injected to the reservoir. Nevertheless, during the evolution of the oxidation process, other oxidant agents are produced, particularly $\bullet OH$ and $HO_2\bullet$. Although the ISC literature does not attribute to $HO_2\bullet$ a high reactive character and the $\bullet OH$ role has not been largely explored, their effect in the process was analyzed. Table 5.7 presents the energy reaction results during the initiation event having as oxidant agents $\bullet OH$ and $HO_2\bullet$. All surrogates were analyzed except PA, because the addition of both oxidant agents did not lead to the formation of stable species as the optimization calculations showed that the individual species are more stable than when combined. This analysis was carried out in order to explore changes in reaction energies, routes and species obtained by the interaction of $\bullet OH$ and $HO_2\bullet$ with hydrocarbons; however, it is important to highlight that the equilibrium concentration of these species has not been determined during ISC and therefore, it is not possible to determine if they roles are important or not in the dynamic of the process. From the results in Table 5.7, it was possible to identify $\bullet OH$ as an effective oxidant agent with a high reactivity. Initiation reactions carried out by this agent are exothermic, because it is very unstable and one of the products from this type of interaction is water, which is a highly stable molecule. Water is one of the main products in a combustion process, once water molecules are produced, high energy is required to disturb them. In the case of $HO_2\bullet$, it was identified as a low reactive oxidant agent. Initiation reactions promoted by this agent required higher energy reactions than in the cases analyzed for O_2 . This suggests that the radical $HO_2\bullet$ is more a hydrogen-transportation species than as an oxidant agent.

Table 5.7: Summary of LTO initiation event with $\bullet OH$ and $HO_2\bullet$ as oxidant agents by the intermolecular H-abstraction route

Route	Oxidant Agent	Surrogate	Reaction energy (kcal/mol)	Products
Intermolecular H-abstraction	$\bullet OH$	CS	-17.61	Tertiary free radical and water
		NS	-7.92	Primary free radical and water
		MA	-21.33	Primary free radical stabilized by resonance and water
		Olefin	-30.27	Secondary free radical
	$HO_2\bullet$	CS	15.37	Tertiary free radical and hydrogen peroxide
		NS	25.06	Primary free radical and hydrogen peroxide
		MA	11.66	Primary free radical stabilized by resonance and hydrogen peroxide
		Olefin	–	Secondary free radical

5.2.2. Propagation

This event considered as reactants the products of the initiation event in the LTO process (Figure 5.7). The study of the most-accepted reaction mechanisms proposed for LTO indicated four types of reactions that occur in this event: β -scission, intermolecular and intramolecular H-abstraction and intermolecular addition of O_2 . Except for the radical produced by the olefin surrogate, the chemical evolution of all radicals were analyzed during this event. This is because the radical produced by the alkene compound is a secondary radical that makes part of a normal alkane; therefore, all conclusions made for the radical produced by the NS apply to the radical obtained from the olefin.

- β -scission: the presence of dangling bonds in hydrocarbon molecules weakens the bonds with surrounding atoms, which leads to the scission of the β bonds. This type of reactions were applied to the radicals obtained by the initiation event (Figure 5.7). In the case of the radicals from MA and PA, the aromatic ones, their structures did not allow the application of this type of reactions. A β -scission reaction for MA radical would imply a breaking in double or resonant

bonds that is not possible at ISC conditions. On the other hand, in the case of PA, it would generate a breaking in the oxygen-sulfur bond, which goes against the oxidation process.

Figure 5.8 presents the radicals and olefins structures produced. In the case of the tertiary cyclic radical, several options for olefin formation were evaluated. The one presented required the lowest energy for its formation (Figure 5.8 a). On the other hand, for the terminal radical from NS surrogate, there was only one option of breaking, which produced ethylene (Figure 5.8 c) and a terminal radical (Figure 5.8 b).

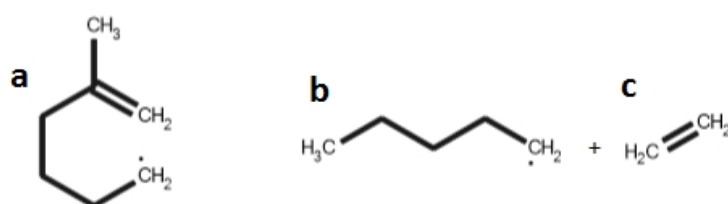


Figure 5.8: LTO propagation products from β -scission reactions. a) Radical olefin from CS. b) $\bullet R$ radical from NS. c) Ethylene from NS

- Intermolecular H-abstraction: depending on the products formed this type of interactions may be considered as propagation or termination reactions. Reactions that form at least a radical compound are classified as propagation; the formation of species without dangling bonds as a termination reaction. In this case, these reactions formed the radical $HO_2\bullet$. Figure 5.9 shows the structures for the products obtained by the study of this type of reactions. Figures 5.9 a and b presents the two possible olefin structures obtained by the H-abstraction in the tertiary radical from CS surrogate. On the other hand, from the terminal radical obtained from NS, only one olefin was likely to produce in an H-abstraction reaction, it is shown in Figure 5.9 c.

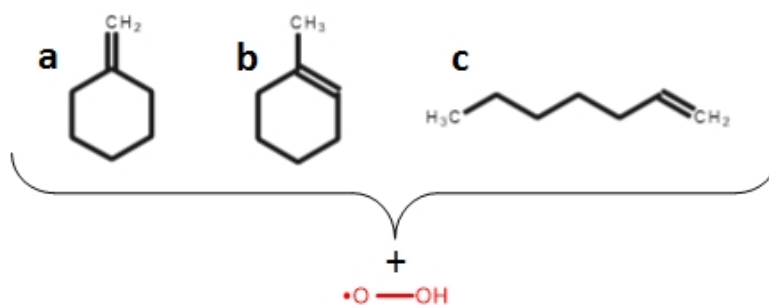


Figure 5.9: LTO propagation products from intermolecular H-abstraction. a) External olefin from CS. b) Internal olefin (methylcyclohexene) from CS. c) Terminal olefin from NS

- Intramolecular H-abstraction: peroxy radicals ($ROO\bullet$) contain a dangling bond in one of the oxygen molecules. Some authors [9,12,14,15] have studied the capacity of those oxygen molecules to rotate inside a molecular system, which allows to abstract a hydrogen molecule. That type of abstraction leads to the formation of a peroxide with a dangling bond in a carbon atom in the same molecule. Figure 5.10 shows the radical molecules obtained by this type of reactions. The $\bullet QOOH$ radicals produced by the surrogates CS, NS, MA and PA are shown by Figures 5.10 a to d respectively.

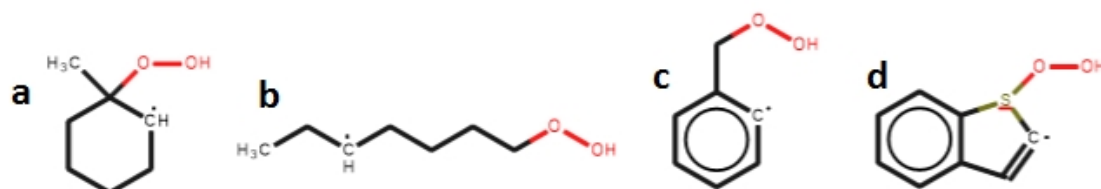


Figure 5.10: LTO propagation products from intramolecular H-abstraction. a) $\bullet QOOH$ radical from CS. b) $\bullet QOOH$ radical from NS. c) $\bullet QOOH$ radical from MA. d) $\bullet QOOH$ radical from PA.

- Intermolecular addition of O_2 : this type of reaction is the most important in the oxidation process as it allows to form bonds among free radicals ($\bullet R$) from initiation with oxygen molecules (O_2). It has been considered as the certain first step in an oxidation process, taking into account that the initiation process is a means to activate hydrocarbon molecules. Figure 5.11 shows the compounds obtained from intermolecular addition of O_2 reactions. The products were peroxy radicals ($ROO\bullet$) from the CS (Figure 5.11 a), NS (Figure 5.11 b) and MA (Figure 5.11 c). This transformation was already considered in the PA radical case, as the initiation reaction.

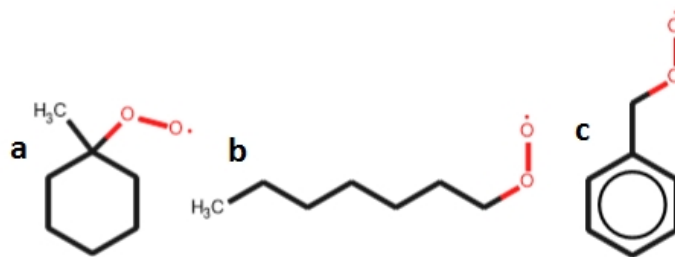


Figure 5.11: LTO propagation products from intermolecular addition of O_2 . a) $ROO\bullet$ from CS. b) $ROO\bullet$ from NS. c) $ROO\bullet$ from MA.

Table 5.8 summarizes reactants, routes, reaction energies and products from this event. Reaction energies for β -scission reactions had an average value of 25 kcal/mol. Chapter 6 gives more details about this type of reactions, given their importance in the thermal cracking process.

The intermolecular H-abstraction reactions, which produced an olefin and a $HO_2\bullet$ radical, presented energies of approximately -49 and -44 kcal/mol, for the formation of n-heptene (Figure 5.9 c) and methylcyclohexene (Figure 5.9 b) respectively. In addition, from the CS radical, it was evaluated the formation of the double bond out of the cycle, which would require 9kcal/mol to occur (Figure 5.9 a). On the other hand, all intramolecular H-abstraction reactions were identified as endothermic, with energy values from 22 and 32 kcal/mol. The highest value was for the abstraction of a hydrogen atom inside an aromatic ring (Figure 5.10 c) and the lowest for the abstraction in a secondary carbon in an alkane (Figure 5.10 b). In the case of intermolecular O_2 addition reactions, they presented an exothermic nature, which indicates the higher stability of the new peroxy radicals formed compared to the initial free radicals. The most stable radical, the one affected by resonance (Figure 5.11 c), has the highest energy release for these reactions, which could be assigned to its stability. The energy releases by bond formation depends on the stability of species implied, the higher the stability the higher the energy released. That fact explains the energy reaction results in Table 5.8 where the lowest energy released, -60.46 kcal/mol (Figure 5.11 c), was for the most stable radical and the highest one, -75.14 kcal/mol (Figure 5.11 b), for the most most unstable radical.

Table 5.8: Summary of LTO propagation event

Route	Reactant	Reaction energy (kcal/mol)	Products
β -scission	Tertiary radical from CS	25.52	Terminal olefin with a dangling bond
	Primary radical from NS	25.1	Alkyl radical and ethylene
Intermolecular H-abstraction	Tertiary radical from CS	-44.22	Olefin with double bond out of the cycle and $HO_2\bullet$
		9.44	Cyclohexene and $HO_2\bullet$
	Primary radical from NS	-48.81	1-heptene and $HO_2\bullet$
Intramolecular H-abstraction	Tertiary radical from CS	23.70	Hydrogen peroxide with a dangling bond
	Primary radical from NS	22.15	
	Aromatic radical from MA	35.15	
	Secondary radical from PA	24.28	
Intermolecular O_2 addition	Tertiary radical from CS	-73.62	Peroxyl radical
	Primary radical from NS	-75.14	
	Aromatic radical from MA	-60.46	

5.2.3. Termination and degenerate branching steps

The peroxy radicals (Figure 5.11) and the peroxides with dangling bonds (Figure 5.10) formed during the evolution of the previous event were the reactants for this event. Several pathways were derived from the possible interactions among the mentioned radicals and other species in the reactive media such as $R-H$, $\bullet OH$, O_2 and $HO_2\bullet$. The chemical evolution of each of these radicals constituted a route that leads to the formation of countless products by the occurrence of several reactions. Products formed by these radicals led to the formation of other species by the occurrence of subsequent reactions. That process has been named by some authors [9, 12] as degenerate branching step and is also explained in this section.

- Peroxides with dangling bonds: given the presence of a dangling bond, several species may interact with this compound. Figure 5.12 presents a reaction scheme that summarizes the routes from

the different possible interactions among the species in the reactive media. In the Stage 1, the peroxide radical has four options: to form a cyclic ether by its own or to undergo H-abstraction or addition reactions with $\bullet OH$, $HO_2\bullet$ and O_2 producing several oxygenated compounds, those that are highlighted in the diagram with bold types. In most of the cases, those molecules contained two or more oxygen atoms that may constitute different functional groups such as, alcohols, peroxides, ketones, ethers and carboxylic acids. In the Stage 2, the oxygenated compounds were named as $QOOH$, those that led to the formation of $QO\bullet$ and $\bullet OH$ radicals, by breaking of $O - O$ bonds. Those $QO\bullet$ radicals had two options for reacting, producing alcohols, aldehydes, ketones and new $\bullet R$ radicals.

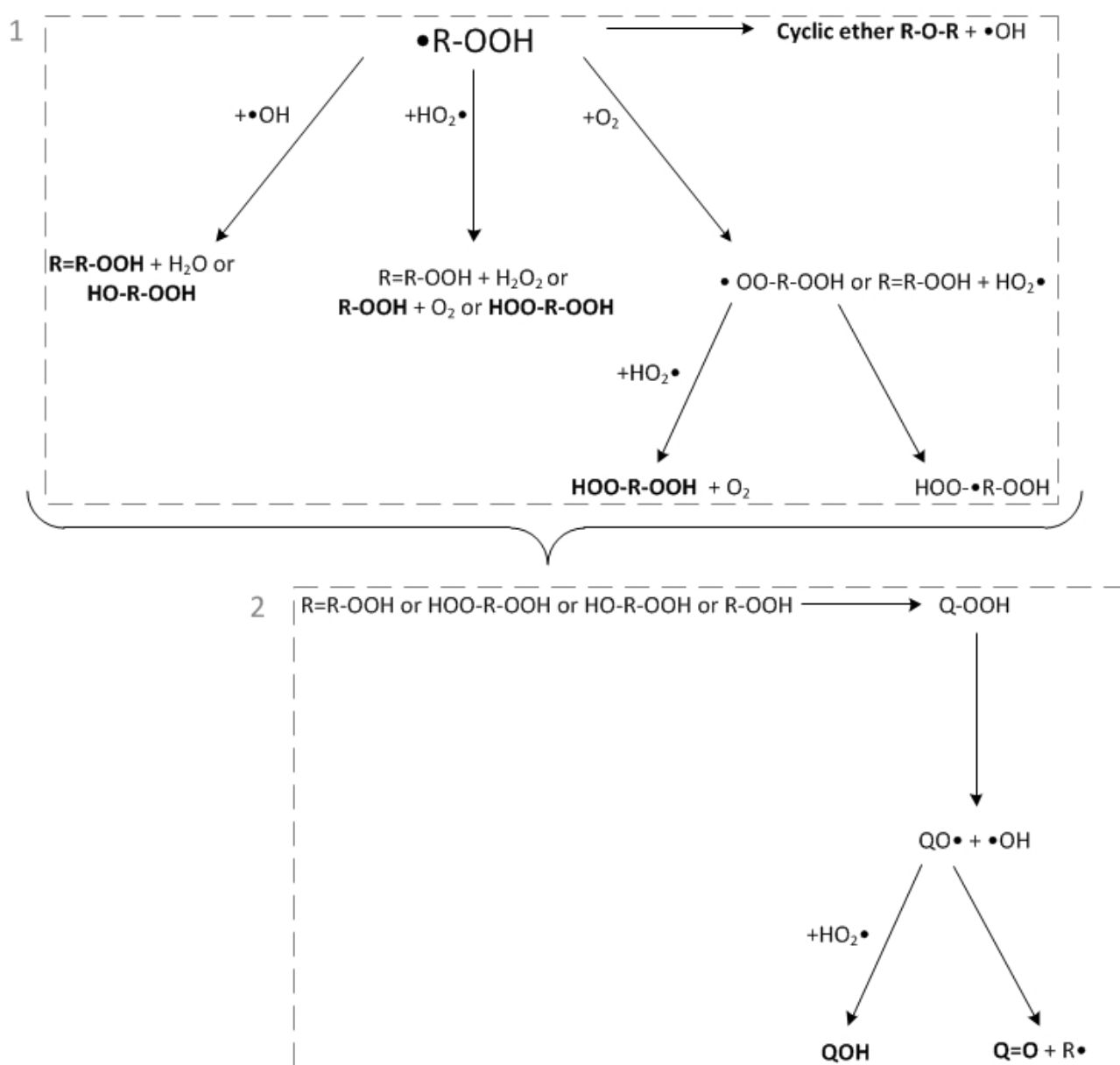


Figure 5.12: Reaction scheme for the evolution of radical peroxides

- Peroxyl radicals: Figure 5.13 presents the possible reaction routes underwent by peroxy radicals. In the Stage 1, the evolution of a peroxy radical proceeded always by the abstraction of a hydrogen atom, from another molecule that may be a hydrocarbon or a $HO_2\bullet$ radical. This stage led to the production of peroxides, compounds that tended to undergo breaking in their $O - O$ bonds, producing $RO\bullet$ and $\bullet OH$ radicals. Next, the presence of both types of radicals allowed the formation of ketones, aldehydes and alcohols during the Stage 2. $\bullet R$ radicals were also an important product from this part of the oxidation process.

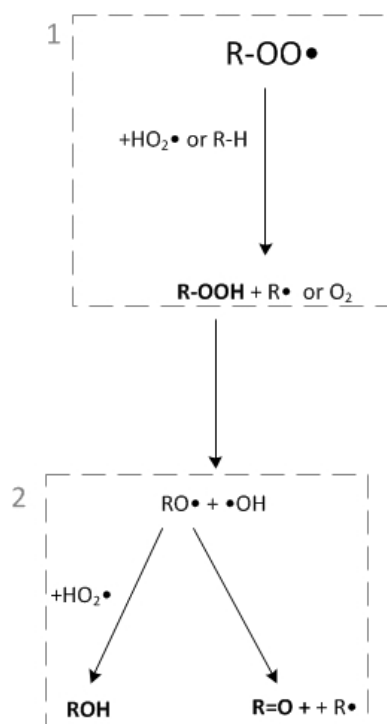
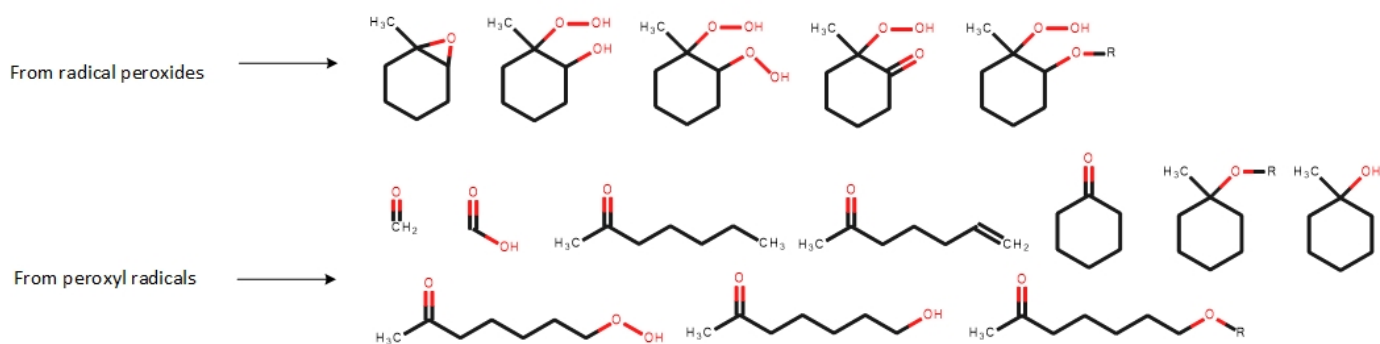
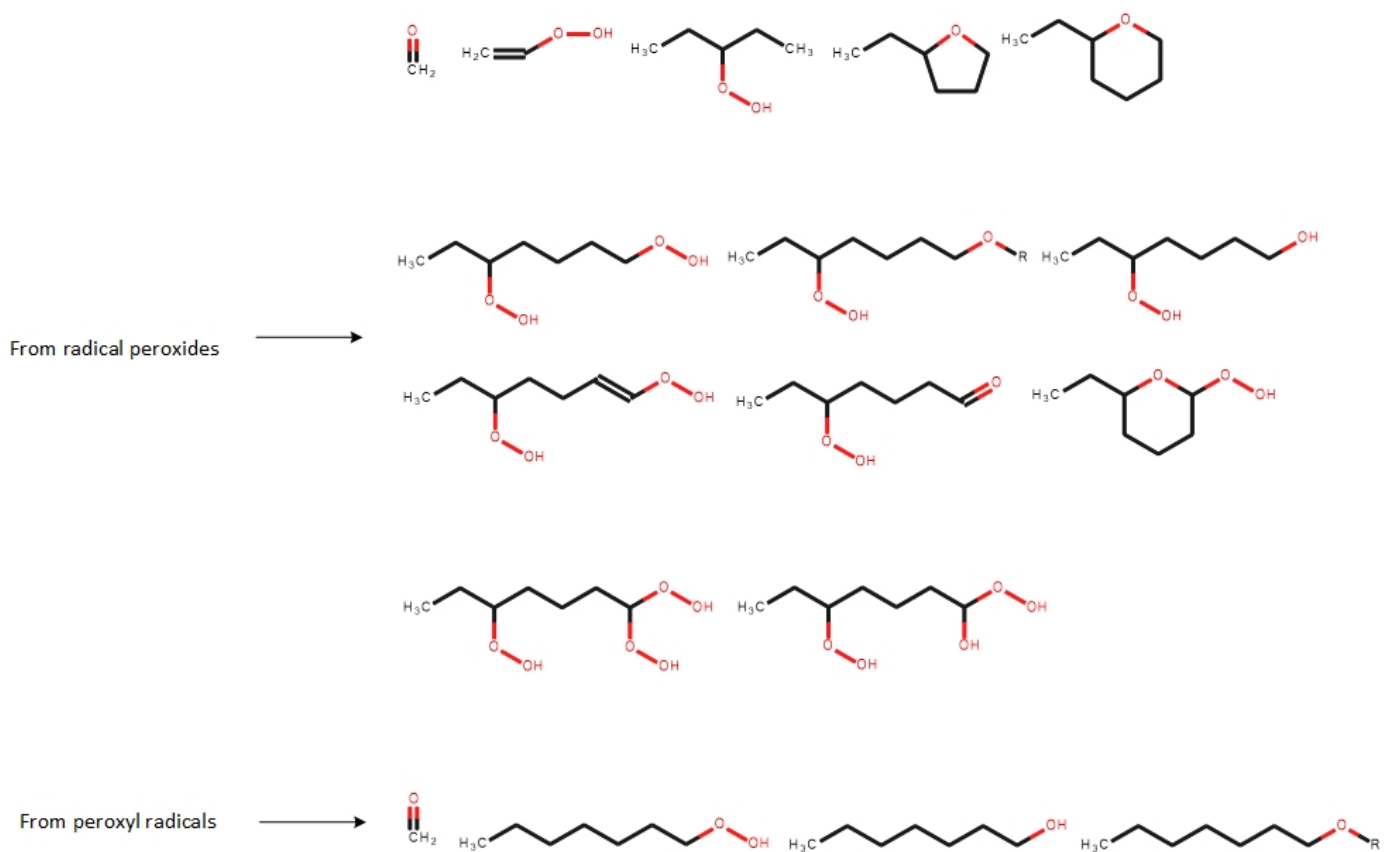


Figure 5.13: Reaction scheme for the evolution of peroxy radicals

Figures 5.14 to 5.17 show the structures of the products derived from the evolution of the peroxides with dangling bonds and peroxy radicals studied. The species produced by the application of the reactions defined agreed with those registered data in the literature [9, 12–15, 63] for ISC.

**Figure 5.14:** Termination event products from CS surrogate**Figure 5.15:** Termination event products from NS surrogate

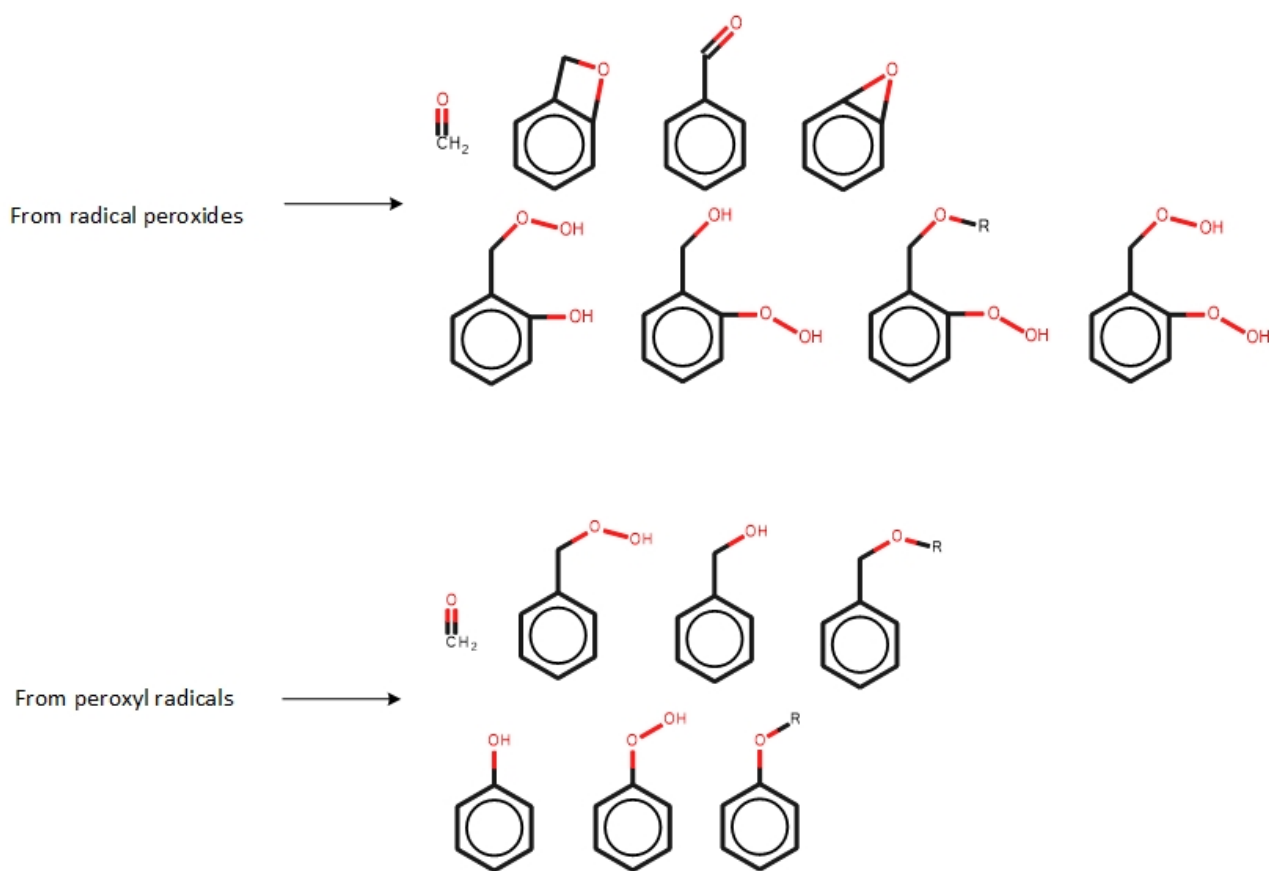


Figure 5.16: Termination event products from MA surrogate



Figure 5.17: Termination event products from PA surrogate

Table 5.9 presents the reaction energies calculated for the reactions considered in this event. The table contains the functional groups formed, the possible interaction with a second reactant, reactions and the energy range obtained. From the results presented, it was possible to identify six of the nine

routes as exothermic. The energy varies in the range of 3 to 4 kcal/mol, which could be considered as very small, except in three cases: formation of alcohols (by intermolecular addition of $\bullet OH$), ketones-aldehydes and cyclic ethers. The possible explanation for the mentioned deviations may be the high dependence in the reactants nature of this type of reactions, e.g. the formation of a cyclic ether depends on the number of atoms in the ring, whereas the formation of ketones and aldehydes depends on the bond that underwent the breaking process.

Table 5.9: Summary of LTO termination event

Functional group formed	Second reactant	Reaction	Reaction energy (kcal/mol)
Alcohol	$HO_2\bullet$	Intermol. H-abstraction	13.37 - 14.44
	$\bullet OH$	Intermol. addition	-95.11 - -113.03
Peroxide	$HO_2\bullet$	Intermol. H-abstraction	5.92 - 8.21
		Intermol. addition	-79.67 - -68.09
Olefin	$\bullet OH$	Intermol. H-abstraction	-76.27 - -74.09
	O_2	Intermol. H-abstraction	\approx -45.51
Cyclic ether	-	Intramol. addition	-41.46 - -19.23
Aldehydes and ketones	-	Intramol. addition	9.24 - 26.27

For more information about the reactions and species explored, please go to the Appendix section at the end of this thesis.

5.3. Analysis for resin and asphaltene surrogates

Given the complexity of the structures selected as surrogates and the nature of this reactive process that commonly gives rise to the formation of larger molecules, the analysis was limited to determine the most reactive sites in their structures, which allowed to make predictions about their behavior during the oxidation process. In order to define reactive sites, the ECFE was calculated for both compounds. Figures 5.18 and 5.19 show the identified sites.

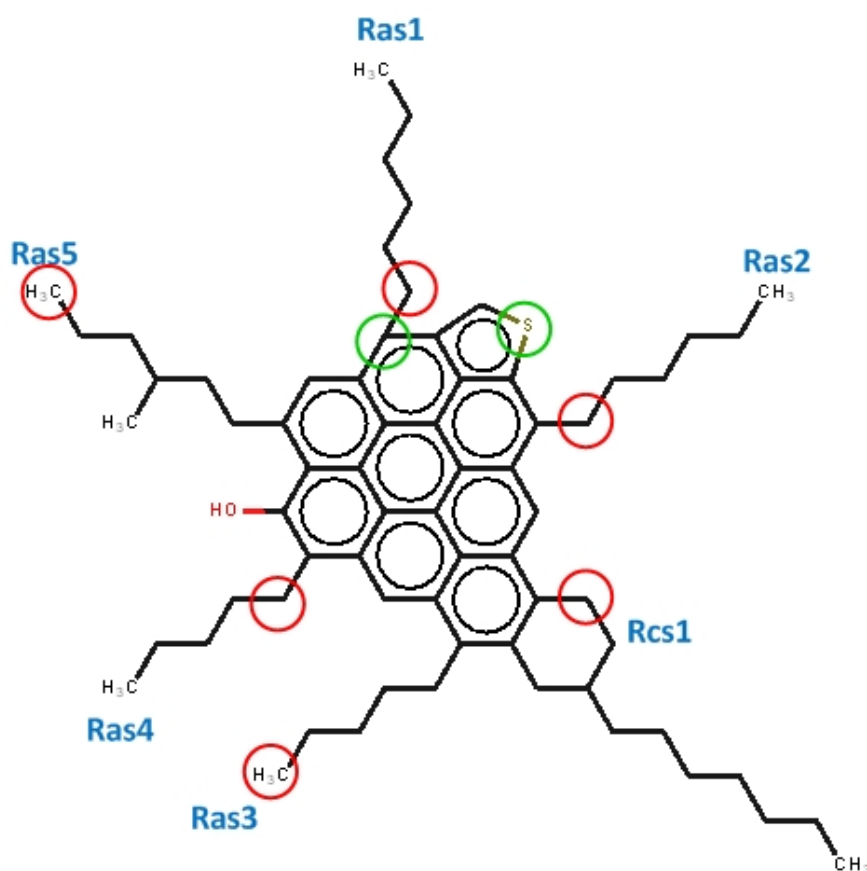


Figure 5.18: Reactive sites (circles) in the CR structure with substituent labels

- Castilla Resin (CR): in the case of the CR surrogate, eight sites were identified as highly reactive (Figure 5.18). In the large condensed aromatic structure, a carbon and a sulfur atoms (Figure 5.18 green circles) presented the highest values. In spite of this, the position of the carbon atom allowed to discard it as a site for an electrophilic attack, as a reaction in this site would imply the alteration of the structure aromaticity, which is not a viable option according to the study carried out above for aromatic molecules (MA and PA). In the case of the sulfur atom, the study conducted for PA identified this as a possible place for the addition of oxygen; however, during the evolution of the oxidation process, oxygen tended to leave the sulfur atom to form bonds with other atoms in the surroundings. Based on that fact, the addition of oxygen to the sulfur atom may be considered but, oxygen is not expected to stay bonded to that site.

Other sites of the CR structure also presented reactive characteristics. In four (Ras1, Ras2, Rcs1 and Ras4) of the six substituents the most-reactive atom is one of the *H* atoms bonded to the nearest carbon to the large aromatic structure, which was expected because the abstraction of those types of atoms lead to the production of highly-stable radicals. Based on the type of radical

that these abstractions may produced, those reactive sites are expected to present the behavior showed by the molecules produced in the oxidation process of MA (Monocyclic aromatic). On the other hand, in the substituents Ras3 and Ras5, the most reactive sites were found at the end of the chains. Based on this, an H-abstraction reaction in those places would form primary radicals, those that were analyzed in the previous sections for the NS (Normal Saturate). Therefore, these sites of the CR could evolve as the NS surrogate did.

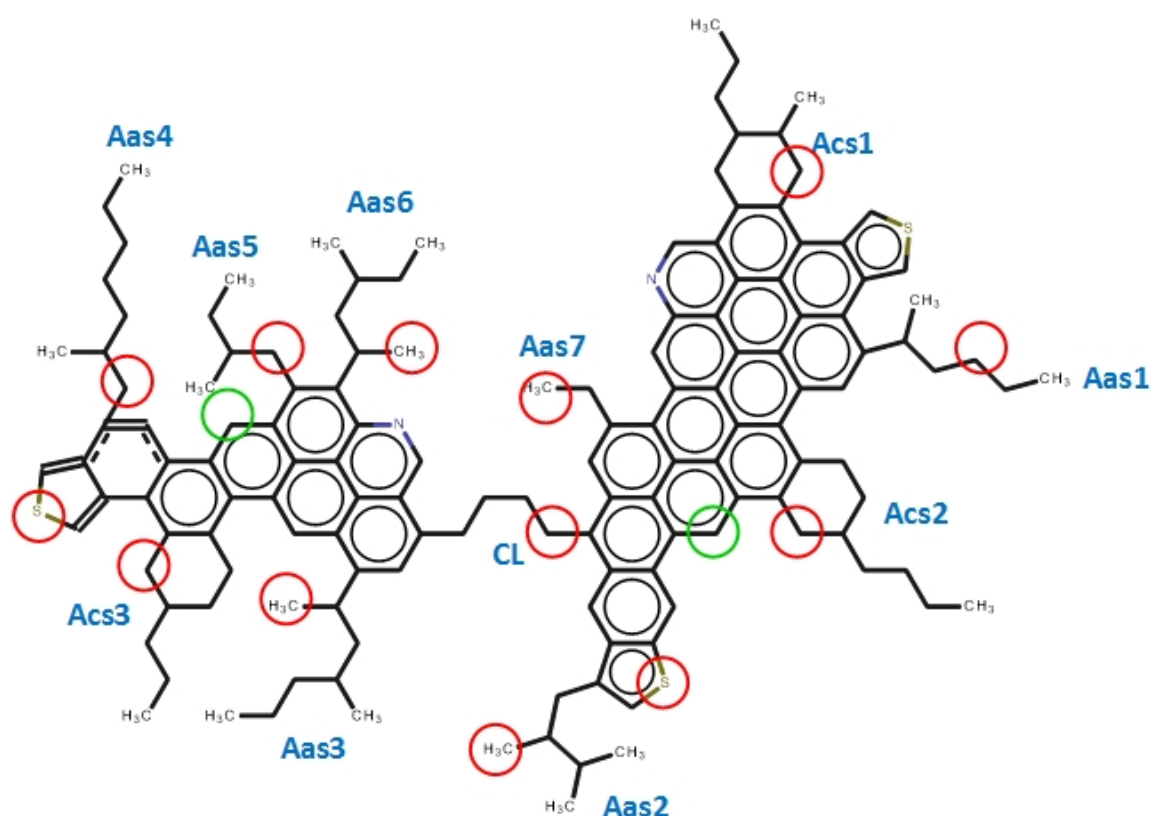


Figure 5.19: Reactive sites (circles) in the CA structure with substituent labels

- Castilla Asphaltene (CA): given the great size of the surrogate structure, 15 places were identified as highly reactive (Figure 5.19). In two of those places, those that involve sulfur atoms, the reactive character is high and, as in the CR case, it is possible that an oxidation process conducted in this place tends to move to another atoms in the surroundings. The rest of the atoms identified are hydrogen in different parts of the structure, in the substituents and in the large condensed structure. Acs1, Acs2, CL, Acs3, Aas4 and Aas5 presented a behavior closer to the one showed by the MA surrogate, i.e. the formation of resonance-stabilized radicals. On the other hand, the places marked with the green circles could be places for an electrophilic attack if the steric hindrance introduced by the several substituents allows. Given that, during the evolution of MA

a benzene radical was produced, that information applies to describe the oxidation process in green sites. Aas2, Aas3, Aas6 and Aas7 are located in sites that allow the formation of primary radicals. In spite of this, it is not possible to affirm that they may proceed as NS did, because their structures are branched alkanes and not normal alkanes; therefore, the evolution, energies and products could change. Finally, in the Aas1 substituent, a hydrogen atom in the middle of the chain was identified as the one with the highest reactivity, result that could not be identified as similar to another one in this study.

5.4. Conclusions

- The electrophilic topological and electrophilic condensed Fukui function calculations carried out for saturates and aromatic surrogates identified the same high reactive sites in the CS, NS, MA and PA molecules.
- The PA and olefin surrogates did not proceed by the H-abstraction route in the initiation event of the LTO process. Given the presence of a sulfur atom or a double bond, those molecules underwent the initiation process by the intermolecular addition of O_2 and even the alternative oxidant agent $\bullet OH$.
- The role of $\bullet OH$ could be considered by future ISC studies as this species may act as an effective oxidant agent. Reactions that involve this reactant were highly exothermic, which certainly increases the lifetime of their products. Nevertheless, it is important to highlight that the contribution of this radical to the oxidation process, depends on its equilibrium concentration and temperature conditions.
- $HO_2\bullet$ was identified as a compound for the transport of hydrogen atoms. In the beginning of the process, oxygen abstracts a hydrogen atom from hydrocarbon molecules to form $\bullet R$ and $HO_2\bullet$ radicals. In the subsequent steps, $HO_2\bullet$ releases the hydrogen atom to allow the formation of compounds such as alcohols or peroxides.
- Several olefins were formed during the oxidation process by β -scission and intermolecular H-abstraction reactions, during the propagation and termination events. These routes constituted the explanation for the formation of lighter hydrocarbons during an oxidation process.
- Two types of molecules were identified as fundamental in the oxidation process, peroxy radicals and peroxides with dangling bonds. From the evolution of those species several routes such as

intermolecular and intramolecular H-abstractions and intermolecular additions were identified to produce many oxygenated products.

- Each of the saturate and aromatic surrogates underwent an oxidation process producing several oxygenated compounds such as, ketones, peroxides, aldehydes, ethers (cyclic and long chain) and acids. The products obtained also contained two or more functional groups associated to oxygen.
- The molecules obtained in the development of the reaction pathways for the LTO process were in agreement to the results obtained by some ISC studies [13, 63], which have attempted to describe, by experimental methodologies, the evolution of species during the ISC oxidation process at low temperature.

Chapter 6

Thermal cracking reaction pathways

This chapter describes the formulation of the thermal cracking reaction pathways. As in the LTO case, for saturate and aromatic surrogates, the reactions were studied in detail, whereas, for resin and asphaltene molecular systems, a less detailed analysis was carried out based on the conclusions made for the lighter surrogates.

The first section of the chapter presents a methodology diagram, which condenses the step to develop the LTO reaction pathways. Next, the section that describes the results is presented. In that section six main topics are discussed: Formation of free radicals, Initiation, Propagation, Other intermediate formation and termination, Reaction route for coke formation and Thematic Database results. Finally the chapter finalizes with a section for conclusions .

During the chapter, the author explains the development of the pathways; however, detailed reaction schemes are in the appendixes. Based on that, for more detail in the structures and reaction energies obtained from the study of the reactions in the different events see the appendixes of this thesis.

6.1. Methodology

Figure 6.1 shows the diagram that explains the steps followed to analyze the chemical evolution of species during the thermal cracking process. The chapter 3 presented a more detailed explanation about the steps condensed in the diagram. In the Step 1, the surrogate structures are optimized to obtain ground state structures. The Step 2 considers the performance of NBO simulations to calculate bond orders (through Wiberg Index). During the Step 3, bond orders for all surrogate structures are analyzed to determine the most probable breaking sites. The Step 4 involves the analysis of the formation of free radicals, which considers bond orders and reaction energies of bond dissociation reactions. In the Step 5, initiation reactions are considered with surrogate structures as reactants and several radicals are the products for the event. Step 6 takes into account the radicals produced

during the Step 5 to apply propagation reactions, producing alkenes and more radicals ($\bullet R$). The Step 7 involves radicals produced during the Step 6 as reactants for the Other intermediate formation and Termination events, with several radicals and hydrocarbons as products. Additionally, compounds considered in the Steps 5 to 7 are simulated in the Step a to obtain optimized structures and its energies in order to calculate reaction energies in the Step b. In the last step, Step 8, chemical structures and reaction energies considered and calculated during the previous steps were taken into account in order to build reaction schemes.

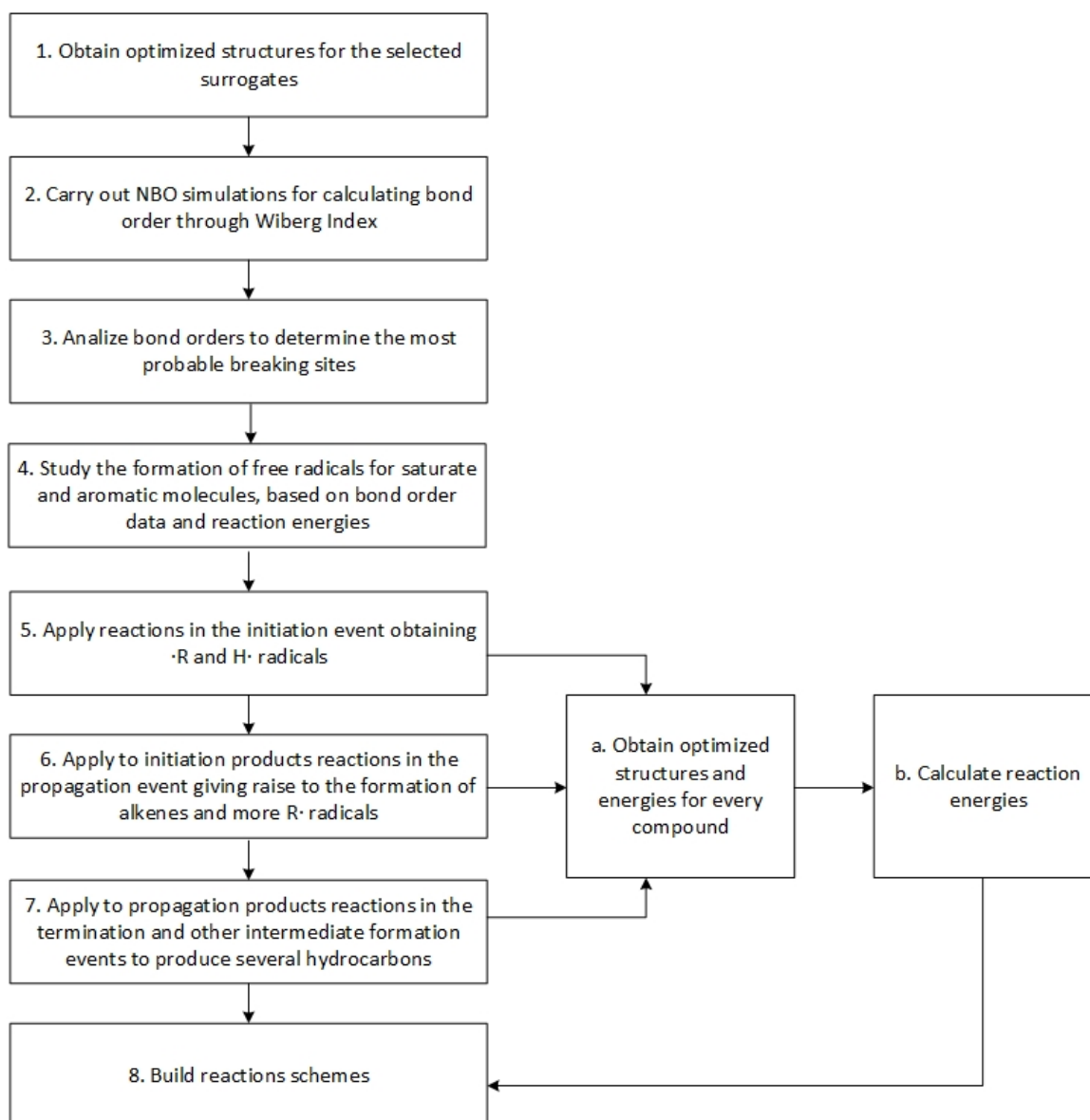


Figure 6.1: Methodology diagram for the formulation of the thermal cracking reaction pathways

6.2. Results

6.2.1. Formation of free radicals

The most accepted reaction mechanisms [21–36,65] in this field described that at thermal cracking ISC conditions the chemical evolution of hydrocarbon molecules proceeds by free radical formation. Those species have as main characteristic dangling bonds that constitute active sites, and its production takes place by bond breaking. Based on that, the information to analyze the production of free radicals was obtained from NBO calculations by the analysis of bond orders (through Wiberg index).

For the saturate and aromatic surrogates, the breakings of carbon-hydrogen ($C - H$) and carbon-carbon ($C - C$) bonds were analyzed based on a radical formation study that identified the weakest $C - C$ and $C - H$ bonds, linking bond order data with reaction energies. In addition, given the structures of saturate and aromatic surrogates, it was possible to identify some symmetry planes. The presence of a symmetry plane in a molecule could imply, atoms in both sides of the plane had the same characteristics, hence only the breaking of bonds in one the sides of the molecules were studied. On the other hand, for resin and asphaltene surrogates, since only $C - C$ bonds breaking were taken into account, a study as the one mentioned before was not necessary.

- Saturates: the free radical formation study involved the simulation of all possible breaking of bonds in the molecules: Cyclic Saturate (CS) and Normal Saturate (NS). Starting structures with their symmetry planes are showed in Figure 6.2 a for the CS surrogate and in Figure 6.2 b for the NS structure. Tables 6.1 and 6.2 present the results obtained from the free radical study. They include type of bond, $C - H$ or $C - C$, label numbers of the bonded atoms, bond orders and energy reactions. For both surrogate structures, CS and NS, it was possible to determine that there were two bonds that were more likely to undergo the breaking process. In the case of CS, the bonds 7 and 12 were selected; each of them had the lowest bond order and energy reaction in their type, $C - H$ and $C - C$ bonds respectively. For NS, the bonds 8 and 11 were selected. As in the CS case, both bonds presented the lowest bond orders and energy reactions in their categories. In addition, for NS, it was possible to identify that each of the two hydrogen atoms bonded to the carbon atoms in the molecule, had the same bond order and reaction energy, which implies that, as expected, no distinctions have to be done between hydrogen atoms bonded to the same carbon atom in a normal saturate. It is important to mention that symmetry restriction were not taking into account during calculations with the aim to obtain electronic structure information.

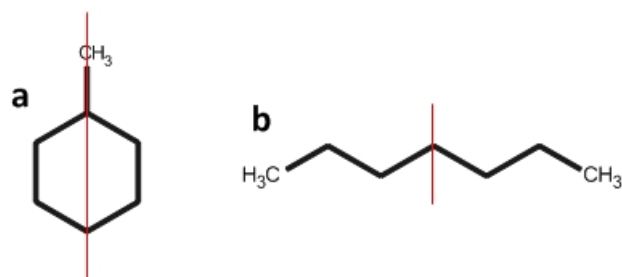


Figure 6.2: Symmetry planes of saturate structures. a) Symmetry planes for the CS surrogate. b) Symmetry planes for the NS surrogate.

Table 6.1: Results of free-radical formation study for Cyclic Saturate (CS)

Type of bond	Bond number	Atom 1	Atom2	Bond order	Reaction energy (kcal/mol)
<i>C – H</i>	1	1	10	0.9179	104.19
	2	1	11	0.9184	104.19
	3	2	8	0.9178	103.80
	4	2	9	0.9175	103.80
	5	3	7	0.9185	103.97
	6	3	17	0.9183	103.97
	7	4	12	0.9012	98.61
	8	18	19	0.9328	107.09
	9	18	21	0.9329	107.09
<i>C – C</i>	10	1	2	1.0125	87.69
	11	2	3	1.0121	87.47
	12	3	4	0.9972	83.35
	13	4	18	1.0112	87.81

Table 6.2: Results of free-radical formation study for Normal Saturate (NS)

Type of bond	Bond number	Atom 1	Atom2	Bond order	Reaction energy (kcal/mol)
<i>C – H</i>	1	1	3	0.9336	108.30
	2	1	4	0.9334	108.34
	3	1	5	0.9334	108.34
	4	2	7	0.9173	104.62
	5	2	8	0.9173	104.62
	6	6	10	0.9168	104.54
	7	6	11	0.9168	104.54
	8	9	12	0.9165	104.45
	9	9	13	0.9165	104.45
<i>C – C</i>	10	1	2	1.0284	93.06
	11	2	6	1.0156	89.39
	12	6	9	1.0164	89.71
	13	9	14	1.0163	89.70

- Aromatics: the free radical formation study for aromatic surrogates, involved the simulation of all possible *C – C* and *C – H* bond breakings in the Monocyclic Aromatic (MA) and Polycyclic Aromatic (PA) molecules. The scission of *C = C* bonds was not analyzed because it was determined that this type of breaking is not possible at ISC temperatures. A symmetry plane was identified for the MA structure. Figure 6.3 shows the mentioned plane. In the case of the PA, the presence of heteroatoms and the mixture of sizes in the aromatic rings did not allow to identify any symmetry planes.

Tables 6.3 and 6.4 present the results obtained from the free radical study carried out for MA and PA. For MA surrogate, bond 4 was selected as the weakest one, by the two criteria applied, bond order and reaction energy. In the PA case, it was possible to identify two *C – H* bonds, as the most likely places for the breaking. Bonds 2 and 5 were selected because, only in this case, the bond with the lowest bond order was not the one with the lowest energy reaction. Based on that, the two *C – H* cleavages were considered, the one with the lowest bond order and the one with the lowest energy reaction. The author attributes this deviation in the normal behavior of bond order data to the presence of the sulfur atom in PA, which affects the resonance character of the aromatic rings.

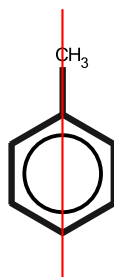


Figure 6.3: Symmetry planes of aromatic structures

Table 6.3: Results of free-radical formation study for Monocyclic Aromatic (MA)

Type of bond	Bond number	Atom 1	Atom2	Bond order	Reaction energy (kcal/mol)
<i>C – H</i>	1	1	7	0.9173	117.23
	2	2	8	0.9175	117.12
	3	6	11	0.9173	117.70
	4	12	13	0.9128	94.90
	5	12	14	0.9278	94.90
	6	12	15	0.9282	94.90
<i>C – C</i>	7	3	12	1.0288	104.84

Table 6.4: Results of free-radical formation study for Polycyclic Aromatic (PA)

Type of bond	Bond number	Atom 1	Atom2	Bond order	Reaction energy (kcal/mol)
<i>C – H</i>	1	1	7	0.9111	117.87
	2	4	8	0.9138	117.68
	3	5	9	0.9158	117.87
	4	6	10	0.9155	117.80
	5	11	14	0.9022	120.14
	6	13	15	0.9088	122.16

6.2.2. Initiation

Based on the information provided by the section of study of free radical formation, the initiation event products were determined for the six surrogates.

- Saturates: Figure 6.4 presents the structures of the radical species obtained from the selected $C - C$ and $C - H$ breakings in the CS and NS molecular systems. These species are called, from now on, Saturate Initiation Products (SIP). Breaking of the CS bonds led a tertiary cyclic radical (Figure 6.4 b), an alkyl chain biradical (Figure 6.4 c) and a hydrogen radical atom (Figure 6.4 a). Free radicals increase their stability directly proportional to their order. Based on that, the most stable compound produced was the tertiary free radical, followed by the alkyl biradical that combines a secondary and a primary free radical, and finally, the hydrogen radical atom that is the least stable. In addition, breaking of NS bonds produced one secondary (Figure 6.4 d), two primary (Figure 6.4 f and g) and one hydrogen radical (Figure 6.4 e). The most stable compound produced was the secondary free radical, followed by the two primary and the hydrogen.

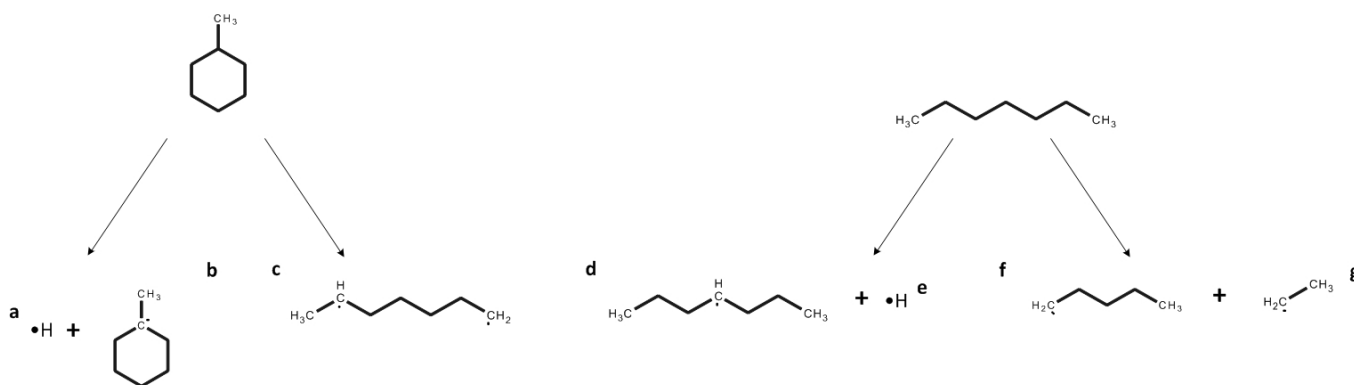


Figure 6.4: Saturate initiation products (SIP). a) Hydrogen radical from CS. b) Tertiary cyclic radical from CS. c) Biradical from CS. d) Secondary radical from NS. e) Hydrogen radical from NS. f and g) Primary radicals from NS

Table 6.5 presents the energy results obtained from the study of the unimolecular initiation reactions for saturate and aromatic surrogates. For CS, the production of the tertiary and the hydrogen radical required an energy of 98.61 kcal/mol, whereas, the formation of the biradical presented an energy of 83.35 kcal/mol. Based on these and other results presented in this chapter, one can conclude that in general the breaking of a $C - H$ bond requires a higher energy compared to the breaking of a $C - C$ bond. For the radicals produced from NS, as in the CS case, the highest reaction energy was calculated for the production of the hydrogen radical atom, 104.44 kcal/mol. On the other hand, the breaking of $C - C$ bond that led to the formation of two primary radicals, presented an energy of 89.39 kcal/mol.

Table 6.5: Summary of unimolecular initiation reactions for saturate and aromatic surrogates

Reactant	Route	Products	Reaction energy (kcal/mol)
CS	$C - H$ cleavage	Tertiary and hydrogen radicals	98.61
	$C - C$ cleavage	Biradical	83.35
NS	$C - H$ cleavage	Secondary and hydrogen radicals	104.44
	$C - C$ cleavage	Two primary radicals	89.39
MA	$C - H$ cleavage	Stabilized by resonance and hydrogen radicals	94.90
PA	$C - H$ cleavage	Secondary and hydrogen radicals	117.68
		Secondary and hydrogen radical	120.14

- Aromatics: according to the literature review carried out, unsaturated molecules such as olefins or aromatics could undergo unimolecular and bimolecular initiation reactions. Unimolecular reactions consist the breaking of $C - C$ and $C - H$ bonds, whereas, bimolecular reactions involve the transference of a hydrogen atom by the contact of two unsaturated molecules, in order to produce two radical species.

Figure 6.5 presents the structures of the radical species obtained from unimolecular and bimolecular initiation reactions. These species are referred, from now on, as Aromatic Initiation Products (AIP). Breaking in the MA and PA surrogates produced two secondary (Figure 6.5 b and d), two hydrogen (Figure 6.5 c and e) and one primary radicals (Figure 6.5 a). Contrary to the theory that describes free radical stability, the primary radical formed by MA (Figure 6.5 a) is the most stable one, because of the resonance from the benzene ring. The flow of electrons from the aromatic structure mitigates the effect of the dangling bond, which has a big influence in the radical stability. This result constituted a great contribution from the aromatic reaction pathway to the study of the chemical evolution of resin and asphaltene surrogates, because, given the presence of large aromatic nuclei in their structures, those molecules tended to form in most of the cases radicals stabilized by resonance.

From the bimolecular initiation reactions, different kind of radicals (Figure 6.5) were obtained:

two primary stabilized by resonance (Figure 6.5 f and h) and four secondary (Figure 6.5 g, i, j and k). Five of these radicals (Figure 6.5 f, h, i, j and k) were also produced by the unimolecular initiation reactions previously explained; however, the radical in Figure 6.5 g could be produced only by a bimolecular initiation reaction, i.e. the addition of a hydrogen molecule to the MA ring. The production of this radical changed in the aromaticity of MA, which gave rise to the formation of a dihexene radical from an aromatic molecule, result that constituted an important fact in order to explain the production of lighter species from aromatic compounds.

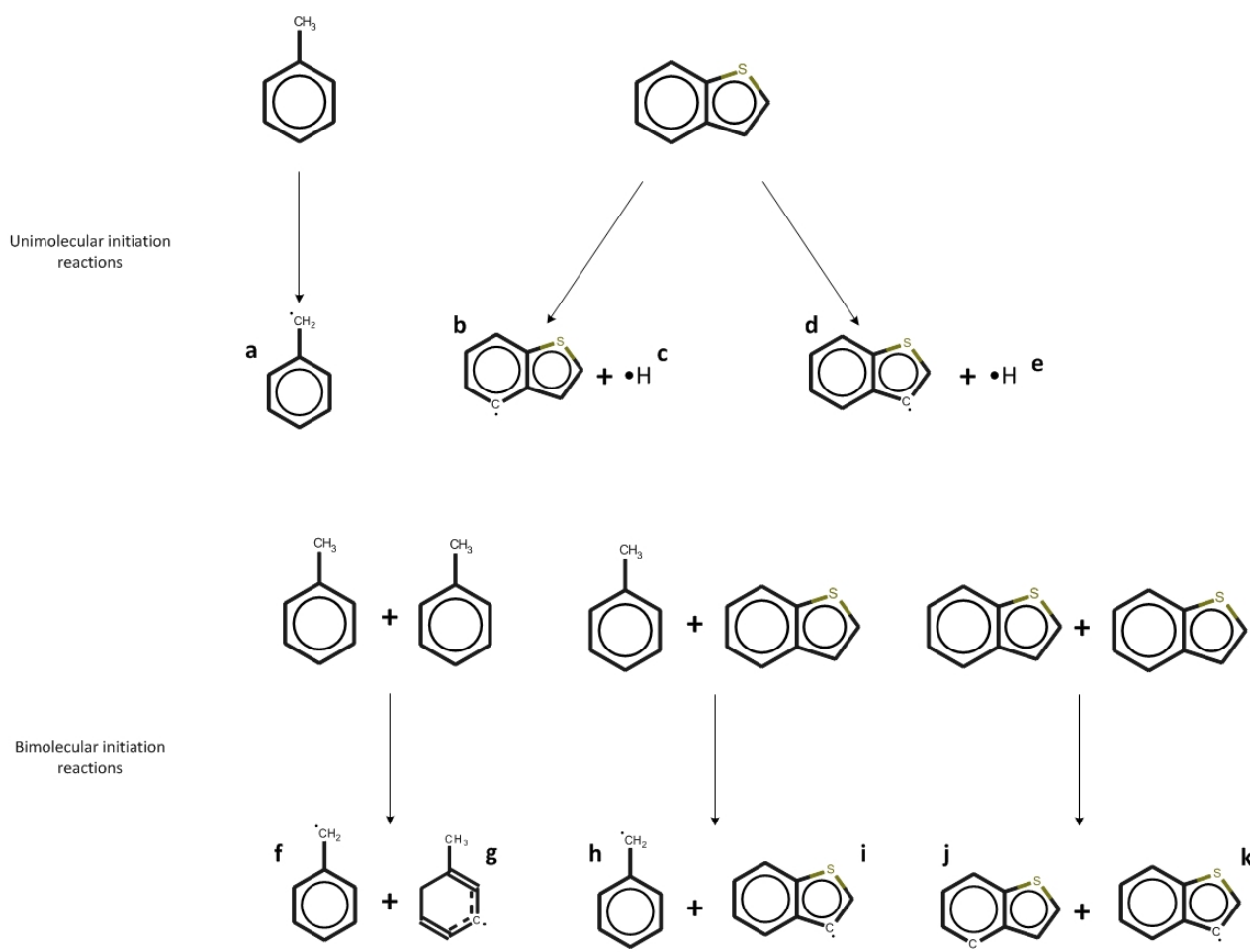


Figure 6.5: Aromatic unimolecular and bimolecular initiation products (AIP). Unimolecular initiation reactions: a) Stabilized by resonance radical from MA b) Secondary radical from PA c) Hydrogen radical from PA d) Secondary radical from PA e) Hydrogen radical from PA. Bimolecular initiation reactions: f) Stabilized by resonance radical from MA g) Dihexene radical from MA h) Stabilized by resonance radical from MA i) Secondary radical from PA j) Secondary radical from PA k) Secondary radical from PA.

The reaction energies for the formation of the aromatic radicals by $C-H$ and $C-C$ cleavages varied from 94.9 to 120.14 kcal/mol. For the bimolecular initiation reactions, reaction energies presented in Table 6.6 varied from 52.43 to 75.22 kcal/mol. The calculated energies were highly affected by the stabilization of radicals and the presence of sulfur atoms, which tended to reduce and increase, respectively, the reaction energies related to the reactions associated to MA and PA.

Table 6.6: Summary of bimolecular initiation reactions for aromatic surrogates

Reactant 1	Reactant 2	Products	Reaction energy (kcal/mol)
MA	MA	Stabilized by resonance and dihexene radicals	65.26
MA	PA	Stabilized by resonance and secondary radicals	52.43
PA	PA	Two secondary radicals	75.21

- Castilla Resin (CR): the surrogate structure selected to represent the resin fraction has 168 bonds. Figure 6.6 presents the distribution of bond orders for the 168 bonds. The figure makes evident the existence of three ranges of bond orders. The red square groups bond orders from 1.09 to 1.53, which represent the double or resonant carbon-carbon bonds and double, resonant or simple carbon-heteroatom (oxygen or sulfur) bonds. These bond orders have an average value of 1.3; however, some of them presented lower or higher values, which depends in the aromatic character, e.g. a double bond has a higher bond order than a resonant bond. In the case of the carbon-heteroatom bonds, for the two bonds that involved the sulfur, bond order values were 1.09 and 1.2, whereas, for the carbon-oxygen bond was 1.01. In the case of the carbon-sulfur bonds, although both of them connect with the same sulfur atom, the presence of other substituents in the surroundings may cause weakening or strengthening, which explains the difference in bond order values and hence, their reactivity behavior.

The blue square delimits the bond order interval for carbon-carbon bonds. It has an average value of 1.01. Deviations from this value results from the existence of different types of $C-C$ bonds in the structure. Some bonds made part of the cyclohexane structures, those had a lower bond order when compared to the average value. The rest of the bonds made part of alkyl chains. Three differences were found among those bonds. i) The bond between an alkyl chain and an aromatic structure was, in most cases, the weakest and presented lower bond orders. ii) Internal $C-C$ bonds in alkyl substituents presented values close to the average, with some

exceptions when chains were branched, which implies changes in the weakest bonds because breaking of branched chains may lead to the formation of high order radicals. iii) In general, terminal bonds of the chains presented higher bond orders, because breaking of these type of bonds would produce methyl radicals, which are highly unstable.

The last interval in Figure 6.6 is the one defined by the green square, which groups bond order data for $C - H$ bonds. As in the $C - C$ case, it was possible to identify three different types: hydrogens near to the aromatic nucleus, hydrogen bonded to internal carbon atoms and terminal hydrogens. The lowest bond order values were calculated for those near to the aromatic nucleus, whereas, the highest for terminal hydrogens.

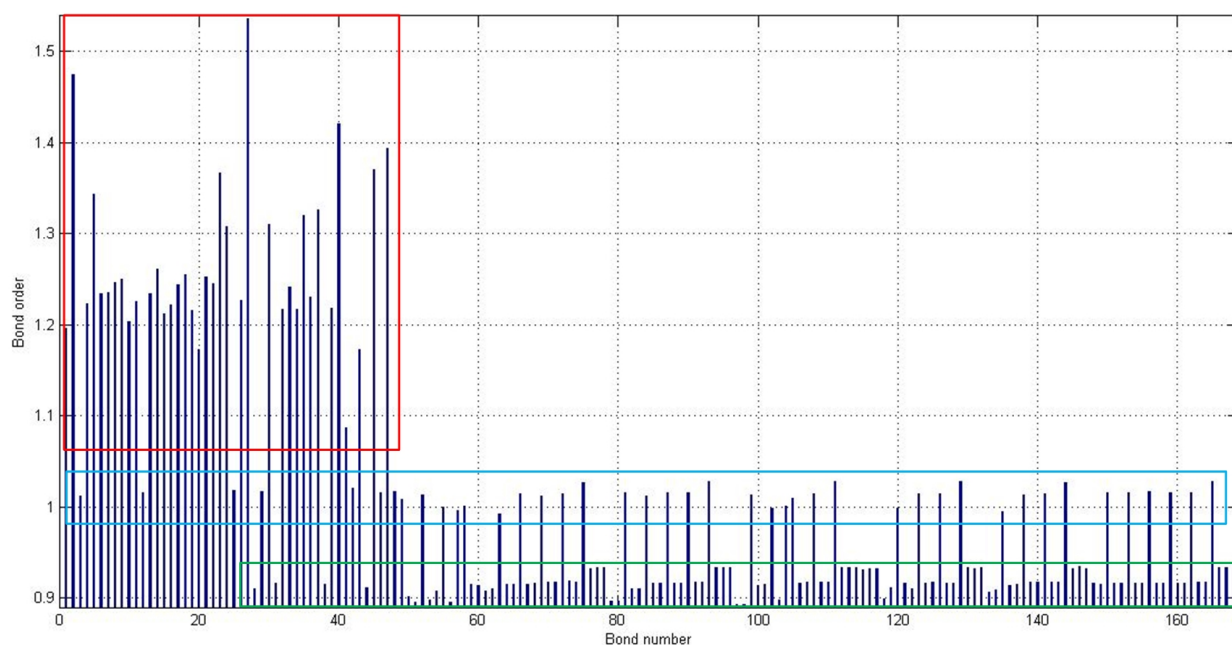


Figure 6.6: Frequency plot for bond order for the bonds in the CR surrogate

Based on the analysis of these data, the breaking of the $C - C$ bonds with the lowest value for each of the parts in the resin structure, was considered. Figure 6.7 shows the resin structure with the proposed breaking sites as red lines.

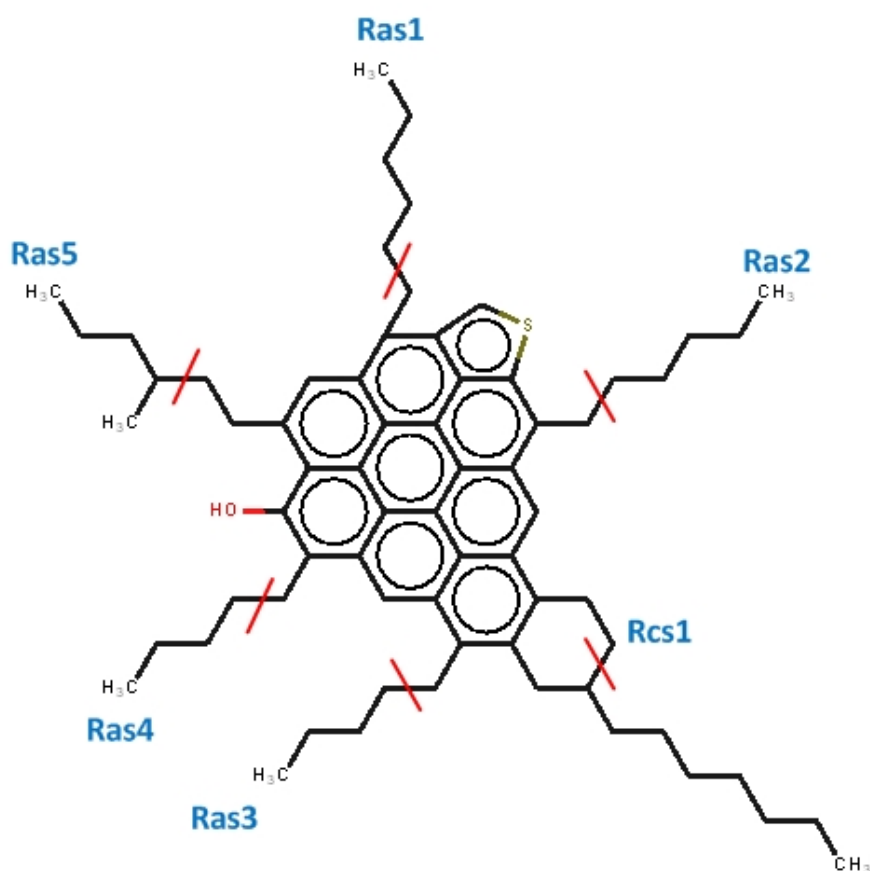


Figure 6.7: Castilla Resin structure. The red lines indicate the places where it is more possible that the bonds break

Table 6.7 summarizes the reactant site, products and reaction energies obtained from the selected breakings. For the breakings in Ras1, Ras2, Ras3 and Ras4 the energy reaction calculated was 76 kcal/mol. This case constituted the most common one, because the formation of radicals stabilized by resonance is the most likely breaking event in this type of structures. Due to its frequent occurrence, the value associated to this kind of breaking was used as a comparison point. In the case for the opening of the Rcs1 structure, the energy required was determined as 83 kcal/mol, which is higher when compared to the most probable breaking. This result is explained because the opening in a chair hexane structure produced two radicals and, although one of the them was also stabilized by resonance, the formation of two radical species required higher energy. The breaking of the branched chain (Ras5) did not produce stabilized radicals; therefore, the reaction energy was 84 kcal/mol, higher when compared to the value of 76 kcal/mol. As it was explained in the Chapter 3, the calculation of a reaction energy imply the performance of optimization calculations that required high computational costs. Based on that, Table 6.7

presents approximated reactions energies that were calculated by the simulation of parts of the molecule.

Table 6.7: Summary of $C - C$ cleavage as initiation reactions for Castilla Resin (CR)

Reactant site	Products	Reaction energy (kcal/mol)
Ras1		
Ras2	Stabilized by resonance and primary radicals	≈ 76
Ras3		
Ras4		
Rcs1	Secondary bonded to the aromatic nucleus and primary radicals	≈ 83
Ras5	Primary bonded to the aromatic nucleus and secondary radicals	≈ 84

Figure 6.8 shows the structures of the radicals produced by the initiation event for the resin structure. Those radicals were named Resin Initiation Products (RIP).

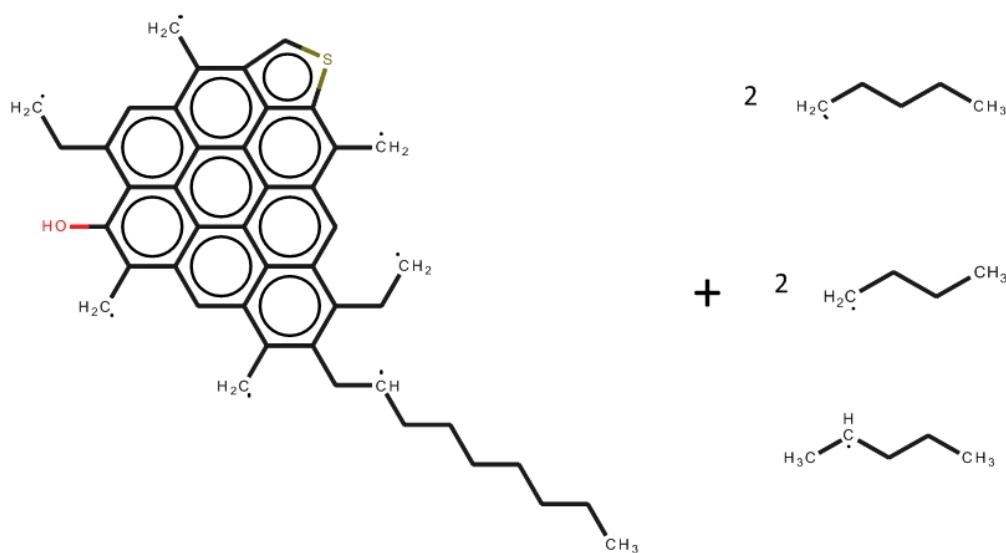


Figure 6.8: Castilla resin initiation products (RIP)

- Castilla Asphaltene (CA): the surrogate structure selected consisted of 335 bonds. For the asphaltene molecule, the graphic obtained from bond order data analysis is not presented by this thesis because, given the similarities between CR and AR structures, the same zones identified for the CR molecule were shown by this structure. Figure 6.9 presents the most-likely breaking

sites in the asphaltene structure.

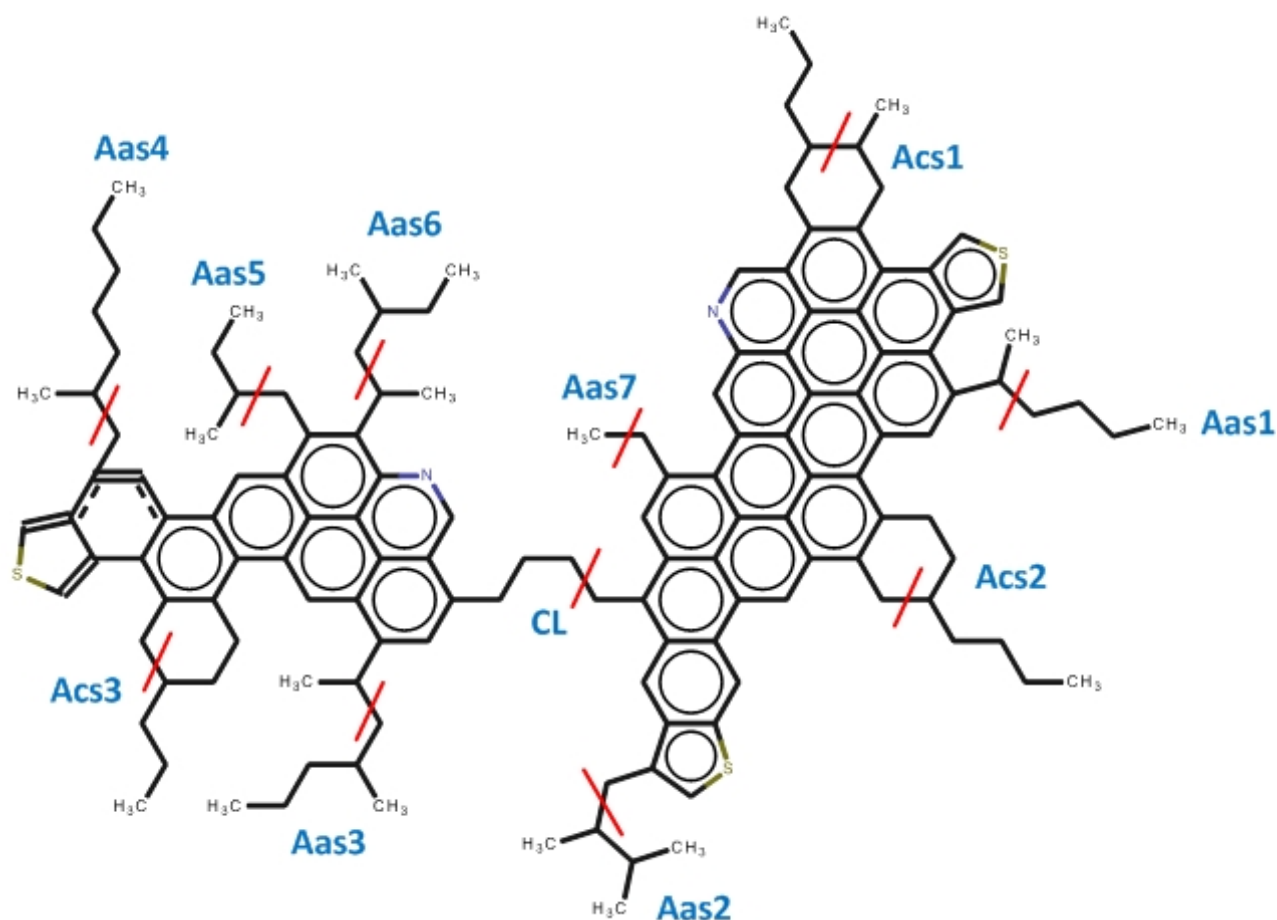


Figure 6.9: Castilla Asphaltene structure. The red lines indicate the places where it is more possible that the bonds break

Table 6.8 summarizes the reactant site, products and reaction energies obtained from the selected breakings for the Castilla asphaltene. In bonds Aas1, Aas3, Aas4 and Aas5, the fragmentation left at least one carbon atom bonded to the big aromatic structure and produced a primary or a secondary free radical; the energy needed for this to occur was calculated as 71 kcal/mol. As was the case for the CR, this kind of breaking is the most common during the process, because one of the atoms with the dangling bond is highly stabilized by the electron flow (resonance), from the big aromatic structure.

A fragmentation in the sites Acs1, Acs2 and Acs3 produced an opening in the chair structure of a cyclohexane. This reaction has an energy difference of 83 kcal/mol, which is higher compared to the reference value. Nevertheless, this reaction produces two radical species, one of them stabilized by resonance. The rise in the reaction energy could be due to the fact that it affects

a cyclic hydrocarbon, which has a chair configuration in its structure. In spite of the proximity of heteroatoms that usually affect the normal electronic behavior of the big aromatic structure, the breakings in Aas2 and Aas6 had reaction energies of 67.59 kcal/mol and 68.77 kcal/mol respectively; which are close to the most common result, 71 kcal/mol. On the other hand, the breaking in Aas7 needed 79 kcal/mol, a higher amount if it is compared to the most common case. The reason for this higher value is the production of a methyl radical, which is more unstable than the other primary radicals produced. In the case of site CL, where the two big aromatic structures were separated, the energy difference of the reaction is 76.06 kcal/mol, which is also near to the reference value.

Table 6.8: Summary of $C - C$ cleavage as initiation reactions for Castilla Asphaltene (CA)

Reactant site	Products	Reaction energy (kcal/mol)
Aas1 Aas3	Stabilized by resonance and primary radicals	≈ 71
Aas4 Aas5	Stabilized by resonance and secondary radicals	≈ 68
Acs1	Two secondary radicals (come from chair cyclohexane structure opening)	≈ 83
Acs2 Acs3	Stabilized by resonance and secondary radicals (come from chair cyclohexane structure opening)	≈ 79
Aas2	Stabilized by resonance (near to a sulfur atom) and secondary radicals	≈ 68
Aas6	Stabilized by resonance (near to a nitrogen atom) and primary radicals	≈ 67
Aas7	Stabilized by resonance and methyl radicals	≈ 79
CL	Stabilized by resonance and primary radicals (breaking in the alkyl chain that tied the aromatic nuclei)	≈ 76

The radicals obtained from this process are shown in Figure 6.10. Those are referred from now on as asphaltene initiation products (AsIP).

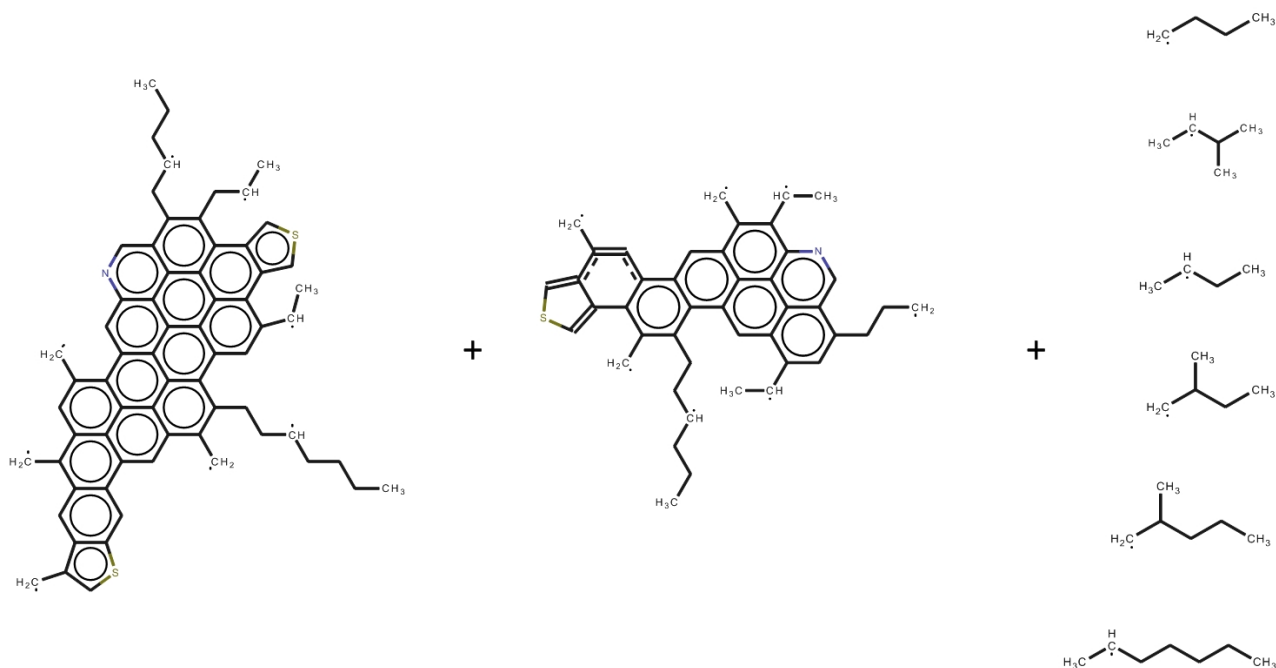


Figure 6.10: Castilla Asphaltene (CA) initiation products (AsIP)

6.2.3. Propagation

Three types of reactions have been identified in this event: intermolecular H-transfer, β -scission and isomerization.

- Intermolecular H-transfers: important for species that contained less than 20 carbon atoms. Intermolecular H-transfer reactions did not constitute a probable route when large compounds were involved, as it would imply a direct contact between two molecular structures; that would not be easy taking into account the size of the structures selected for the resin and asphaltene fractions and the effect of steric hindrance. The products from this type of reactions were hydrocarbon species without dangling bonds and radicals. The reaction energies related to this type of reactions were in the range from -5 to ≈ 0 kcal/mol. These reactions did not form final products, the hydrocarbon species produced by these transformations always tend to undergo breaking processes as those explained for the initiation event.
- β -scission: constitute fundamental reactions in a thermal cracking process and have been identified as the main responsible for the formation of terminal olefins during the process. The reaction energies calculated for β -scission reactions were of ≈ 25 kcal/mol when breaking a $C-C$ β bond. For a $C-H$ bond the energy required for the breaking was of ≈ 44 kcal/mol.
- Isomerization: only the exothermic isomerization reactions were studied. Reaction energies for

these reactions were calculated, obtaining a range from approximately -5 to values near to 0 kcal/mol. These reactions do not occur when resonance radicals are produced. The resonance effect that made of those radicals stable highly increases the energy required for isomerization reactions. In addition, the application of these reactions to the large aromatic radicals in Figures 6.8 and 6.10 became impossible given the lack of alkyl substituents that may form the cyclic transition states, which have been defined as a requirement for the occurrence of isomerization reactions.

6.2.4. Other intermediate formation and Termination

The last steps on the thermal cracking process are the formation of other intermediate species and termination. During these events, free radicals formed and transformed during previous stages, could follow three types of routes: i) size reduction because of additional fragmentation by $C - C$, $C - H$ cleavage or β -scission reactions. ii) constant size but changes in the bond structure by intermolecular H-transfer, disproportion or reverse radical disproportion (RRD) reactions. iii) size increase by recombination or radical addition reactions.

- Other intermediate formation: given the possible interaction of several compounds inside the reservoir, most of the reactions previously explored such as, $C - H$ and $C - C$ cleavages, reverse radical disproportion or bimolecular initiations, isomerizations, intermolecular H-transfers and β -scission reactions were considered once again. This event is named as other intermediate formation, because its products are mainly radical species.

Table 6.9 summarizes the interactions considered in this event. The presence of saturates and radical species gave rise to the occurrence of cleavage and β -scission reactions, which produced $\bullet R$ and $\bullet H$ radicals and terminal olefins. Cleavage reactions presented reaction energies in the range from 70 to 120 kcal/mol, as expected given the high dependence of the energy for this type of reactions on reactants and products. The stability of the radicals formed highly condition the reaction energy of a cleavage reaction. β -scission reactions presented energies between 25 and 44 kcal/mol, where the lowest values, i.e. close to 25 kcal/mol were for the breaking of $C - C$ bonds, whereas highest values were calculated for those reactions that involved the breaking of $C - H$ bonds. This event took into account the interaction between many types of compounds. The interaction between saturates and radicals gave rise to H-transfer reactions, which presented reaction energies from -5 to 0 kcal/mol, producing saturates and more stable radical species. The contact between olefins led to RRD reactions that produced saturates and radical species with reaction energies from 50 to 75 kcal/mol. Finally, the interaction between olefins and radicals

presented to reaction options: i) radical addition with reaction energies from -44 to -25 kcal/mol and heavier radicals as products ii) H-transfer with saturates and resonance-stabilized radicals as products, which presented reaction energies from -20 to -9 kcal/mol. The reaction energies obtained for the interactions among olefins and radicals were exothermic because from less stable species such as radicals, higher order radicals and other kind of more stable species were produced. This did not happen in the cases of cleavage reactions, where stable compounds such as saturates formed radicals that constituted less stable species leading to endothermic transformations.

Table 6.9: Summary of Other intermediate formation

Reactant 1	Reactant 2	Route	Products	Reaction energy range (kcal/mol)
Saturate	-	$C - C$ and $C - H$ cleavages	$\bullet R$ and $\bullet H$ radicals	$\approx 70 - 120$
Radical	-	β -scission	Terminal olefins and radicals	$\approx 25 - 44$
Saturate	Radical	H-transfer	New saturates and radical species	$\approx -5 - 0$
Olefin	Olefin	RRD	Saturates and radical species	$\approx 50 - 75$
Olefin	Radical	Radical addition	Heavier radicals	$\approx -44 - -25$
Olefin	Radical	H-transfer	Saturates and stabilized by resonance radical	$\approx -20 - -9$

- Termination: as its name expresses in this event the thermal cracking process terminates. For this event the interactions between two radical species produces species without dangling bonds. The reactions considered during this event were intermolecular addition and disproportion. By a intermolecular addition, two free radical molecules formed a bond producing a new hydrocarbon molecule. Regarding the disproportion reactions, two free radical molecules interacted producing an olefin and a saturated molecules. In this case one of the free radicals interacts with the other one by abstracting a hydrogen atom connected to a carbon atom next to a one with a lack in its valence, the formation of a double bond between the two carbon atoms is very possible. The energetic nature of this group of reactions was always exothermic and highly dependent on the reactants. The more unstable the reactants the higher the reaction energy. Table 6.10

summarizes the interactions, products and energies for these reactions.

Although both, intermolecular addition and disproportion reactions, were exothermic, clearly the energy ranges obtained were large compared to those showed for other types of reactions such as the ones studied in the propagation event. The explanation for those energy results is the high dependence of these reactions on the reactants involved. For example, the energy released by the addition of two hydrogen radicals cannot be comparable to the one produced by the addition of two tertiary radicals. In fact, the formation heats for these reactions depends on several structural conditions of the reactants, such as the order of the radicals.

Table 6.10: Summary of Termination

Reactants	Route	Products	Reaction energy range (kcal/mol)
Two radicals	Intermolecular addition	Heavier hydrocarbon molecules	$\approx -109 - -58$
	Disproportion	Olefin and a saturated molecules	$\approx -84 - -3$

6.2.5. Reaction route for coke formation

The chemical evolution of the large aromatic radicals, as those formed by the thermal cracking of resin and asphaltene compounds led to the formation of coke, which is a carbonaceous material important in the application of the ISC thermal recovery technique. This section focuses on the description of the route for coke formation from the asphaltene surrogate, Castilla Asphaltene (CA).

- First step: the formation of large aromatic radicals occur. The energetic nature and characteristics of these reactions were already explained. Figure 6.11 shows the surrogate structure and the radicals produced.

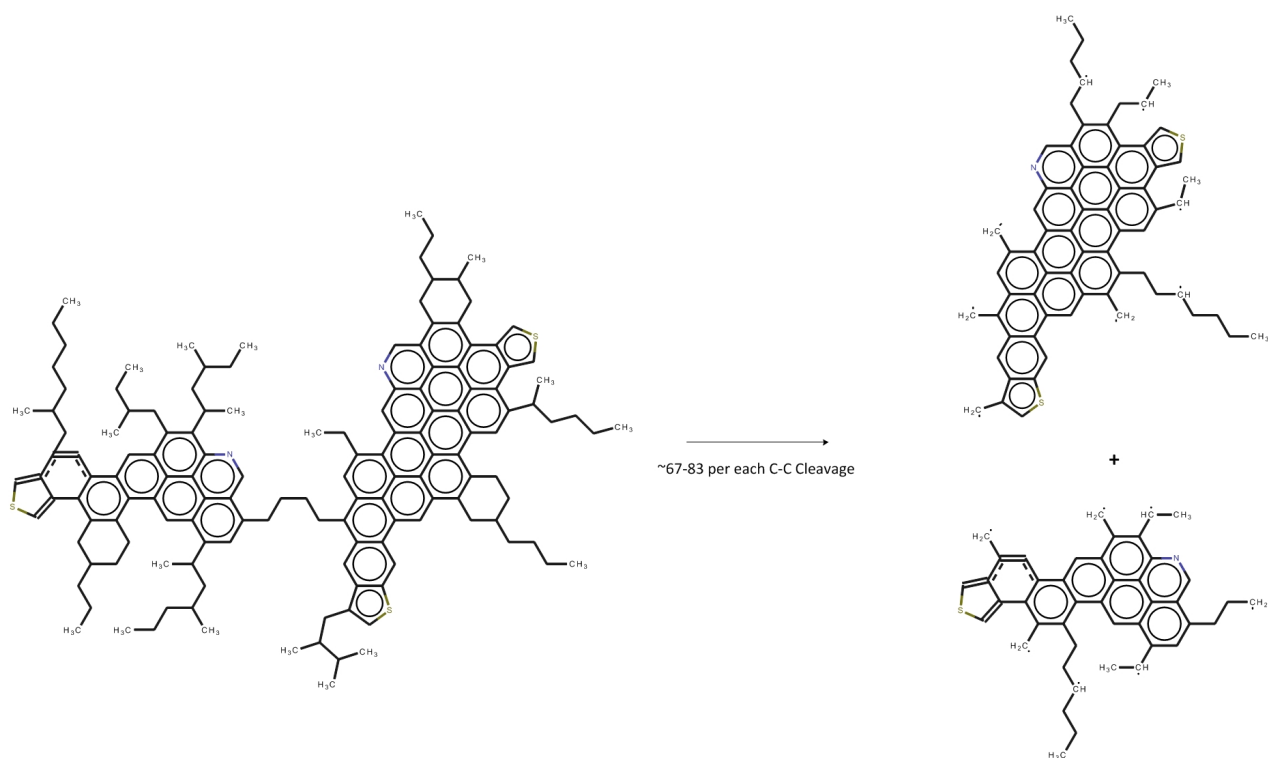


Figure 6.11: First step in the reaction route for coke formation - Initiation reactions. Reaction energies in kcal/mol

- Second step: the large aromatic radicals underwent β -scission reactions as the only propagation reaction possible to occur in this type of structures. From this type of reactions some reactive sites become species without dangling bonds. Figure 6.12 shows the species involved in this step.

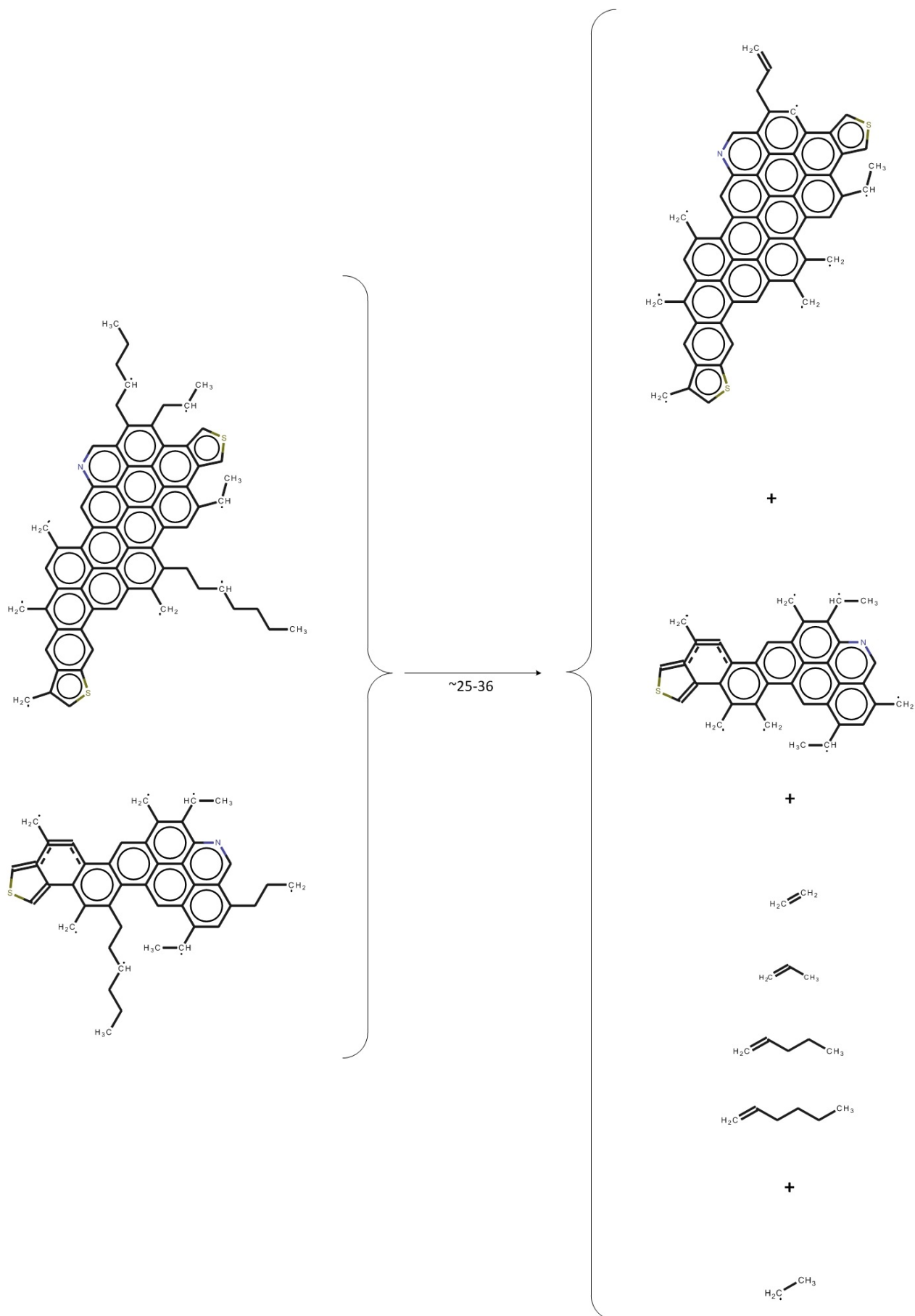


Figure 6.12: Second step in the reaction route for coke formation - Propagation reactions. Reaction energies in kcal/mol

- Third step: for the third step of the process coke molecules were formed. From disproportion reactions, the remaining reactive sites became saturated and led to the formation of several olefin compounds, the structures are shown in Figure 6.13. So far, there is not a defined and global structure accepted to represent the carbon-rich residue called coke. The structure of this material is highly dependent on the way it was produced. Thermal cracking, catalytic cracking and low temperature oxidation processes produce coke. In order to characterize and have an idea about coke composition, different parameters have been established to identify this complex material and, the hydrogen-carbon ratio (H/C) is one of the most used and it is usually a key parameter analyzed in coke samples. ISC studies have reported H/C values for coke produced by thermal cracking processes which are between 0.62 and 1.45. Based on those values and calculating the H/C ratios for the two aromatic nuclei produced in the reactions in Figure 6.13, it was possible to say that the compounds produced that have H/C ratios of 0.64 and 0.84, are possible examples of coke, which has been identified as the most abundant product from asphaltenes thermal cracking during ISC.

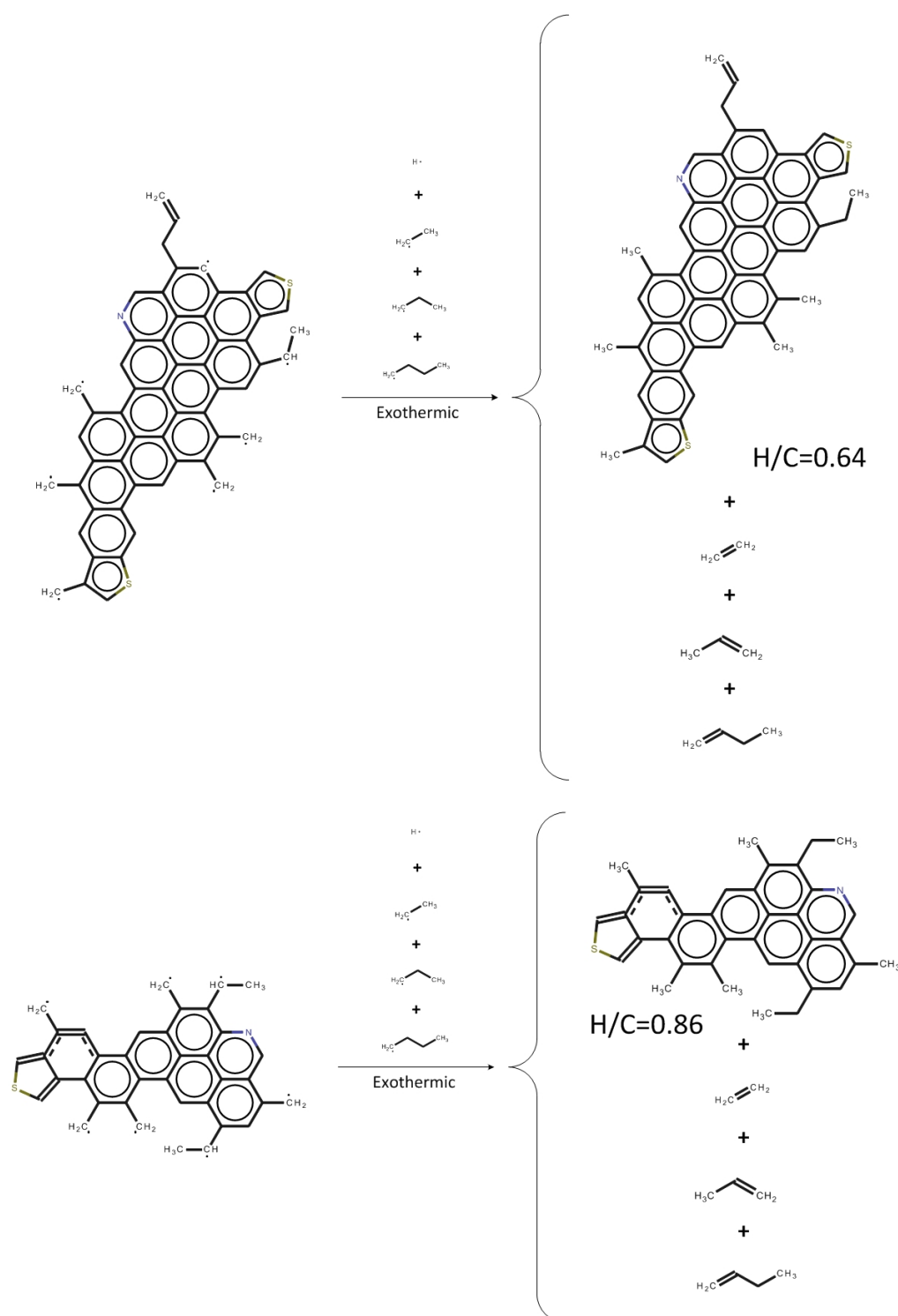


Figure 6.13: Third step in the reaction route for coke formation - Coke formation

- Fourth step: coke underwent a maturation process due to the increment in its energy through the heating process. This maturation process involves the release of gases [100] such as methane and hydrogen. Analyzing the coke structures proposed (Figure 6.13), producing these type of gases was possible. If the energy of these molecules increases, the only possible route to follow is a new

fragmentation process by $C-C$ and $C-H$ bonds cleavage. With the coke structures as reactants, the available sites to undergo breakings were those carbons bonded to the big aromatic nuclei and the hydrogen molecules connected to them. Figure 6.14 summarizes the reactions in the maturation process. In the first step, both coke molecules underwent several breaking processes to produce an olefin, many methyl radicals and several radicals in the aromatic nuclei. Next, the methyl radicals obtained by these fragmentation processes could easily make contact to other saturate, olefin or even saturated sites in the coke structure in order to abstract hydrogen atoms to produce methane or hydrogen. Another route that the methyl radicals could follow was the intermolecular addition to form other heavier gases such as ethane or propane. On the other hand, the radicals produced in the coke structures during the second step of this maturation process, underwent saturation processes to produce new coke molecules with H/C ratios of 0.43 and 0.6.

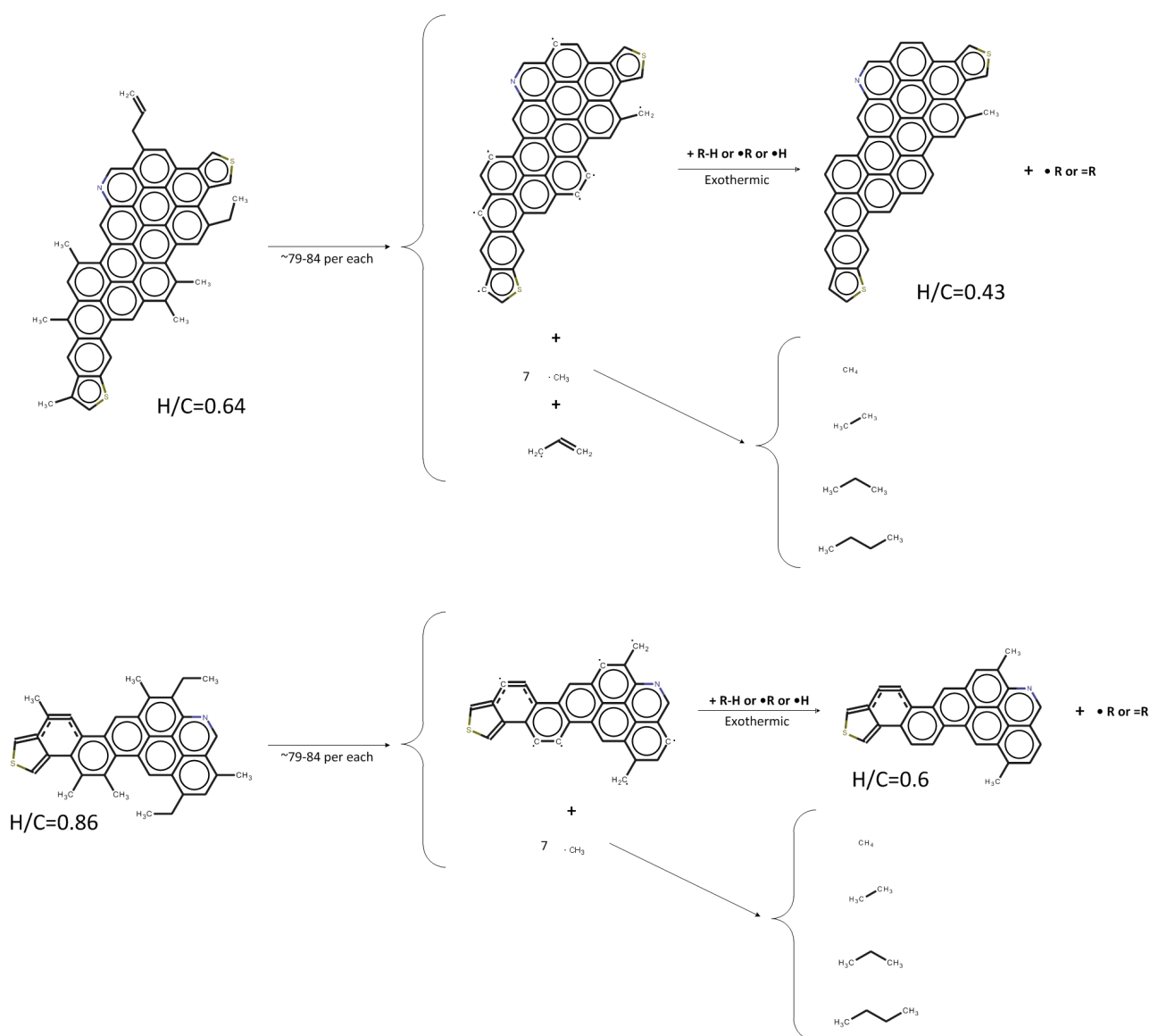


Figure 6.14: Fourth step in the reaction route for coke formation - Maturation. Reaction energies in kcal/mol

6.2.6. Thematic DataBase results

The study of the thermal cracking process for the surrogates selected to represent the saturate fraction of a crude oil derived in a great amount of species. Currently, it is of high importance to count with reaction models that offer accurate explanations of the chemistry phenomena but that, at the same time, could be applied for simulation studies. Based on this, it has been common to study reductions in the size of mechanisms that allow more condensed models. Taking this into account, a Thematic DataBase was built in order to apply some reduction criteria. The initial pathway presented 332 reactions originated from two surrogates.

The first criteria studied for carrying out the reduction process was the calculation of approximations to activation energies for the four initiation reactions underwent by saturate surrogates. Table 6.11 presents the results for relaxed scan calculations. In the case of the CS two routes were considered as initiation and based on the results, it was possible to eliminate one of the reactions, the one that produced the tertiary and hydrogen radicals. The approximation to activation energy presented by these reactions was of 139.19 kcal/mol, whereas, the one that competed with it presented an approximation to activation energy of 114.37 kcal/mol. Contrary to this case, for NS no reactions could be eliminated. Both of the possible transformations underwent by NS surrogate, presented similar approximations for activation energies, 130.82 and 131.20 kcal/mol.

Table 6.11: Summary of results for scan relaxed calculations applied to Saturate surrogates

Reactant	Route	Products	Approximation to activation energy(kcal/mol)
CS	<i>C – H</i> cleavage	Tertiary and hydrogen radicals	139.19
	<i>C – C</i> cleavage	Biradical	114.37
NS	<i>C – H</i> cleavage	Secondary and hydrogen radicals	130.82
	<i>C – C</i> cleavage	Two primary radicals	131.20

The second criteria applied for reducing the amount of reactions in the mentioned reaction scheme was the consideration of the more stable transformations. A pair of compounds could follow several reactions, e.g. two radicals that make contact may undergo an intermolecular addition or a disproportion reactions; therefore, based on the reaction energies calculated it was possible to determine the most stable reaction options. After the application of these reduction criteria, a reaction scheme with 139 reactions was obtained, which meant a reduction of 42%.

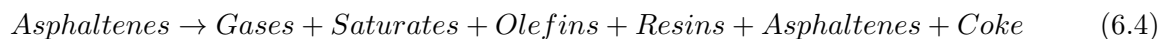
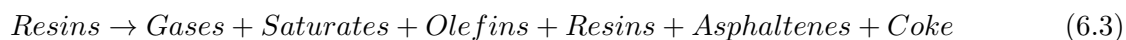
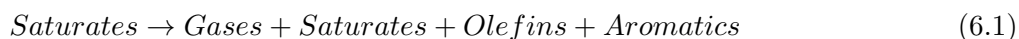
The developed thematic DataBase constitutes a tool to obtain more condensed mechanisms from the reactions schemes developed in this thesis. Those type of condensed mechanisms have been required for the performance of simulation tools where the use of extended mechanisms is not possible or practical.

6.3. Validation

Reactions 6.1 to 6.5 present the reaction model by pseudocomponents obtained from the analysis of the thermal cracking process of ISC. Most of these reactions agree with the reaction scheme based on experiments and proposed by Freitag and Exelby [55]. The Reaction 6.1 proposes that the ther-

mal cracking of the saturate fraction led to the formation of gases, saturates, olefins and aromatic compounds. The cracking of the aromatic fraction (Reaction 6.2) gave rise to the formation of gases, saturates, aromatics and resins. In addition, resins (Reaction 6.3) that is one of the heavier fractions, formed several types of compounds such as gases, saturates, olefins, resins, asphaltenes and coke, which is one the most important species in the ISC process. The Reaction 6.4 presents the products from the asphaltenic fraction: gases, saturates, olefins, resins, asphaltenes and coke. Finally, coke through a maturation process produced gasea and coke with lower H/C ratios. Urán [100] obtained the same results for coke maturation process by an experimental methodology.

The products obtained by the analysis of the thermal cracking process have been reported by other three researches [54, 55, 100], which validates the proposed pathways.



6.4. Conclusions

- In the initiation event, the highest bond dissociation energies were calculated for the $C - H$ bonds, except in the cases where those formed stabilized by resonance radicals that, given their high stability, led to the lowest dissociation energies in the thermal cracking process.
- The presence of a sulfur atom in the PA structure affected the bond order data and energy reactions calculated, as its presence changed the electronic structure of the molecule. For the PA surrogate, the breaking patterns and reaction energies ranges determined for the rest of the molecules changed.
- The most stable radicals in the events analyzed were those in a carbon atom tied to aromatic structures. In the evolution of resin and asphaltene molecules, the formation of those radicals

was fundamental for explaining coke formation. The carbon atoms bonded to the large aromatic nucleus underwent breaking during the maturation process leading to produce gases such as, methane and hydrogen.

- The reverse radical disproportion reactions (bimolecular initiations) were identified as the possible reaction route that lead to the formation of saturate and non aromatic compounds from the aromatic fraction of a crude oil. Given that the breaking of double or resonant bonds is not possible at ISC temperature conditions, this study is the first one in the referred literature that takes into account the formation of non-aromatic species from the aromatic fraction of a crude oil.
- Several olefin compounds were produced and two routes were identified as responsible: disproportion and β -scission reactions. The main difference between these routes is that the olefins produced by β -scission reactions are always terminal, whereas, those formed by disproportion reactions may be both terminal or secondary; however, the secondary olefins presented lower reaction energies.
- Compounds in the saturate fraction of a crude oil follow three different routes during the thermal cracking process: i) formation of lighter species such as methane, ethylene and hydrogen. ii) production of unsaturated species such as olefins and dienes, that may condense to form cyclohexene compounds that produce aromatic rings. iii) formation of heavier saturated hydrocarbon species.
- Aromatic species of a crude oil may undergo three reaction routes during the thermal cracking process: i) formation of gases and lighter species by breaking in $C - C$ and $C - H$ bonds. ii) reduction of their aromaticity by the addition of a hydrogen radical produce saturated or olefin compounds. iii) interaction with other aromatic species by intermolecular addition or disproportion reactions, producing heavier aromatic species.
- Resin and asphaltene molecules, mainly undergo $C - C$ breaking reactions to produce gases, light saturated compounds, olefins and coke.

Chapter 7

Conclusions

This thesis developed a new methodology to formulate reaction pathways by the application of mechanistic studies theories to the ISC process. The formulated methodology described the evolution of crude oil fractions during the low temperature oxidation and thermal cracking stages.

Computational chemistry calculations were successfully employed to describe the chemical evolution of crude oil fractions during the ISC process. The exploration of this kind of tools expanded the computational methodologies traditionally used to study ISC and in general, petroleum processes. Although high computational capacities are needed to carry out calculations for large molecules, they are excellent complement to the more traditional experimental methods that are not anymore the only option to study kinetic and thermodynamic characteristics of the reactions involved in a petroleum process.

During the LTO stage, oxygenated products such as cyclic ethers, ethers, ketones, aldehydes, peroxides and carboxylic acids were produced. Two main routes, intermolecular and intramolecular H-abstraction, were determined as responsible of peroxy radicals evolution. The intermolecular route produced in most of the cases most of the mentioned products and also allowed to study the possible conversion of hydroperoxyl radicals with low reactivity into new oxygen molecules, which contributed to the advance of the oxidation process. The intramolecular route was the main responsible for cyclic ethers formation, which was meaningful taking into account that those products have not been identified by any other ISC chemistry study.

For the thermal cracking stage, it was possible to determine the products from this process as coke, methane, hydrogen, lighter and heavier saturates and olefins. For coke, which is one of the most important products in ISC process, H/C ratios from 0.8 to 0.6 were obtained, values that fit into the ranges found by experimental studies.

Introducing the role of new species such as lighter saturates and olefins improves the typical

chemical approach of ISC, where the thermal cracking of crude oil fractions only produces asphaltenes, gas and coke. The fact that these products that have economical value can be produced from all the SARA oil fractions, even from asphaltenes suggests that it is possible to achieve a partial upgrade process inside the reservoir. Studies such as the ones in this thesis that improves the understanding of chemistry of the ISC process are fundamental if such an upgrade is desired.

This thesis proposed approximately 800 thermal cracking reactions and 120 low temperature reactions that aim to get a better understanding on the chemical processes involved in the ISC.

7.1. Future work

This study explored wide research field that apply other simulation tools to study processes that involve crude oil. The developed reaction pathways help to better understand the chemical processes that occur during the ISC technique; however, they could be extended and complemented by the incorporation of new reactions, species or even kinetic data, which could be determined by computational or experimental methodologies.

References

- [1] P. S. Sarathi, “In - Situ Combustion Handbook - Principles and practices,” tech. rep., 1999.
- [2] I. Akkutlu and Y. C. Yortsos, “The dynamics of in-situ combustion fronts in porous media,” *Combustion and Flame*, vol. 134, pp. 229–247, Aug. 2003.
- [3] A. Hart, M. Greaves, and J. Wood, “A comparative study of fixed-bed and dispersed catalytic upgrading of heavy crude oil using-CAPRI,” *Chemical Engineering Journal*, vol. 44, pp. 1–11, 2015.
- [4] N. Mahinpey, A. Ambalae, and K. Asghari, “In Situ Combustion in Enhanced Oil Recovery (EOR): a Review,” *Chemical Engineering Communications*, vol. 194, no. 8, pp. 995–1021, 2007.
- [5] D. Subramanian, K. Wu, and A. Firoozabadi, “Ionic liquids as viscosity modifiers for heavy and extra-heavy crude oils,” *Fuel*, vol. 143, pp. 519–526, 2015.
- [6] D. D. Mamora, H. J. Ramey, W. E. Brigham, and L. M. Castanier, *Kinetics of In Situ Combustion*. PhD thesis, 1993.
- [7] P. R. Kapadia, M. S. Kallos, and I. D. Gates, “A Comprehensive Kinetic Theory to Model Thermolysis, Aquathermolysis, Gasification, Combustion, and Oxidation of Athabasca Bitumen Hydrogen Generation from Pyrolysis and Aquathermolysis : Experimental Data,” in *Improved Oil Recovery Symposium*, pp. 1–31, 2010.
- [8] J. Belgrave, R. Moore, M. Ursenbach, and D.W. Bennion, “A Comprehensive Approach to In-Situ Combustion Modeling,” *SPE Advanced Technology Series*, vol. 1, no. 1, pp. 98–107, 1993.
- [9] F. Battin-Leclerc, “Detailed chemical kinetic models for the low-temperature combustion of hydrocarbons with application to gasoline and diesel fuel surrogates,” *Progress in Energy and Combustion Science*, vol. 34, no. 4, pp. 440–498, 2008.

- [10] F. Buda, R. Bounaceur, V. Warth, P. a. Glaude, R. Fournet, and F. Battin-Leclerc, "Progress toward a unified detailed kinetic model for the autoignition of alkanes from C4 to C10 between 600 and 1200 K," *Combustion and Flame*, vol. 142, no. 1-2, pp. 170–186, 2005.
- [11] N. P. Freitag, "Chemical Reaction Mechanisms That Govern Oxidation Rates During In-Situ Combustion and High-Pressure Air Injection," in *SPE Heavy Oil Conference-Canada*, pp. 1–16, Society of Petroleum Engineers, June 2014.
- [12] P. A. Glaude, O. Herbinet, S. Bax, J. Biet, V. Warth, and F. Battin-Leclerc, "Modeling of the oxidation of methyl esters-Validation for methyl hexanoate, methyl heptanoate, and methyl decanoate in a jet-stirred reactor," *Combustion and Flame*, vol. 157, no. 11, pp. 2035–2050, 2010.
- [13] Z. Khansari, *Low temperature oxidation of heavy crude oil: Experimental study and reaction modeling*. PhD thesis, University of Calgary, 2014.
- [14] E. Ranzi, T. Faravelli, P. Gaffuri, and A. Sogaro, "Low-temperature combustion: Automatic generation of primary oxidation reactions and lumping procedures," *Combustion and Flame*, vol. 102, no. 1-2, pp. 179–192, 1995.
- [15] J. M. Simmie, "Detailed chemical kinetic models for the combustion of hydrocarbon fuels," *Progress in Energy and Combustion Science*, vol. 29, pp. 599–634, Jan. 2003.
- [16] S. Touchard, R. Fournet, P. a. Glaude, V. Warth, F. Battin-Leclerc, G. Vanhove, M. Ribaucour, R. Minetti, D. M. Golden, and J. Troe, "Modeling of the oxidation of large alkenes at low temperature," *Proceedings of the Combustion Institute*, vol. 30 I, no. 1, pp. 1073–1081, 2005.
- [17] X. Wang, "Mechanism Generation for Hydrocarbon Fuels," Master's thesis, Brandenburgische Technische Universität Cottbus, 2011.
- [18] V. Warth, F. Battin-Leclerc, R. Fournet, P. Glaude, G. Come, and G. Scacchi, "Computer based generation of reaction mechanisms for gas-phase oxidation," *Computers & chemistry*, vol. 24, pp. 541–60, July 2000.
- [19] O. Welz, J. Zádor, J. D. Savee, L. Sheps, D. L. Osborn, and C. a. Taatjes, "Low-temperature combustion chemistry of n-butanol: Principal oxidation pathways of hydroxybutyl radicals," *Journal of Physical Chemistry A*, vol. 117, no. 46, pp. 11983–12001, 2013.
- [20] C. K. Westbrook, J. Warnatz, and W. J. Pitz, "A detailed chemical kinetic reaction mechanism for the oxidation of iso-octane and n-heptane over an extended temperature range and its appli-

- cation to analysis of engine knock,” *Symposium (International) on Combustion*, vol. 22, no. 1, pp. 893–901, 1989.
- [21] S. Benson and W. DeMore, “Gas Kinetics,” *Nature*, vol. 204, no. 4962, pp. 965–966, 1964.
- [22] R. Bounaceur, V. Burklé-Vitzthum, P.-M. Marquaire, and L. Fusetti, “Mechanistic modeling of the thermal cracking of methylcyclohexane near atmospheric pressure, from 523 to 1273K: Identification of aromatization pathways,” *Journal of Analytical and Applied Pyrolysis*, vol. 103, pp. 240–254, Sept. 2013.
- [23] R. O. Canaz and C. Erkey, “Process intensification for heavy oil upgrading using supercritical water,” *Chemical Engineering Research and Design*, vol. 92, pp. 1845–1863, Oct. 2014.
- [24] Q. Chen and G. F. Froment, “Thermal cracking of substituted aromatic hydrocarbons. II. Kinetic study of the thermal cracking of n-propylbenzene and ethylbenzene,” *Journal of Analytical and Applied Pyrolysis*, vol. 21, no. 1-2, pp. 51–77, 1991.
- [25] Q. Chen and G. F. Froment, “Thermal cracking of substituted aromatic hydrocarbons. I. Kinetic study of the thermal cracking of i-propylbenzene,” *Journal of Analytical and Applied Pyrolysis*, vol. 21, pp. 27–50, Sept. 1991.
- [26] J. M. Cuquerella, “Craqueo térmico y catalítico, con y sin vapor de agua, de alcanos sobre zeolitas, cinética, desactivación y estabilización del catalizador,” *Zhurnal Eksperimental’noi i Teoreticheskoi Fiziki*, 2009.
- [27] D. Fuentes-Cano, A. Gómez-Barea, S. Nilsson, and P. Ollero, “The influence of temperature and steam on the yields of tar and light hydrocarbon compounds during devolatilization of dried sewage sludge in a fluidized bed,” *Fuel*, vol. 108, pp. 341–350, June 2013.
- [28] B. S. Greensfelder, H. H. Voge, and M. G. Good, “Catalytic and Thermal Cracking of Pure Hydrocarbons,” *Industrial and Engineering Chemistry*, vol. 41, no. November, pp. 2573–2584, 1949.
- [29] D. M. Hernandez-Baez, B. Tohidi, A. Chapoy, A. Reid, and R. Bounaceur, “Establishing the Maximum Carbon Number for Reliable Quantitative Gas Chromatographic Analysis of Heavy Ends Hydrocarbons . Part 1 . (Low Conversion Thermal Cracking Modeling). Pyrolysis risk inside a Gas,” *Energy & Fuels*, pp. 1–22, 2012.
- [30] F. Khorasheh and M. R. Gray, “High-pressure thermal cracking of n-hexadecane,” *Industrial & Engineering Chemistry Research*, vol. 32, pp. 1853–1863, Sept. 1993.

- [31] F. D. Kopinke, G. Zimmermann, and B. Ondruschka, "Tendencies of aromatization in steam cracking of hydrocarbons," *Industrial & Engineering Chemistry Research*, vol. 26, no. 11, pp. 2393–2397, 1987.
- [32] A. Kubátová, J. ŠtÁvová, W. S. Seames, Y. Luo, S. M. Sadrameli, M. J. Linnen, G. V. Baglayeva, I. P. Smoliakova, and E. I. Kozliak, "Triacylglyceride Thermal Cracking: Pathways to Cyclic Hydrocarbons," *Energy & Fuels*, vol. 26, pp. 672–685, Jan. 2012.
- [33] X. Qin, H. Chi, W. Fang, Y. Guo, and L. Xu, "Thermal stability characterization of n-alkanes from determination of produced aromatics," *Journal of Analytical and Applied Pyrolysis*, vol. 104, pp. 593–602, Nov. 2013.
- [34] F. Rice and K. Herzfeld, "The thermal decomposition of organic compounds from the standpoint of free radicals. VI. The mechanism of some chain reactions," *Journal of the American Chemical Society*, vol. 1262, no. 4, pp. 284–289, 1934.
- [35] K. M. Sundaram and G. F. Froment, "Modeling of Thermal Cracking Kinetics. 3. Radical Mechanisms for the Pyrolysis of Simple Paraffins, Olefins, and Their Mixtures," *Industrial & Engineering Chemistry Fundamentals*, vol. 17, no. 3, pp. 174–182, 1978.
- [36] C. Xu, A. S. Al Shoaibi, C. Wang, H.-H. Carstensen, and A. M. Dean, "Kinetic modeling of ethane pyrolysis at high conversion.," *The journal of physical chemistry. A*, vol. 115, pp. 10470–90, Sept. 2011.
- [37] O. Herbinet, P.-A. Glaude, V. Warth, and F. Battin-Leclerc, "Experimental and modeling study of the thermal decomposition of methyl decanoate," *Combustion and Flame*, vol. 158, no. 7, pp. 1288–1300, 2011.
- [38] M. J. Frisch, G. W. Trucks, H. B. Schlegel, G. E. Scuseria, M. A. Robb, J. R. Cheeseman, G. Scalmani, V. Barone, B. Mennucci, G. A. Petersson, H. Nakatsuji, M. Caricato, H. P. H. X. Li, A. F. Izmaylov, J. Bloino, G. Zheng, J. L. Sonnenberg, M. Hada, M. Ehara, K. Toyota, R. Fukuda, J. Hasegawa, M. Ishida, T. Nakajima, Y. Honda, O. Kitao, H. Nakai, T. Vreven, J. A. Montgomery, J. E. P. Jr., F. Ogliaro, M. Bearpark, J. J. Heyd, E. Brothers, K. N. Kudin, V. N. Staroverov, T. Keith, R. Kobayashi, J. Normand, K. Raghavachari, A. Rendell, J. C. Burant, S. S. Iyengar, J. Tomasi, M. Cossi, N. Rega, J. M. Millam, M. Klene, J. E. Knox, J. B. Cross, V. Bakken, C. Adamo, J. Jaramillo, R. Gomperts, R. E. Stratmann, O. Yazyev, A. J. Austin, R. Cammi, C. Pomelli, J. W. Ochterski, R. L. Martin, K. Morokuma, V. G. Zakrzewski, G. A.

- Voth, P. Salvador, J. J. Dannenberg, S. Dapprich, A. D. Daniels, O. Farkas, J. B. Foresman, J. V. Ortiz, J. Cioslowski, and D. J. Fox, "Gaussian 09," 2013.
- [39] P. R. Kapadia, M. S. Kallos, and I. D. Gates, "A review of pyrolysis, aquathermolysis, and oxidation of Athabasca bitumen," *Fuel Processing Technology*, vol. 131, pp. 270–289, 2015.
- [40] G. Scheffknecht, L. Al-Makhadmeh, U. Schnell, and J. Maier, "Oxy-fuel coal combustion-A review of the current state-of-the-art," *International Journal of Greenhouse Gas Control*, vol. 5, no. SUPPL. 1, pp. 16–35, 2011.
- [41] V. Warth, N. Stef, P. a. Glaude, F. Battin-Leclerc, G. Scacchi, and G. M. Côme, "Computer-aided derivation of gas-phase oxidation mechanisms: Application to the modeling of the oxidation of n-butane," *Combustion and Flame*, vol. 114, no. 1-2, pp. 81–102, 1998.
- [42] T. Wall, Y. Liu, C. Spero, L. Elliott, S. Khare, R. Rathnam, F. Zeenathal, B. Moghtaderi, B. Buhre, C. Sheng, R. Gupta, T. Yamada, K. Makino, and J. Yu, "An overview on oxyfuel coal combustion-State of the art research and technology development," *Chemical Engineering Research and Design*, vol. 87, no. 8, pp. 1003–1016, 2009.
- [43] G. M. Côme, V. Warth, P. a. Glaude, R. Fournet, F. Battin-Leclerc, and G. Scacchi, "Computer-aided design of gas-phase oxidation mechanisms-Application to the modeling of n-heptane and iso-octane oxidation," *Symposium (International) on Combustion*, vol. 26, no. 1, pp. 755–762, 1996.
- [44] R. G. Moore, S. A. Mehta, M. Ursenbach, and C. J. Laureshen, "Strategies for Successful Air injection-based IOR process," in *7th Unitar International Conference on Heavy Crude and Tar Sands held on Beijing, China*, pp. October 27–30, 1998.
- [45] J. Taber, F. Martin, and R. Seright, "EOR Screening Criteria Revisited - Part 1: Introduction to Screening Criteria and Enhanced Recovery Field Projects," *SPE Reservoir Engineering*, vol. 12, no. 3, pp. 189–198, 1997.
- [46] B. Hascakir, a. Texas, and A. R. Kovsky, "Analysis of In-Situ Combustion Performance in Heterogeneous Media," *SPE Heavy Oil Conference-Canada*, no. June, pp. 1–18, 2014.
- [47] L. M. Castanier and W. E. Brigham, "Upgrading of crude oil via in situ combustion," *Journal of Petroleum Science and Engineering*, vol. 39, no. 1-2, pp. 125–136, 2003.
- [48] B. E. Hoekstra, *Impact of chemical reactions in the gas phase on the in-situ combustion process: an experimental study*. PhD thesis, Delft University of Technology, 2011.

- [49] M. Prats, "The Heat Efficiency of Thermal Recovery Processes Resulting From Non-Uniform Vertical Temperature Profiles," *SPE Latin America Petroleum Engineering Conference*, 1992.
- [50] Y. Ren, N. Freitag, and N. Mahinpey, "A Simple Kinetic Model for Coke Combustion During an In Situ Combustion (ISC) Process," *Proceedings of Canadian International Petroleum Conference*, June 2005.
- [51] M. Absi-Halabi, A. Stanislaus, and D. Trimm, "Coke formation on catalysts during the hydro-processing of heavy oils," *Applied Catalysis*, vol. 72, pp. 193–215, May 1991.
- [52] S. Abu-Khamsin, W. Brigham, and H. Ramey Jr., "Reaction Kinetics of Fuel Formation for In-Situ Combustion," *SPE Reservoir Engineering*, vol. 3, no. 4, 1988.
- [53] K. Adegbesan, J. Donnelly, R. Moore, and D. Bennion, "Low-Temperature Oxidation Kinetic Parameters for In-Situ Combustion Numerical Simulation," *Society of Petroleum Engineers*, no. November, 1987.
- [54] D. K. Banerjee, K. J. Laidler, B. N. Nandi, and D. J. Patmore, "Kinetic studies of coke formation in hydrocarbon fractions of heavy crudes," *Fuel*, vol. 65, pp. 480–484, Apr. 1986.
- [55] N. Freitag and D. Exelby, "A SARA-Based Model for Simulating the Pyrolysis Reactions That Occur in High- Temperature EOR Processes Waxy Mixtures," *Proceedings of Canadian International Petroleum Conference*, June 2002.
- [56] N. P. Freitag and B. Verkoczy, "Low-temperature oxidation of oils in terms of SARA fractions: Why simple reaction models don't work," *Journal of Canadian Petroleum Technology*, vol. 44, no. 3, pp. 54–61, 2005.
- [57] E. Cavanzo and S. Muñoz, "Kinetics of Wet In-Situ Combustion : A Review of Kinetic Models," *SPE Heavy and extra heavy oil conference*, 2014.
- [58] K. H. Coats, "In-Situ Combustion Model," *SPE Society of Petroleum Engineers of AIME*, no. December, pp. 533–554, 1980.
- [59] M. Hayashitani, D. W. Bennion, J. K. Donnelly, and R. G. Moore, "THERMAL CRACKING MODELS FOR ATHABASCA OIL SANDS OIL," *Society of Petroleum Engineers of AIME*, 1978.
- [60] J. Millour, R. Moore, D. Bennion, M. Ursenbach, and D. Gie, "A Simple Implicit Model for Thermal Cracking of Crude Oils," *Society of Petroleum Engineers*, 1985.

- [61] D. E. Dmitriev and a. K. Golovko, "Transformations of resins and asphaltenes during the thermal treatment of heavy oils," *Petroleum Chemistry*, vol. 50, no. 2, pp. 106–113, 2010.
- [62] M. R. Kristensen, M. G. Gerritsen, P. G. Thomsen, M. L. Michelsen, and E. H. Stenby, "Efficient Reaction Integration for In-Situ Combustion Simulation," *Transport in Porous Media Porous Med*, 2006.
- [63] Z. Khansari, P. Kapadia, I. Gates, and N. Mahinpey, "Kinetic Models for Low Temperature Oxidation Subranges based on Reaction Products," *Proceedings of 2013 SPE Heavy Oil Conference-Canada*, June 2013.
- [64] J. Warnatz, U. Mass, and R. W. Dibble, *Combustion: physical and chemical fundamentals, modeling and simulation, experiments, pollutant formation*. Springer, 4 ed., 1999.
- [65] X. Chen, D. E. Corporation, Z. Chen, R. G. Moore, S. Mehta, M. G. Ursenbach, and T. G. Harding, "Kinetic Modeling of the In-Situ Combustion Process for Athabasca Ramped Temperature Oxidation (RTO) Experiments and Pseudo Component Modeling Process," in *SPE Heavy Oil Conference*, pp. 1–19, 2014.
- [66] G. Liu, Y. Han, L. Wang, X. Zhang, and Z. Mi, "Supercritical thermal cracking of N-dodecane in presence of several initiative additives: Products distribution and kinetics," *Energy and Fuels*, vol. 22, no. 6, pp. 3960–3969, 2008.
- [67] Y. Xiao, J. M. Longo, G. B. Hieshima, and R. J. Hill, "Understanding the Kinetics and Mechanisms of Hydrocarbon Thermal Cracking: An Ab Initio Approach ," *Industrial & Engineering Chemistry Research*, vol. 36, no. 10, pp. 4033–4040, 1997.
- [68] H. Richter and J. Howard, "Formation of polycyclic aromatic hydrocarbons and their growth to soota review of chemical reaction pathways," *Progress in Energy and Combustion Science*, vol. 26, pp. 565–608, Aug. 2000.
- [69] B. Haynes and H. Wagner, "Soot formation," *Progress in Energy and Combustion Science*, vol. 7, pp. 229–273, Jan. 1981.
- [70] Z. Zhu, G. Q. Lu, J. Finnerty, and R. T. Yang, "Electronic structure methods applied to gas-carbon reactions," *Carbon*, vol. 41, no. 4, pp. 635–658, 2003.
- [71] A. E. Sánchez-Pino, *Effect of O2 and CO2 on Nitrogen Compound Emissions during Fluidized Bed Oxy-Combustion Reactions*. PhD thesis, Universidad de Antioquia, 2011.

- [72] S. Bell, T. J. Dines, B. Z. Chowdhry, and R. Withnall, "Computational Chemistry Using Modern Electronic Structure Methods," *Journal of Chemical Education*, vol. 84, no. 8, pp. 1364–1370, 2007.
- [73] C. J. Cramer and D. G. Truhlar, "Density functional theory for transition metals and transition metal chemistry.," *Physical chemistry chemical physics : PCCP*, vol. 11, no. 46, pp. 10757–10816, 2009.
- [74] N. Chen and R. T. Yang, "Ab initio molecular orbital calculation on graphite: Selection of molecular system and model chemistry," *Carbon*, vol. 36, no. 7-8, pp. 1061–1070, 1998.
- [75] Y. Zhao and D. G. Truhlar, "Density functionals with broad applicability in chemistry," *Accounts of Chemical Research*, vol. 41, no. 2, pp. 157–167, 2008.
- [76] S. N. Pieniazek, F. R. Clemente, and K. N. Houk, "Sources of error in DFT computations of C-C bond formation thermochemistries: $\pi\sigma$ transformations and error cancellation by DFT methods," *Angewandte Chemie - International Edition*, vol. 47, no. 40, pp. 7746–7749, 2008.
- [77] S. N. Steinmann, M. D. Wodrich, and C. Corminboeuf, "Overcoming systematic DFT errors for hydrocarbon reaction energies," *Theoretical Chemistry Accounts*, vol. 127, no. 5, pp. 429–442, 2010.
- [78] M. D. Wodrich, C. Corminboeuf, P. R. Schreiner, A. A. Fokin, and P. Schleyer, "How accurate are DFT treatments of organic energies?," *Organic Letters*, vol. 9, no. 10, pp. 1851–1854, 2007.
- [79] J. Tirado-Rives and W. L. Jorgensen, "Performance of b3lyp density functional methods for a large set of organic molecules," *Journal of Chemical Theory and Computation*, vol. 4, no. 2, pp. 297–306, 2008.
- [80] V. Van Speybroeck, G. B. Marin, and M. Waroquier, "Hydrocarbon bond dissociation enthalpies: From substituted aromatics to large polyaromatics," *ChemPhysChem*, vol. 7, no. 10, pp. 2205–2214, 2006.
- [81] Y. Zhao and D. G. Truhlar, "How well can new-generation density functionals describe the energetics of bond-dissociation reactions producing radicals?," *Journal of Physical Chemistry A*, vol. 112, no. 6, pp. 1095–1099, 2008.
- [82] K. Hemelsoet, V. Van Speybroeck, and M. Waroquier, "A DFT-based investigation of hydrogen abstraction reactions from methylated polycyclic aromatic hydrocarbons," *ChemPhysChem*, vol. 9, no. 16, pp. 2349–2358, 2008.

- [83] G. Mallocci, C. Joblin, and G. Mulas, "On-line database of the spectral properties of polycyclic aromatic hydrocarbons," *Chemical Physics*, vol. 332, no. 2-3, pp. 353–359, 2007.
- [84] A. Gaspar, E. Zellermann, S. Lababidi, J. Reece, and W. Schrader, "Characterization of Saturates, Aromatics, Resins, and Asphaltenes Heavy Crude Oil Fractions by Atmospheric Pressure Laser Ionization Fourier Transform Ion Cyclotron Resonance Mass Spectrometry," *Energy & Fuels*, vol. 26, no. 6, pp. 3481–3487, 2012.
- [85] L. Navarro, M. Álvarez, J. L. Grosso, and U. Navarro, "Separación y caracterización de resinas y asfaltenos provenientes del crudo Castilla. Evaluación de su interacción molecular," *CT y F - Ciencia, Tecnología y Futuro*, vol. 2, no. 5, pp. 53–67, 2004.
- [86] A. Lapene, G. Debenest, M. Quintard, L. M. Castanier, M. G. Gerritsen, and A. R. Kovscek, "Kinetics oxidation of heavy oil. 1. Compositional and full equation of state model," *Energy and Fuels*, vol. 25, no. 11, pp. 4886–4896, 2011.
- [87] A. M. McKenna, J. M. Purcell, R. P. Rodgers, and A. G. Marshall, "Heavy petroleum composition. 1. Exhaustive compositional analysis of athabasca bitumen HVGO distillates by fourier transform ion cyclotron resonance mass spectrometry: A definitive test of the boduszynski model," *Energy and Fuels*, vol. 24, pp. 2929–2938, May 2010.
- [88] A. E. Miller, "Review of American Petroleum Institute Research Projects on Composition and Properties of Petroleum," in *4th World Petroleum Congress*, (Rome), 1955.
- [89] M. R. Fassihi and W. E. Brigham, "Analysis of Fuel Oxidation in In-Situ Combustion Oil Recovery," tech. rep., U.S. Department of Energy, Bartlesville, Oklahoma, 1982.
- [90] B. S. Greensfelder and H. H. Voge, "Catalytic Cracking of Pure Hydrocarbons. Cracking of paraffins," *Industrial and Engineering Chemistry*, vol. 37, no. 6, pp. 514–520, 1945.
- [91] C. Mabery, "Composition of Petroleum and Its Relation to Industrial Use," *Transactions of the AIME*, vol. 65, no. 01, pp. 505–521, 1921.
- [92] S. R. Serguienko, B. E. Davydov, I. Delonfi, and M. Teterina, "Composition and Properties of High Molecular Petroleum Compounds," in *4th World Petroleum Congress*, (Rome), 1955.
- [93] M. J. Frisch, G. W. Trucks, H. B. Schlegel, G. E. Scuseria, M. A. Robb, J. R. Cheeseman, G. Scalmani, V. Barone, B. Mennucci, G. A. Petersson, H. Nakatsuji, M. Caricato, H. P. H. X. Li, A. F. Izmaylov, J. Bloino, G. Zheng, J. L. Sonnenberg, M. Hada, M. Ehara, K. Toyota, R. Fukuda, J. Hasegawa, M. Ishida, T. Nakajima, Y. Honda, O. Kitao, H. Nakai, T. Vreven, J. A.

- Montgomery, J. E. P. Jr., F. Ogliaro, M. Bearpark, J. J. Heyd, E. Brothers, K. N. Kudin, V. N. Staroverov, T. Keith, R. Kobayashi, J. Normand, K. Raghavachari, A. Rendell, J. C. Burant, S. S. Iyengar, J. Tomasi, M. Cossi, N. Rega, J. M. Millam, M. Klene, J. E. Knox, J. B. Cross, V. Bakken, C. Adamo, J. Jaramillo, R. Gomperts, R. E. Stratmann, O. Yazyev, A. J. Austin, R. Cammi, C. Pomelli, J. W. Ochterski, R. L. Martin, K. Morokuma, V. G. Zakrzewski, G. A. Voth, P. Salvador, J. J. Dannenberg, S. Dapprich, A. D. Daniels, O. Farkas, J. B. Foresman, J. V. Ortiz, J. Cioslowski, and D. J. Fox, "Gaussian 09," 2010.
- [94] R. I. Dennington, T. Keith, and J. M. Millam, "GaussView 5.0.8."
- [95] T. Lu and F. Chen, "Multiwfn: A multifunctional wavefunction analyzer," *Journal of Computational Chemistry*, vol. 33, no. 5, pp. 580–592, 2012.
- [96] O. Karacan and M. V. Kok, "Pyrolysis analysis of crude oils and their fractions," *Fuel and Energy Abstracts*, vol. 38, no. 6, p. 391, 1997.
- [97] "MarvinSketch 15.2.2, ChemAxon," 2015.
- [98] T. Fan, J. Wang, and J. S. Buckley, "Evaluating Crude Oils by SARA Analysis," *Improved Oil Recovery Symposium*, pp. 1–7. SPE-75228, 2002.
- [99] H. M. Lababidi, H. M. Sabti, and F. S. AlHumaidan, "Changes in asphaltenes during thermal cracking of residual oils," *Fuel*, vol. 117, pp. 59–67, Jan. 2014.
- [100] L. Urán, "Coke formation during thermal cracking of heavy crude oil," Master's thesis, Universidad Nacional de Colombia - Sede Medellín, 2015.

Appendix A

Reaction schemes

If any problem for visualizing these diagrams please visit:

<http://minas.medellin.unal.edu.co/gruposdeinvestigacion/biofrun/index.php/2-uncategorised/32-reaction-pathways-luisa-carvajal> .

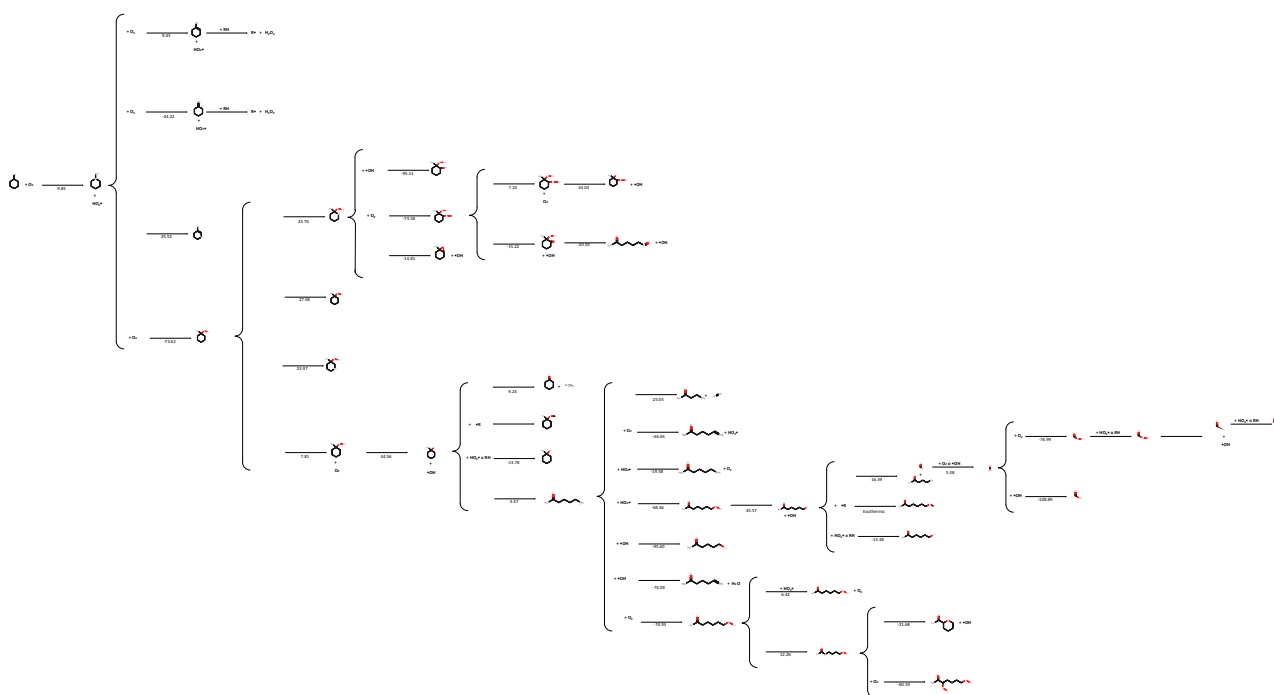


Figure A.1: Reaction scheme for the LTO of the CS surrogate

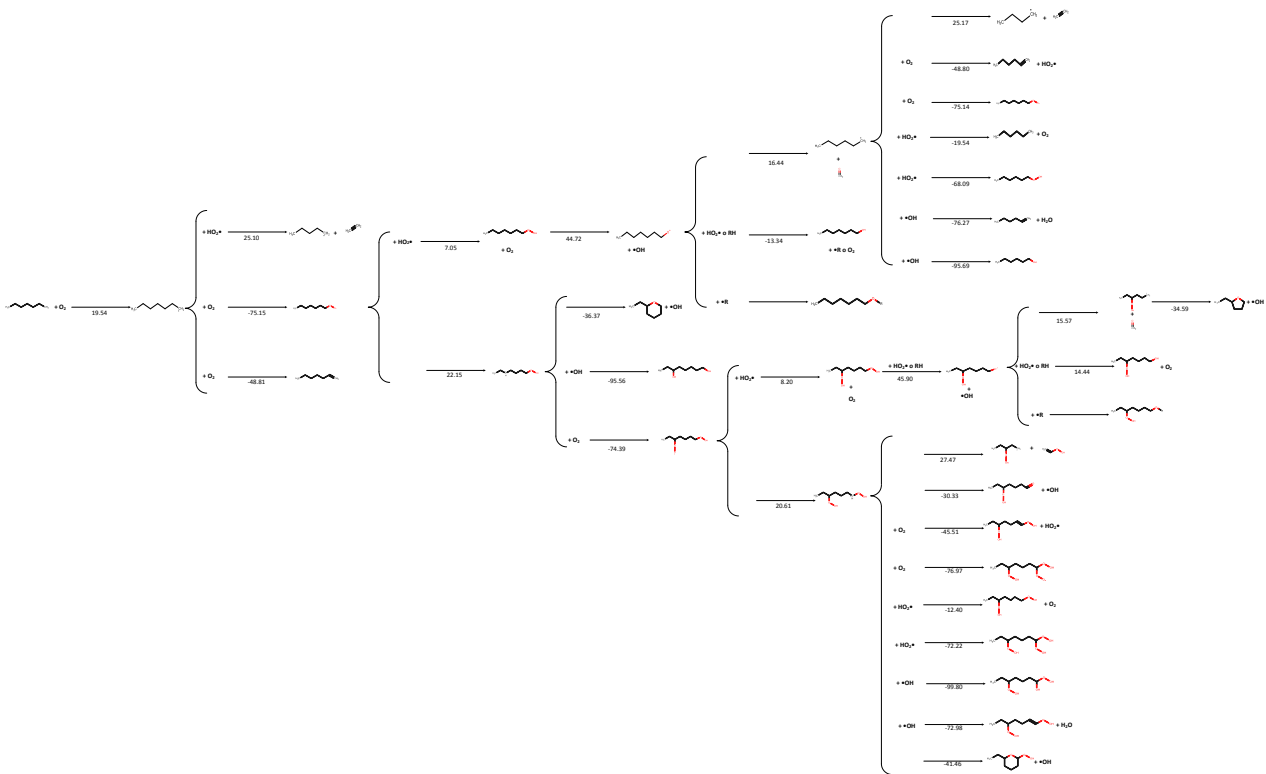


Figure A.2: Reaction scheme for the LTO of the NS surrogate

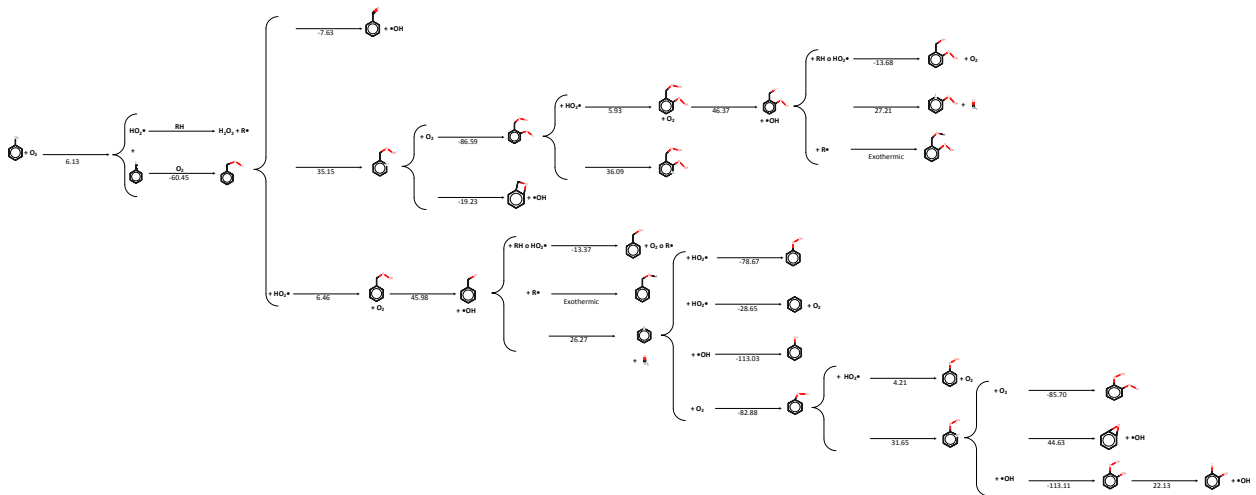


Figure A.3: Reaction scheme for the LTO of the MA surrogate

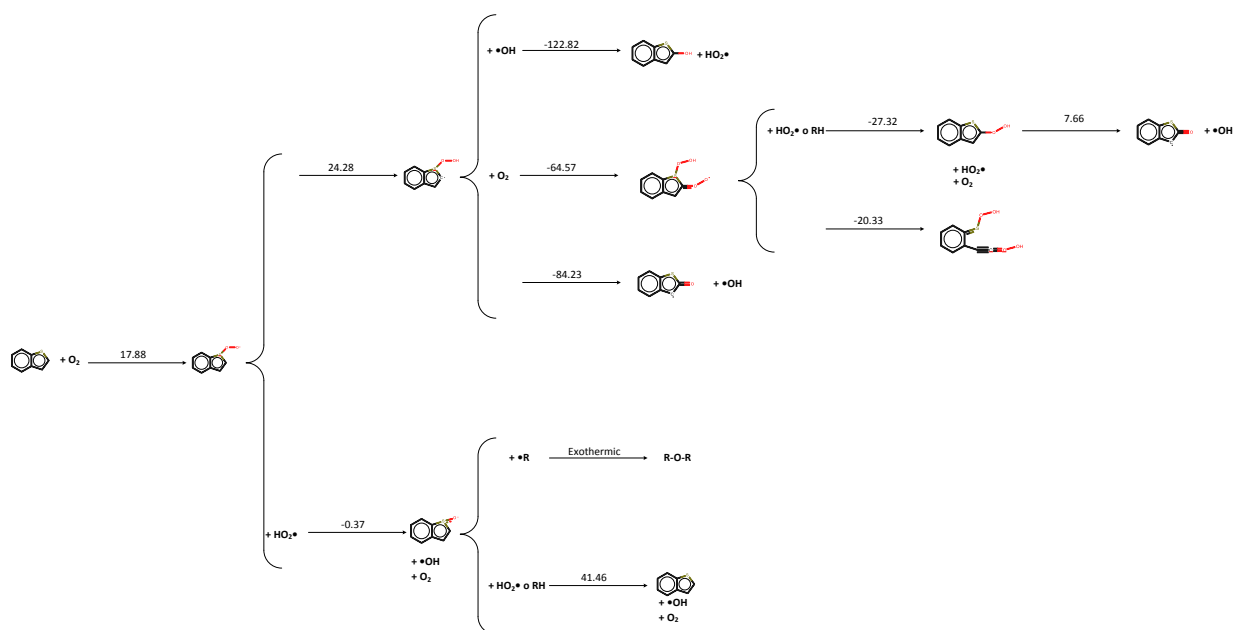


Figure A.4: Reaction scheme for the LTO of the PA surrogate

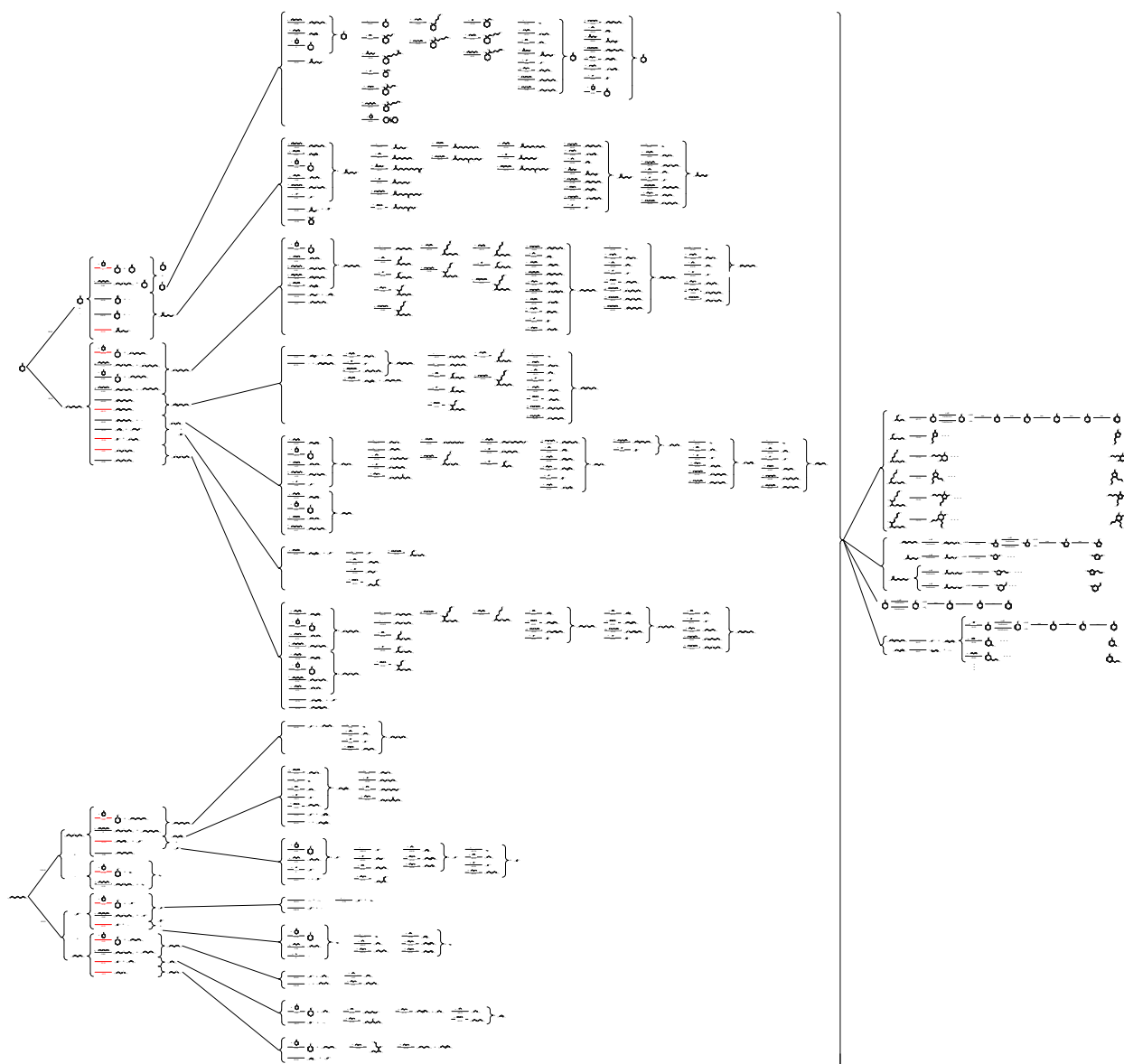


Figure A.5: Reaction scheme for the thermal cracking of the saturate surrogates

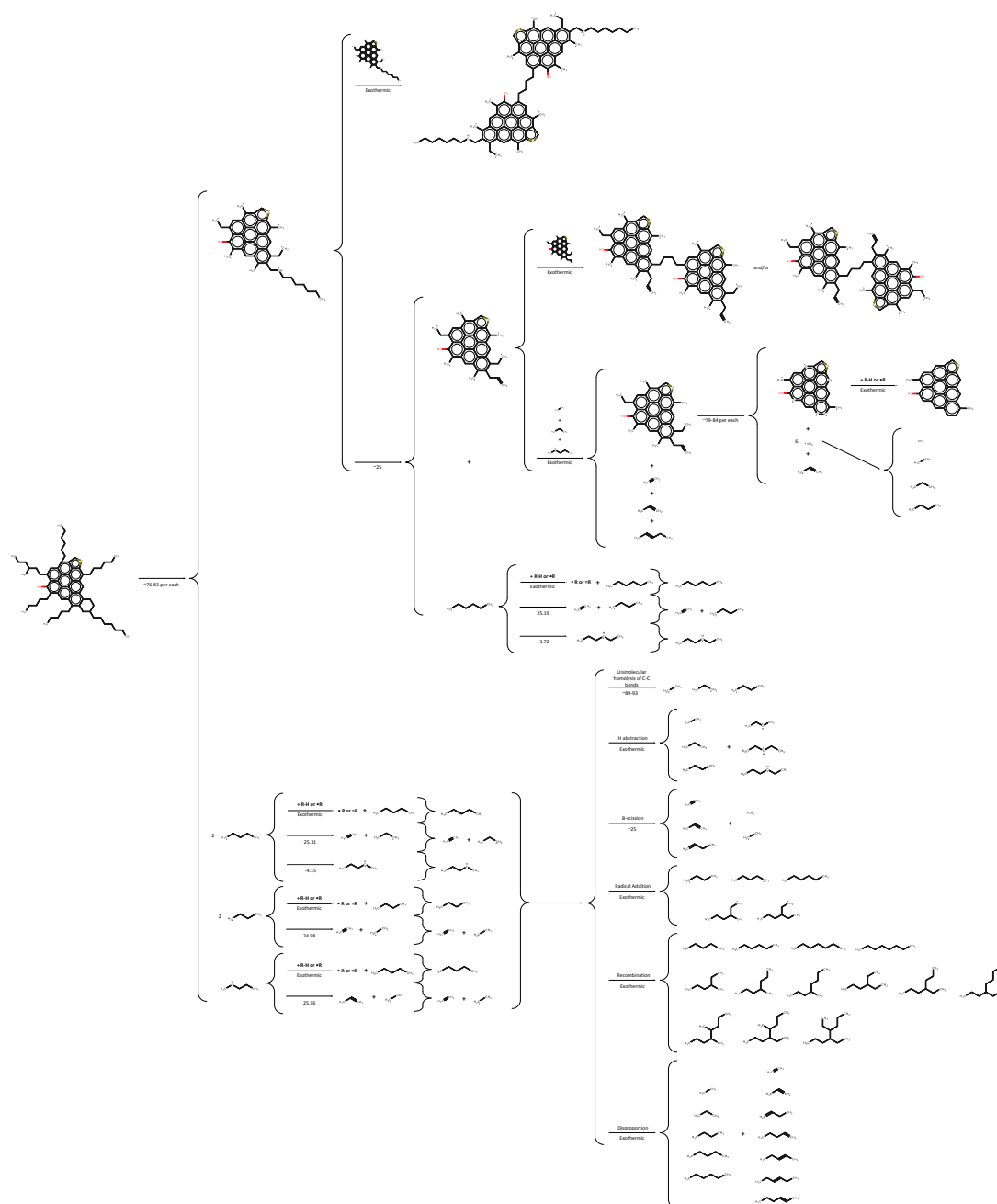


Figure A.6: Reaction scheme for the thermal cracking of the resin surrogate

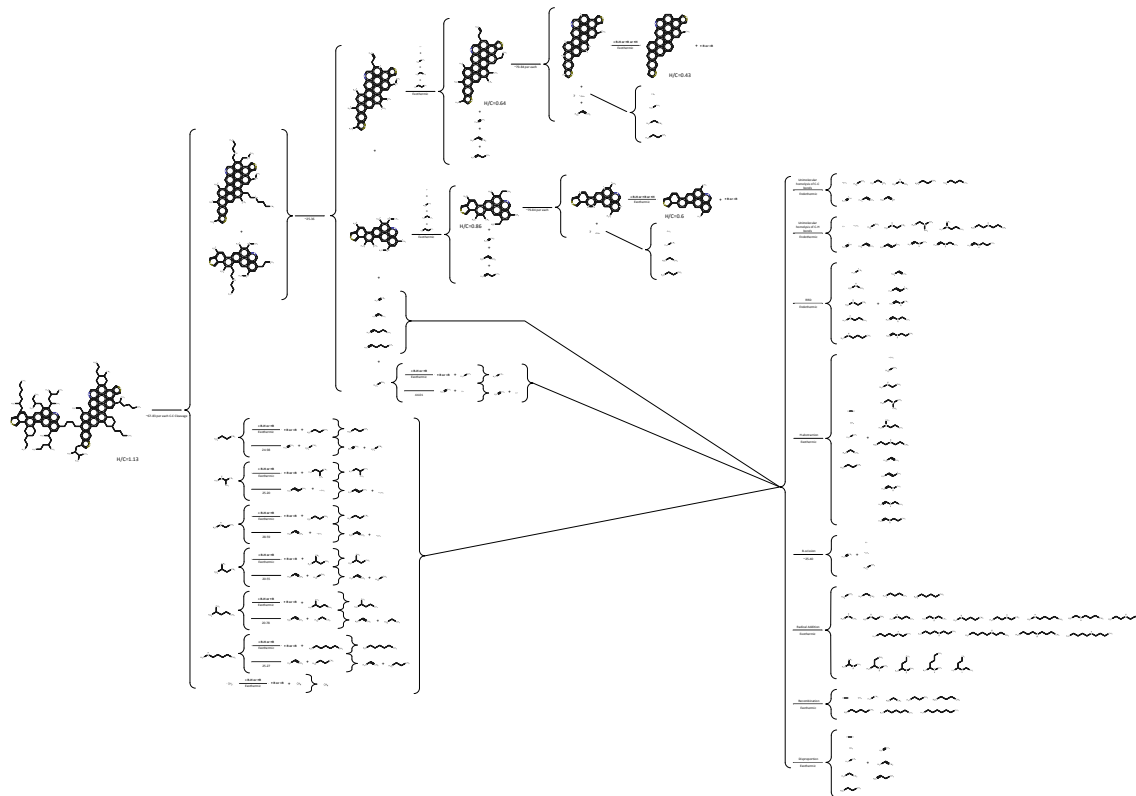


Figure A.7: Reaction scheme for the thermal cracking of the asphaltene surrogate